Monitoring oxidative stress enables predictions of personalised glucose targets in diabetic patients

A thesis

Submitted in partial fulfillment of the requirements

of the degree of

Doctor of Philosophy

By

Rashmi Govind Kulkarni

20103083

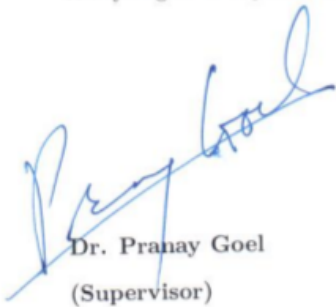INDIAN INSTITUTE OF SCIENCE EDUCATION AND RESEARCH PUNE

April 2017

To my parents

Thank you for being there, *always.*

Certificate

I certify that the thesis entitled "**Monitoring oxidative stress enables predictions of personalised glucose targets in diabetic patients**" presented by **Ms. Rashmi Govind Kulkarni** was carried out by the candidate, under my supervision. The work presented here or any part of it has not been included in any other thesis submitted previously for the award of any degree or diploma from any other University or Institution.

Dr. Pranay Goel

(Supervisor)

Date: 14 Dec'16

Declaration

I declare that this written submission represents my idea in my own words and where others' ideas have been included; I have adequately cited and referenced the original sources. I also declare that I have adhered to all principles of academic honesty and integrity and have not misrepresented or fabricated or falsified any idea/data/fact/source in my submission. I understand that violation of the above will be cause for disciplinary action by the Institute and can also evoke penal action from the sources which have thus not been properly cited or from whom proper permission has not been taken when needed.

Ms. Rashmi Govind Kulkarni

(20103083)

Date: 14|12|2016

Acknowledgements

There are many people who have influenced my PhD endeavour - directly or indirectly. This piece of work will be incomplete if I do not express my gratitude towards them.

Foremost, I would like to thank my Research Advisory Committee members Professor Saroj Ghaskadbi, Dr. Richa Rikhy and Dr. Nishikant Subhedar for taking an interest in my work. I have been immensely benefitted from your critical comments. I especially like to thank Professor Saroj Ghaskadbi, also a collaborator, for sharing the diabetic patient's dataset and for her words of encouragement and appreciation.

I would sincerely like to thank the panel of referees - Dr. Krasimira Tsaneva-Atanasova (University of Exeter, United Kingdom), Dr. Bradford E. Peercy (University of Maryland, Baltimore County, USA) and Dr. Ganesh A Viswanathan (IIT Bombay, India) - for evaluating my thesis work. Their comments and suggestions helped me improve my thesis work and understand it better.

I would like to acknowledge Professor L. S. Shashidhara and Dr. Girish Ratnaparkhi for their useful suggestions and for their out of the way support, when it was required the most. Thanks are due to Dr. Nagaraj Balasubramanian for allowing me to use his lab facilities for experimental work. I would like to extend my thanks to the administrative and technical staff of IISER-Pune, for their timely help.

To my colleagues and friends through the years - I am fortunate to have a large interdisciplinary network of friends from Physics, Mathematics, and Biology. They have directly and indirectly contributed towards this endeavour - making this journey pleasurable - in numerous, uncountable ways. I specifically like to thank Snehal Shekatkar for helping me

with the thesis formatting. I can not forget my colleagues from Pune-Bio Modelling group - from organising conferences to attending monthly group meetings; I have learned much from these informal interactions. Special thanks to Dr. Chetan Gadgil, for his guidance on the critical issues, who introduced me to the area of computational biology for the first time.

To my family for their patient support throughout and admiring my efforts. Thank you for being there, especially during the trying times. I am grateful to my parent-in-laws for their understanding, support and care during the last spell of my PhD.

To my husband - Sameer. Thank you for bearing with me, for your affection and constant encouragement. Most importantly, because you *always* understood.

Most of all, I would like to thank my advisor - Dr. Pranay Goel. I have gained much from your style of critically evaluating and formulating scientific theories. Of asking directed and pointed questions, paying attention to the details. I must say, it has always given me a perspective to look at the things differently, in scientific matters and in general. I can not thank you enough for giving me freedom to think independently, to question my assumptions, and encouraging my efforts at the same time. You have imparted into me the importance of communicating ideas in the most unbiased manner - it is helping me to develop a structured thinking and writing style, which I will continue to improve. Thank you for everything.

Rashmi Kulkarni

Abstract

The principal cause of hyperglycemia-mediated post-diabetic complications (PDCs) is - oxidative stress (OS). Therefore, establishing a quantitative relationship between OS and glycemic status (GS) of a diabetic individual could help in deciding how much and how long OS should be controlled via external anti-glycemic treatment. To monitor serial changes in OS (as measured by glutathione or GSH, an OS marker), a group of newly diagnosed type 2 diabetic patients kept on anti-diabetic treatment were followed for the period of 8 weeks. A cluster analysis performed on the GSH values pooled from non-diabetics and diabetics before and after therapy (0 and 8 weeks) show that GSH can be used to classify individuals based upon their diabetic status, independently of glucose. That is, GSH can be an excellent anti-oxidant to monitor along with glucose in defining diabetes status. Further, GSH levels are found to be inversely correlated with the GS of diabetic individuals. We propose a physiological minimal mathematical model to capture a quantal dose-response relationship between GSH and glucose for each diabetic patient. Individualised diabetic GSH-glucose curves are parameterised by: maximal glutathione level (G_{tot}), glucose concentration when GSH is half maximal (v) and slope of the curve (k). Finally, to relax the assumptions imposed in the physiological model, a statistical phenomenological model is proposed to capture OS-GS trajectories in diabetic patients. We show that a phenomenological model is a statistically better and simple alternative to the physiological minimal model. We propose that individually parameterised GSH-glucose curves can be helpful in deciding optimal glucose control strategies through which OS is maximally controlled. Thus, glucose targets can be personalised based upon the OS state of an individual.

Contents

List of Figures

VII

VIII

List of Tables

Chapter 1

Introduction

Type 2 diabetes (diabetes) has emerged as a pandemic in the last two decades [1]. Diabetes is diagnosed by fasting plasma glucose (FPG) $>$ 126 mg/dL (7.0 mmol/L) and glycated hemoglobin (HbA_{1c}) $\geq$ 6.5% (48 mmol/mol). HbA_{1c} reference assay for defining diabetic state was standardised based upon the results from Diabetes Control and Complications Trial [2]. A pre-diabetic state is characterised by an FPG range of 100 - 125 mg/dL (5.5-6.9 mmol/L) or HbA_{1c} range 5.7-6.4% (American Diabetes Association [3]; The International Expert Committee [4]). Currently, there are 350 million individuals affected due to diabetes worldwide, and an equal number of people are in the pre-diabetic state (International Diabetes Federation (IDF) Diabetes Atlas [5]). The worldwide spread of diabetes seems to have a complex, multifactorial origin. Obesity -another emergent epidemic- has a strong association with metabolic disorders like diabetes, hypertension and cardiovascular disease (Yoon [6]; Kahn *et al.* [7]). In general, a sedentary lifestyle (Tuomilehto *et al.* [8]; Hamilton *et al.* [9]), and over consumption of food and sugar-sweetened drinks (Hu and Malik [10]; Pereira *et al.* [11]), together with the lack of physical activity or exercise (Sigal *et al.* [12]; Colberg *et al.* [13]) are contributing to the spread of metabolic diseases. However, along with environmental factors, ethnicity - the genetic and anthropometric characteristics of a population - also play a crucial role in the development of diabetes (Harris *et al.* [14]; Abate and Chandalia [15]). If the current spread of diabetes is not controlled, the number of dia-

1

betics is expected to rise by around 55% by 2035 (International Diabetes Federation (IDF), Diabetes Atlas [5]).

Another important aspect of the diabetes management is controlling the rate of post-diabetic complications (PDCs). PDCs fall into two main categories: microvascular and macrovascular disease. Microvascular disorders comprise of retinopathy, nephropathy and neuropathy. Cardiovascular disorders (CVDs) like heart disease and stroke form a major component of macrovascular disorders. Diabetes is the leading cause of retinopathy and end-stage kidney disease, and CVDs are the leading cause of deaths among the diabetic patients (International Textbook of Diabetes, Vol. 2 [16]). The International Federation of Diabetes estimates that an average per person global health expenditure with diabetes ranges between USD 1583 to USD 2842 and an annual global expenditure on diabetes ranges between 612 billion to 1099 billion USD (Rocha *et al.* [17]). The expense on diabetes therapy contributes towards 11% of the total global health expenditure (Zhang *et al.* [18]). In fact, in the United States of America, average lifetime medical expenditure for a diabetic patient is 85,200 USD, of which 53% is on PDCs (Zhua *et al.* [19]). Though diabetes expenditure varies region wise all across the world, the management of PDCs clearly puts a huge burden on healthcare systems.

Persistent hyperglycemia is known to play a significant role in the development of PDCs (Klein [20]; Singh *et al.* [21]): the duration of diabetes and poor glucose control have been correlated with the development of PDCs (International Textbook of Diabetes, Vol. 2 [16]). Consequently, controlling glucose within certain limits remains a key focus of diabetes management. Along these lines, large-scale clinical trials have been performed to assess the impact of glucose control regimens on the rate of development of PDCs (Turnbull *et al.* [22]). The results of these clinical trials are reflected in the current position statement of the American Diabetes Association (ADA) (Inzucchi *et al.* [23]): ADA criticises a *"one-size-fits-all"* approach to diabetes therapy; stating that benefits of tight glucose control should be evaluated in the context of other risk factors like the age of an individual, duration of diabetes, comorbodities associated with diabetes, sex, and general social and health status

of an individual. Therefore, there is a great concern regarding how various phenotypic, pathophysiological and genetic factors can be factored into the personalisation of diabetes treatment [23].

A few personalised algorithms have been devleoped, using various phenotypic indicators of a diabetic patient. Notably, The Italian Association of Medical Diabetologists (Ceriello *et al.* [24]) and Finnish Current Guidelines on Diabetes (Virkamaki *et al.* [25]) suggest decision making algorithms to define person-specific antidiabetic therapy. They use phenotypic factors like the duration of diabetes, BMI of an individual, occupation of the person, age of the diabetic individual, comorbodities associated with diabetes, and side effects of antidiabetic drug treatments like hypoglycemia to recommend antidiabetic strategies. However, it is important to note that **there are no consensus algorithms available which would predict personalised glucose targets, and this is an important open area in the field of diabetes treatment.**

Glucose metabolism leads to production of reactive oxygen species (ROS) *via* the Tricarboxylic Acid Cycle (TCA) cycle. ROS production is the natural byproduct of the energy metabolism, and in fact, they often play an important role of secondary messenger molecules in various cell signalling mechanisms. The redox state of the cell is maintained by a balance between the pro-oxidant and antioxidant systems of the cell. This balance is upset in hyperglycemic state leading to an unbalanced production of ROS, which leads to oxidative stress (OS). Brownlee *et al.*, using cell lines and animal models, established that mitochondrial overproduction of ROS is a unifying causal pathophysiological feature of hyperglycemia-mediated diabetic microvascular and macrovascular complications (Brownlee [26]; Giacco and Brownlee [27]). Therefore, controlling hyperglycemia is expected to improve the OS status of the cell. However, an important question in this regard is: what is the optimal glucose control? If OS is causally implicated in the development of PDCs, it stands to reason that optimal glucose control would be one which would improve OS sufficiently such that OS is maximally controlled; and this can be expected to reduce the rate of development of PDCs. Therefore, if the OS response to changes in the glycemic state (GS) can be captured

quantitatively, then OS state of a diabetic patient can be used (a) to monitor the extent of progression of diabetes therapy, and (b) to optimise a glucose target for a patient.

In this thesis we work with data collected as a part of an interventional study conducted on newly-diagnosed Indian diabetic patients. Professor Saroj Ghaskadbi and Dr. Jhankar Acharya from Savitribai Phule Pune University shared a dataset of diabetic patients who were kept on an antidiabetic treatment for around two months (Acharya *et al.* [28]). Blood samples of the study subjects were serially collected at intervals of 0-week, 4-weeks and 8-weeks. Ten OS markers along with plasma glucose, insulin and HbA_{1c} were measured in the study subjects over the study period [28]. **We used this dataset to propose a quantitative algorithm which utilises the OS state of a diabetic patient to predict personalised glucose targets. This novel approach of predicting glucose targets based on monitoring OS along with GS is the central result of the present thesis work**.

Outline of the thesis

In **Chapter 2 we first review literature which shows that OS is a central causal locus for hyperglycemia-mediated development of PDCs.** These studies imply that controlling OS internally using antioxidant molecules might be expected to reduce the rate of PDCs. However, unexpectedly, the use of antioxidants in controlling diabetes has not turned out to be useful; in fact, the use of antioxidants is not recommended for diabetes treatment (Golbidi *et al.* [29]; Johansen *et al.* [30]; Bajaj and Khan [31]).

Since the use of antioxidants is controversial in diabetes therapy, we focus instead on a novel approach of monitoring OS as a function of changes in the GS. We use this to predict personalised glucose targets. This unique approach will be elaborated on in **Chapter 5**.

In **Chapter 3** we present an analysis of the ten OS markers serially measured in newly-diagnosed diabetic patients. In particular, we seek two characteristic features in the OS markers: (a) the marker should respond rapidly to changes in glucose over the short study period of 8-weeks, and (b) the OS marker should distinguish a diabetic state distinctly from the non-diabetic state. These two features serve two purposes: firstly, a distinction between

the diabetic and non-diabetic state indicates a strong involvement of that OS marker in the diabetics pathophysiology. Secondly, if we could quantitatively capture rapid changes in the OS marker with respect to the GS in a model, it can potentially help us define what the optimal glucose control should be. In our view, an optimal glucose control is that in which OS state is maximally controlled in order to reduce the rate of development of PDCs.

We show that glutathione metabolism: GSH_t and activity of the enzyme glutathione peroxidase show these properties. We select glutathione as an OS marker to perform a further detailed analysis for tracking diabetes progression.

In **Chapter 4** we describe an interesting result emerging out of a cluster analysis of glutathione values pooled from non-diabetic subjects and diabetic patients: **we show that glutathione can be used to classify diabetes, independently of the glucose-based classification**. That is, glutathione alone can be used to classify a person as diabetic or non-diabetic with good accuracy.

In **Chapter 5** we present a biophysically motivated minimal mathematical model to explain the following observation: OS (measured in terms of GSH_t) shows an inverse relationship with GS, as diabetes treatment progresses. The minimal model captures the rapid variation in the OS in response to changes in the GS, and does so in an individualised manner. We describe various salient features of the model and explain how predictions of the model can be used to determine glucose targets in a personalised manner in a clinical setting.

Although the physiological model in **Chapter 5** explains the inverse relationship observed between OS and GS, due to its complex functional form it may not be readily usable in a clinical setup. Besides, the glutathione-glucose physiology is made up of a more complex network of reactions than is represented in the minimal model (Reed *et al.* [32]; Raftos *et al.* [33]). We anticipate that some of the underlying assumptions of the physiological model may not be realistic and ought to be relaxed. In **Chapter 6** we therefore shift our modelling approach and propose a simple **phenomenological model** to capture OS-GS trajectories in diabetic patients. A rigorous statistical analysis is then carried out to compare the two models. We show that the phenomenological model with its simple functional form retains

the ability to predict personalised glucose targets and is suited to a clinical setup.

We close this chapter by presenting a comparison of the strengths and weaknesses of the physiological and phenomenological models.

In **Chapter 7** we focus on another aspect of glutathione metabolism in the context of recovery from the diabetes treatment. In Chapter 5 we showed that diabetic patients respond differently to antidiabetic therapies. What influences these different recovery rates of diabetic patients? It is to be expected that initial GS influences the rate of recovery from the diabetes treatment. **Surprisingly, we show that before-therapy GSH_t status also influences the recovery trajectory of a diabetic patient. The exact physiological explanation of this result remains unclear.**

In **Chapter 8** we summarise the main outcomes of the thesis work. We then elaborate on the results of our minimal model in the broader context of the development and progression of diabetes. Our minimal model specifically captures variations in the OS as a function of glucose metabolism. However, changes in the OS state have a more complex origin than represented in the minimal model. Firstly, OS is affected due to several other physiological factors like free fatty acid metabolism and inflammatory responses. These mechanisms may be contributing towards changes in the OS apart from GS. Secondly, OS not only plays a causal role in the development of PDCs but also in the development of hyperglycemia itself. Recent findings suggest that OS plays a key role in the development of insulin resistance and β-cell dysfunction, the ultimate cause of hyperglycemia. Thus, changes in the OS may feed back into the GS via modifying insulin sensitivity and secretory functions. Therefore, the OS-GS relationship would be expected to be made up of a complex network of non-linear interactions than represented in the model. Further, we realise that the interest of redox status is beyond the development of PDCs and there is scope to build complex models of diabetes progression involving OS.

The unifying theme that evolves in these chapters is how monitoring glutathione as an OS marker along with the GS marker, HbA_{1c}, might enable prediction of a personalised glucose target in diabetic patients.

Chapter 2

Problem foundations

This thesis is about utilising OS status for personalization of glucose targets in type 2 diabetes treatment. To understand motivation behind this work, we describe the evidence supporting the role of OS as a major cause of hyperglycemia-mediated diabetic complications. Defining glucose targets to control diabetic complications is a difficult task. There are two relevant components to it: On the one hand, we need to consider the physiological mechanisms which give rise to hyperglycemia. On the other hand, we need to consider various physiological mechanisms which lead to hyperglycemia-mediated diabetic complications. Current diabetes treatment to control hyperglycemia is based on the existing evidence of underlying mechanisms giving rise to hyperglycemia. Ironically, glucose targets are defined based on the association of GS with the rate of development of diabetic complications. Essentially, we need to combine these two apparently distinct arms. That is, we search for a **unifying** physiological principle which (a) influences the development of hyperglycemia, and (b) plays a key role in hyperglycemia- mediated diabetic complications.

In Section 2.2 we ask whether hyperglycemia is sufficient to cause diabetic complications. Though there is ample evidence to support this claim, there are important reasons why controlling hyperglycemia may not be adequate to reduce diabetic complications. **An important question in this respect is: are we truly targeting the cause of diabetic complications while defining glucose targets?** This sets the stage for understanding the

need of (a) personalised medicine in the diabetes treatment, and (b) incorporating markers other than glucose for defining diabetes treatment.

In Section 2.3, we dive deeper into the molecular mechanisms of hyperglycemia-mediated diabetic complications. We seek a unifying mechanism found in the various diabetic tissue damages: such a mechanism is mitochondrial overproduction of ROS, or OS. We summarise the evidence supporting a causal role of OS in the development of PDCs. In fact, OS may emerge as a unique underlying mechanism of diabetes development and progression into diabetic complications. It will serve as a model for generating hypotheses for controlling diabetes development. We shall stress that manipulating OS may be considered as an important therapeutic target for reversing hyperglycemia-mediated PDCs.

Before going into the molecular mechanisms of diabetic complications, we first begin to describe diabetes itself. In Section 2.1 we present a brief history of diabetes and then move into the current theories of the development of diabetes, which will set the stage for discussing the need of personalised glucose targets.

2.1   Diabetes: the problem of impaired glucose homoeostasis

The symptomatic evidence of diabetes can be found in ancient literature as early as from 1500 BC. For example, an Egyptian manuscript documents - "too great emptying of the urine" - probably referring to a diabetic condition, and Indian literature describing "ants getting attracted to a patient's urine" - indicative of the presence of sugar in the urine (Principles of Diabetes Mellitus [34]). Although there were intermittent records of diabetic cases till 18th century, no curative measures were available, because the pathophysiology of diabetes was unclear.

The causal mechanisms underlying diabetes started to emerge only in the 19th century. The credit of discovering the role of pancreas in the pathogenesis of diabetes is given to Joseph von Mering and Oskar Minkowski [35]. In 1889, they performed pancreatectomy in dogs. They showed that dogs developed symptoms of diabetes and died shortly afterwards. This suggested that the deficiency of a chemical from pancreas is responsible for diabetes.

However, it took almost three decades to discover that chemical substance, today known as insulin. The milestone discovery of insulin changed the lives of diabetic patients, for which the credit of discovery goes to Frederick Banting and Charles Best: In 1921, they took a step ahead of Mering and Minkowski's experiment. They injected pancreatic extract from a healthy dog to a diabetic dog and showed a reversal of diabetic symptoms [36]. Further, they discovered the chemical from the pancreatic extract - insulin - for which they got Noble Prize in 1923. Insulin is, therefore, the first effective documented treatment for treating diabetic patients.

However, at this point, it was thought that the lack of insulin is the prime reason for developing diabetes. Later, in 1939, Himsworth proposed that insulin deficiency may not be the only cause for the development of diabetes, but resistance to insulin action may be another reason. He coined the term "insulin insensitivity" for this phenomenon [37]. Insulin insensitivity or resistance can be termed as inability of insulin responsive tissues to uptake glucose, despite presence of insulin in the blood. However, this idea gained support after development of radioimmunoassays to measure plasma insulin (Yalow and Berson [38]) and insulin resistance measures like "glucose-clamp method" in late 60's and 70's (Shen *et al.* [39]; DeFronzo *et al.* [40]). Later, clinical trials showed that most of the diabetic individuals studied were in fact "insulin insensitive" (Ginsberg *et al.* [41]; Reaven [42]). Further, it was showed that insulin resistance could play a predictive role in the development of diabetes (Warram *et al.* [43]; Lillioja *et al.* [44]).

The point of describing historical events is to understand how it has shaped our understanding of the pathophysiology of diabetes. This is also reflected in the way diabetes treatments are developed. Therefore, it is worth taking a brief account of theories of the development of diabetes.

2.1.1 Theories of development of hyperglycemia

The narrow range of fasting normoglycemia (80-100mg/dL) is maintained by the net effect of mechanisms by which glucose enters into the blood circulation and is removed from it.

Food is the main source of the plasma glucose. Elevated plasma glucose levels, after a meal, induce insulin secretion form the pancreas. There are three primary tissues which have insulin-dependent glucose uptake, namely, liver, fat, and skeletal muscle. Insulin binds to receptors to cells in these tissues to facilitate glucose uptake. Another function of insulin is to inhibit gluconeogenesis - the conversion of glycogen into glucose - in the liver. Thus, insulin plays an important role in the effective absorption of the plasma glucose and bringing it back to the normoglycemic range. This process usually takes place within two hours. Following absorption of glucose, insulin secretion is lowered, leading to activation of gluconeogenesis in the liver. The activation of gluconeogenesis helps maintain blood glucose in the fasting range; providing a constant supply of glucose to the brain. Maintenance of glucose homoeostasis is a complex process involving other hormones like glucagon, and organs such as kidneys. Glucose homoeostasis is based upon the interplay of three essential factors: (a) insulin sensitivity: the efficiency of glucose uptake in insulin-dependent tissues in response to secretion of insulin, (b) β-cells' capacity to secrete insulin in response to elevated blood glucose levels and (c) liver gluconeogenesis which plays a crucial role in maintaining fasting plasma glucose levels. Therefore, independent or combined defects in any of these three processes leads to hampered glucose homoeostasis.

The pathophysiological routes which give rise to hyperglycemia have been studied for a long time. For instance, different disease models exist to understand the complex origin of elevated blood glucose levels. Two theories are center-stage in understanding the mechanistic origin of elevated glucose levels in diabetic patients. These (theories) are based on the interplay between the two pathological features of diabetes, namely, insulin resistance and impaired insulin secretion from the β-cells of pancreas.

Of the three insulin-dependent tissues, muscles are the major site of glucose disposal (responsible for nearly 70% of the total glucose disposal). Insulin resistance can be thought of as the inability to take up glucose or process insulin signal despite the presence of insulin in the blood. According to **the classical theory of type 2 diabetes**, insulin resistance develops many years before frank hyperglycemia is observed (DeFronzo [45]). Insulin resistance has

multiple origins. Nutrient overload (free fatty acid metabolism) is considered as one of the important drivers of insulin resistance, along with the inflammatory responses and gut microbial changes (Johanson *et al.* [46]). Cellular and animal models have confirmed that multiple stimuli can potentially induce insulin resistance in these tissues. Inter-dependence of these tissues in maintaining glucose homoeostasis makes insulin resistance a complex phenomenon, and tracing the original cause seems almost difficult.

The mechanistic origin of insulin resistance-driven hyperglycemia is depicted in the Figure 2.1. Insulin resistance leads to transient hyperglycemia, which in turn leads to compensatory hyperinsulin secretion from pancreatic β-cells. Transient hyperinsulinemia, also in principle can induce insulin resistance in insulin responsive tissues. If insulin resistance persists for a longer time, eventually β-cell's secretory capacity gets exhausted, and insulin secretion is not enough to control glucose in non-diabetic glycemic limits. In fact, beyond a point, insulin secretion drops, and the person develops diabetes.
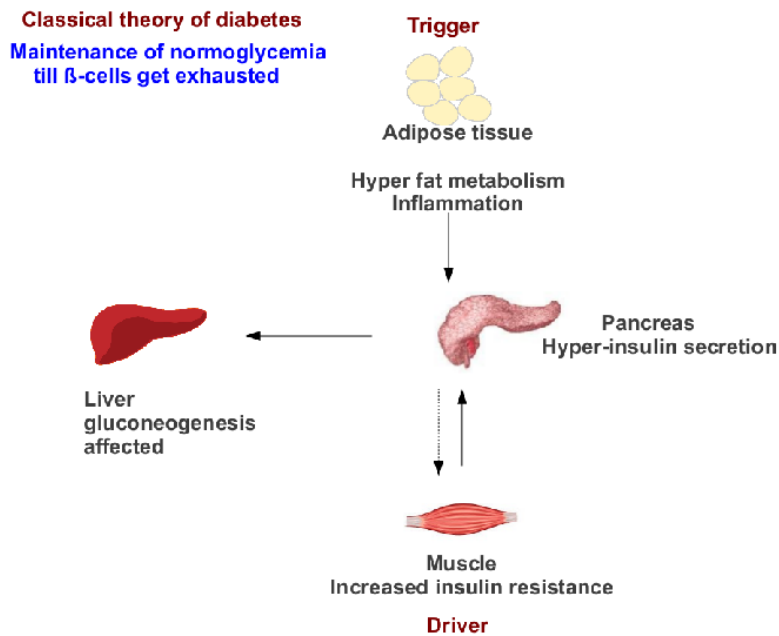
Figure 2.1: Insulin resistance as a driver of development of hyperglycemia. According to the classical theory of diabetes, insulin resistance leads to compensatory hyperinsulin secretion from the pancreas. If insulin resistance persists for a longer time, eventually insulin secretory capacity of the pancreas is exhausted leading to hyperglycemia.

Therefore, the onset of type 2 diabetes is mainly characterised by three hallmark features: (a) Hyperglycemia - excess glucose in the blood plasma and urine (b) Insulin resistance - reduced glucose uptake rate despite presence of insulin in the plasma, and (c) almost 50% reduction in the insulin-secreting β-cell mass in the pancreas. It is important to stress that in the classical theory of type 2 diabetes, insulin resistance is the main driver of diabetes progression, however, until β-cell's capacity to control glucose homoeostasis is not exhausted, frank hyperglycemia does not ensue (DeFronzo and Tripathy [47]).

An alternative theory of the development of type 2 diabetes puts hyperinsulin secretion as the sufficient cause of development of hyperglycemia (Corkey [48]). Corkey hypothesise that there are multiple food components which have entered in the human food chain in the recent times, which can potentially trigger hyperinsulin secretion from the pancreas, without first inducing insulin resistance [49]. This hyperinsulin secretion can cause insulin resistance and further development of hyperglycemia (see Figure 2.2).
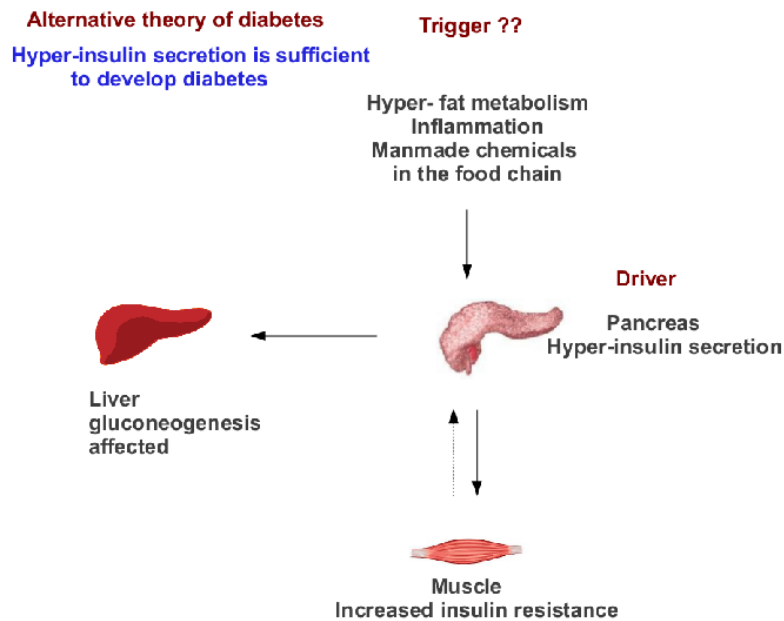
Figure 2.2: Hyperinsulin secretion as a driver of development of hyperglycemia. According to the alternative theory of diabetes, hyperinsulin secretion is sufficient to drive development of hyperglycemia. Hyperinsulin secretion can potentially lead to the development of insulin resistance which can drive development of hyperglycemia.

Both the classical and alternative theories provide disease models for the development of hyperglycemia. At the onset of diabetes, both the defects: insulin resistance as well as β-cell dysfunction, co-exist. However, whether insulin resistance arises first or the major defect is hyperinsulin secretion, in development of hyperglycemia, is an unresolved puzzle. In fact, the relative contribution of the each of the defects is difficult to measure. The development of theories of diabetes is an ongoing research and more complicated diabetes models involving other organs like brain, kidney and adipose tissue may evolve in near future (DeFronzo [50]).

2.2 Hyperglycemia: are we treating the cause of diabetic complications?

It is important to step back and retrospect about how these theories have shaped our view of diabetes diagnosis and treatment. Both theories do not contribute towards identifying a marker apart from glucose to monitor diabetes progression. Even after more than 100 years of discovery of insulin, our classification of diabetes is restricted to glucose ranges (and recently, to HbA_{1c} ranges). Intriguingly, this glucose-based classification may not reflect underlying pathophysiological changes. The current diabetic treatments are designed to reduce insulin resistance, improve insulin secretion or to reduce the rate of gluconeogenesis from the liver. Although we have the models describing the pathophysiology of diabetes, the quantitative contribution from each of these factors in the pathophysiology can not be deciphered. Recently, several other factors like free fatty acid metabolism, inflammation, gut microbial changes have known to be involved in the development of insulin resistance (Johanson *et al.* [46]). While blood glucose is the only accepted feature to define diabetes, these abnormalities may contribute towards the development of diabetic complications. Therefore, while developing the diabetes therapies to reduce diabetic complications, can we be sure that we are targeting the actual cause of diabetic complications?

Hyperglycemia is considered as an initiating cause of diabetic complications. The hyperglycemic state has been associated with diabetic complications in type 1 and type 2 diabetes.

The relationship between poor glucose control and duration of hyperglycemia has long been known to be associated with the degree of complications. The interventional therapies to reduce blood glucose, such as insulin or drugs like metformin, are known to reduce diabetic complication via a reduction in the blood plasma glucose levels. Consequently, tight glucose control regimens were expected to reduce the rate of diabetic complications. However, contrary to this expectation, tight glucose control may not always account for regulation of diabetic complications. What follows next is an account of clinical trials assessing the impact of tight glucose control on the development of diabetic complications.

2.2.1   Aggressive glucose control: findings from the clinical trials

Persistent hyperglycemia influences the development of post-diabetic microvascular (e.g. nephropathy, retinopathy) and macrovascular disorders (especially cardiovascular disorders (CVDs) like myocardial infarction and a fatal or non-fatal stroke). Accordingly, controlling hyperglycemia within a certain limit remains a major concern in the diabetes treatment. Large clinical trials have been conducted in the past decades to define the glucose control regimen for diabetes control. Notably, these clinical trials evaluated the effects of strict versus standard glucose control on the development of microvascular disorders and CVDs. Of these clinical trials, Action to Control Cardiovascular Risk in Diabetes (ACCORD trial [51], n=10,251) and Action in Diabetes and Vascular Disease: Preterax and Diamicron Modified Release Controlled Evaluation (ADVANCE trial [52], n=11,140) were performed on type 2 diabetic patients having one or more micro- or macrovascular events. A strict glucose target employed was reducing HbA_{1c} well below 6% (ACCORD trial [51]) or 6.5% (ADVANCE trial [52]) against the standard glucose reduction criteria of HbA_{1c} range of 7-7.5% or <6.5%., respectively. Another mega clinical trial performed on newly-diagnosed type 2 diabetics in the UK Prospective Diabetes Study (UKPDS [53], n=5,102) compared the effects of a strict glucose regimen of 6 mmol/L as against the standard glucose regimen of 15 mmol/L. On an average, trials were carried out for 4-5 years duration, and more than a thousand patients participated in the each clinical study. Impact of intensive versus standard glucose con-

trol was compared with the proper definition of clinical end-points as micro/macrovascular events.

A meta-analysis conducted on these clinical trials showed that aggressive glucose control helped reduce microvascular events especially retinopathy, but did not lessen the rate of cardiovascular disorders. Aggressively controlled glucose did not reduce the death events caused due to CVD or in overall mortality compared to the standard therapy (Turnbull *et al.* [22]). In fact, intensive glucose control did not affect major macrovascular outcomes in newly-diagnosed diabetics as well. In a different study, Neugebauer *et al.* conducted a clinical trial of 58000 diabetic patients: they divided the cohort into four distinct regimens of HbA_{1c} reduction, ranging from $<7\%$ to $<8.5\%$. They demonstrated that the intensive glucose control, although reduced rate of nephropathies, did not show any beneficial effect on myocardial infarction events over a period of four years [54]. Nonetheless, a couple of other clinical trials showed that an aggressive glucose control in early stages of diabetes, having reduced CVD risk factors, turn out to be beneficial at least during the short study period of 4-5 years (Dailey *et al.* [55]; Chokrungvaranon *et al.* [56]). In almost all the clinical trials, aggressive glucose control enhanced the hypoglycemic events (Turnbull *et al.* [22]). In conclusion, aggressive glucose control may be helpful in the early stage of diabetes to control microvascular disorders but may not reduce the rate of development of CVDs, especially in elderly diabetic patients. Since post-diabetic complications are essentially influenced by multiple factors like duration of diabetes, age of an individual and other risks factors like lipid metabolism, drug-mediated glucose control alone may not be sufficient to turn down the progression of diabetes. Consequently, ADA diabetes guidelines published in 2015 based upon the clinical trials, recommended designing *personalised glucose targets*, taking into account various factors that contribute towards the development of post-diabetic disorders (Inzuchi *et al.*, [57]). In other words, a *one-size-fits-all* strategy of diabetes control is to be abandoned in favour of tailor-made antidiabetic treatment. Also, physiological parameters other than glucose are required to be utilised to define treatment regimen.

Persistent hyperglycemia is known to be the initiating cause of the PDCs, therefore,

glucose control undoubtedly remains as the prime therapy of diabetes management. However, current diabetes treatment has not furnished acceptable glucose targets to prevent onset of the diabetic complications. Therefore, it is important to ask what other molecular players, other than glucose, determine recovery from diabetes. This is also relevant in the context of current diabetic treatments which show interpatient variation in the response to diabetes therapy. In other words, diabetes treatment needs to be *personalised*. Clearly, the pathophysiology of diabetes is too complex to be defined only by GS. Therefore, we need to incorporate other underlying physiological factors while defining individualised glucose targets. To understand which variables (apart from glucose) can be monitored to refine glucose targets, we need to look deeper into the pathophysiology of the development of PDCs.

2.3 OS: a central causal link in the hyperglycemia mediated diabetic complications

Vascular tissues are vulnerable to accumulation of excessive glucose inside the cell. In fact, vascular tissues are not equipped with regulatory mechanisms for dealing with hyperglycemic levels and are therefore prone to damage. There are three main types of diabetic complications : cardiomyopathies, diseases of the microvasculature (retinopathy, nephropathy and neuropathy) and the macrovasculature (cardiovascular disorders for example heart attack and stroke). Four major pathways are known to be activated in the diabetic tissue damage, namely: (1) Polyol pathway (2) Hexosamine pathway (3) Protein kinase C (PKC) pathway, and (4) Advanced glycation end (AGE) products formation. We take a brief account of each of them separately, although they may be activated simultaneously in different vascular tissues.

2.3.1 Increased flux through the polyol pathway

The polyol pathway is known to be activated in the diabetic retinopathy, nephropathy and neuropathy. It is one of the first pathways discovered in the hyperglycemia-mediated diabetic

complications and has been under investigation for almost forty years now.

The polyol pathway is a two-step pathway used for converting excessive glucose into fructose with sorbitol as an intermediate as described in the figure (see Figure 2.3 (A)). Accumulation of the excess glucose inside the cell activates polyol pathway. In the first step, aldose reductase (AR) utilises the reducing equivalent NADPH to convert excessive glucose into sorbitol. In the second step, sorbitol dehydrogenase (SDH) utilises sorbitol to produce fructose and NADH. Activation of polyol pathway leads to diabetic tissue damage in at least three ways: (1) activation of polyol pathway leads to a reduction of NADPH/NADP ratio which is otherwise required for replenishing reduced form of the glutathione, an important redox buffer of the cell (2) A gradual build up of sorbitol and its intermediate biochemical products leads to osmotic imbalance and impairment of Na+/K+ ion channels (Gallgher EJ *et al.* [58]) (3) Fructose gets further converted into fructose-3-phosphate and 3-deoxyglucosone, which are potent glycosylating agents leading to deposition of advanced glycation end products (Chung *et al.* [59]; Tang S *et al.* [60]).

Interventional studies have been performed in animal models and in humans to define the causal role of AR in the the development of PDCs. Overexpression of AR with SDH deficiency in the transgenic mouse model lead to enhanced OS in the liver tissues. In the same mouse model, use of AR inhibitor, epalrestat, showed a reduction in the OS and decreased albuminuria in the urine (Li *et al.* [61]). In a small observational study, Bravi *et al.* [62] showed that intervention with AR inhibitor tolrestat improved erythrocytic NADPH/NADP ratio and GSH concentrations in diabetic patients. A recent meta-analysis performed on the use of AR inhibitors in human clinical trials showed reduction in the diabetic neuropathy (Hu *et al.* [10]; Hotta *et al.* [63]). Undoubtedly, AR inhibitors are the promise for control of diabetic complications, though newer drugs are under investigation.

2.3.2 Increased flux through hexosamine pathway

The fourth pathway found to be activated in the hyperglycemia-mediated diabetic tissue damage is the hexosamine pathway (see Figure 2.3(B)). 2-5% of the total glucose pool gets

diverted into hexosamine pathway in the hyperglycemic conditions (Schleicher and Weigert [64]). The key rate-limiting enzyme of the pathway is glutamine:fructose-6-phosphate amidotransferase (GFAT). GFAT adds an amino group to fructose-6-phosphate producing glucosamine. The end product of the pathway is UDP-N-acetylglucosamine (UDP-GlcNAc).

Activation of hexosamine pathway in hyperglycemic conditions leads to activation of O-glycosylation of transcription factor Sp1 (Du *et al.* [65]). Covalent modification of Sp1 causes overexpression of transforming growth factor-β1 (a cytokine) and plasminogen activator inhibitor-1 (a serine protease inhibitor), which are found to be activated in vascular disorders in diabetes, particularly diabetic nephropathy (Sharma and Ziyadeh [66]; Schleicher and Weigert [64]). The hexosamine pathway also activates NF-kβ in mesangial cells (James *et al.* [67]). Overall, activation of the hexosamine pathway leads to initiation of pro-inflammatory response and modulation of cellular matrix physiology and signalling. In fact, hexosamine pathway has been proposed to play a role in the development of insulin resistance (Buse [68]) and impaired β-cell function (Kaneto *et al.* [69]).

2.3.3   Activation of protein kinase C (PKC) pathway

Hyperglycemia leads to the formation of a metabolic intermediate diacylglycerol (DAG) (Geraldes and King [70]). DAG is known to activate PKC isoforms (mostly β isoforms) in vascular tissues (see Figure 2.3(C)), specially in retinopathy (Shiba *et al.* [71]), neuropathy (Xia *et al.* [72]), nephropathy (Craven *et al.* [73]) and cardiovascular structural deformities (Inoguchi *et al.* [74]; Lee *et al.* [75]; Taher *et al.* [76]).

Increased PKC activation in these tissues have been associated with changes in blood flow, vasodialation, basement membrane thickening, extracellular matrix expansion, abnormal angiogenesis, and excessive apoptosis. PKC activation also leads to changes in enzymatic activity alterations such as MAP kinase, PI3Kinase and Na(+)-K(+)-ATPase (Evcimen and King [77]). In cardiomyocytes, PKC-β activation leads to hampered cardiac function and modulation via impaired Akt-dependent-nitric oxide synthesis (eNOS) (Lei *et al* [78]).

Numerous studies have been performed in diabetic rat and mice models to assess the

efficacy of PKC inhibitors or deletion of PKC gene or overexpression of PKC genes on the development of diabetic vascular complications (Geraldas and King [70]). These studies not only established the role of PKC isoforms in the development of diabetic vascular disorders but also paved a new way of using PKC inhibitors for the treatment of diabetic complications (Durpes *et al* [79]). For example, PKC inhibitors like LY333531 have been useful in improving retinopathy, nephropathy, neuropathy and neuronal dysfunction. (Geraldas and King [70]).

The use of PKC inhibitor, in the clinical trials has been reviewed in detail by Geraldas and King [70] and Idris and Donneley [80]. For example, ruboxistaurin, a PKC-β isoform selective inhibitor, improves renal glomerular filtration rate, endothelial dysfunction and prevents loss of visual acuity (Idris and Donnelly *et al* [80]) and neurological dysfunction (Bansal *et al* [81]) in diabetic patients. The use of Ruboxistaurin for the treatment of diabetic complications is currently under investigation, and PKC inhibitors present a great promise for improvement of debilitating diabetic complications.

2.3.4 Intracellular production of advanced glycation end products

AGEs are nonenzymatically glycated intermediates of proteins, lipids and nucleic acids, produced due to persistent hyperglycemic and oxidative environment inside the cell (see Figure 2.3(D)). Apart from hyperglycemia, smoking and dietary AGEs also contribute towards the pool of AGEs (Brownlee [75]; Goldin *et al.* [82]; Goh and Cooper [83]). AGE formation is a key pathological cause of diabetic vasculature disorders of eyes (Stitt [84]; Milne and Brownstein [85]), kidneys (Forbes *et al.* [86]), nerves (Sugimoto *et al.* [87]), and cardiovascular disease (Meerwaldt *et al.* [88]).

Accumulated AGEs affect physiology by at least three well-known mechanisms. First, AGEs interact with receptors for AGE (RAGE) on the cells. AGE-RAGE interaction leads to enhanced production of OS and activation of nuclear factor NF-k β, which is responsible for modulation of gene expression and activation of pro-inflammatory cytokines like IL-1, IL-6 and tumour necrosis factor-α (TNF-α) (Nessar [89]; Neumann *et al.* [90]; Ramasamy *et al.* [91]). Secondly, AGEs induce cross-linking of proteins like collagen thereby altering

vascular structure (Goh and Cooper [83]). Thirdly, accumulation of AGEs over the time is known to affect renal function. This is mainly due to accumulation and inefficient clearance of AGEs from the kidneys, which further develops into kidney malfunctioning.

Pre-clinical interventional trials using AGE inhibitors (like Aminoguanidine) either for preventing the formation of AGEs or for the removal of AGEs have shown promise in reducing the developments of retinopathies, nephropathies and neuropathies (Goldin *et al.* [82]). A detailed review of animal models and clinical trials performed using AGE inhibitors is due to Goh and Cooper [83], Singh *et al.* [21]. In summary, AGE inhibitors do show promise in small clinical trials, but their long term toxic effects are unclear. Long-term clinical investigations and search for new AGE inhibitors is an ongoing quest to reduce diabetic complications.

2.3.5 Mitochondrial overproduction of ROS: a unifying mechanism of hyperglycemia - mediated diabetic complications

All the above mentioned pathways are known to be activated in diabetic tissue damage. However, is there a common upstream event that regulates all these distinct mechanisms of diabetes tissue damage? Brownlee *et al.* [26] sought to answer this question mainly for two reasons: first, they observed that using inhibitor for one pathway did not suppress the effect of the other. Secondly, clinical trials using combination of inhibitors of these pathways were unsuccessful. This suggested that there might be an upstream missing link which is still mediating its effect (Brownlee [26]). Although the association between OS and hyperglycemia was known for a long time, the exact molecular mechanism linking the two processes was lacking. Brownlee and colleagues found that a common feature of different cell types undergoing diabetic tissue damage is elevated mitochondrial ROS production (Nishikawa *et al.* [92]). They established the causal mechanism of mitochondrial overproduction of ROS in the activation of diabetic tissue damage pathways in three different ways. To begin with, they overexpressed the enzyme manganese superoxide dismutase (MnSOD) in the endothelial cells exposed to hyperglycemia. They showed that the ROS levels were significantly lowered in these cells compared to the control. In another experiment, they
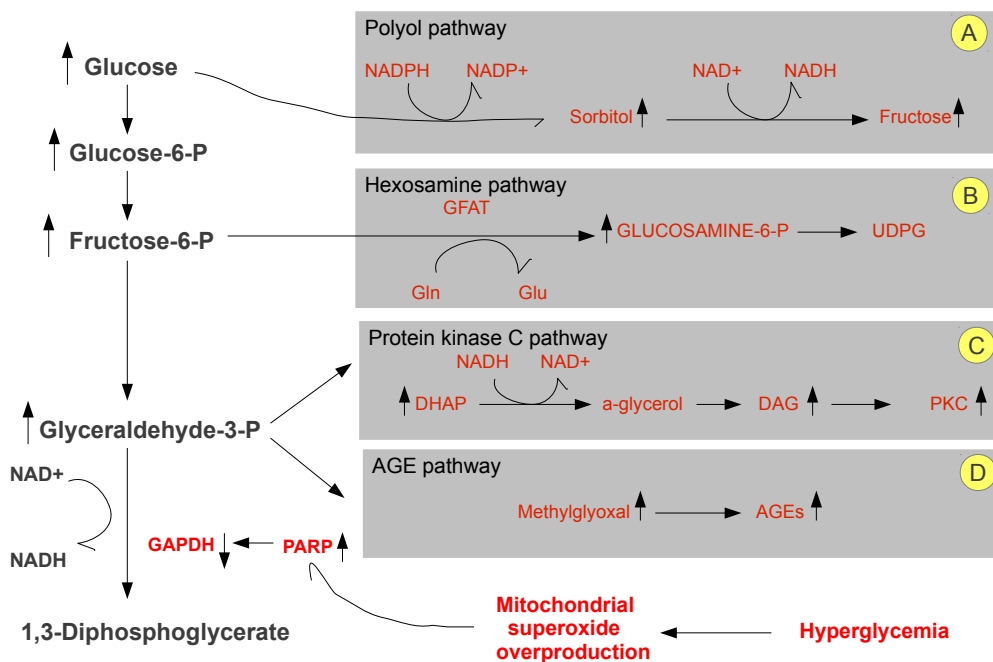
Figure 2.3: Mitochondrial overproduction of ROS is a unifying mechanism in hyperglycemia-mediated diabetic complications. Four main pathways of diabetic tissue damage are: (A) increased flux through the polyol pathway, (B) activation of the hexosamine pathway, (C) activation of the protein kinase C (PKC) pathway, and (D) accumulation of advanced glycation end (AGEs) products. Mitochondrial superoxide overproduction inhibits the activity of the enzyme GAPDH (glyceraldehyde 3-phosphate dehydrogenase). This leads to the accumulation of glycolysis intermediates, which activates the four pathways in the diabetic complications.

generated a mutant endothelial cell line with the deletion of mitochondrial DNA. In these mutant cells, hyperglycemia completely failed to activate the four pathways involved in the hyperglycemic diabetic complications. They confirmed their findings in the diabetic mice models overexpressing MnSOD. They found that in these mice models activation of the four pathways was considerably reduced. These experimental results clearly demonstrated the causal role of mitochondrial ROS production in the activation of pathways involved in the diabetic complication.

Further molecular mechanisms were studied linking the mitochondrial ROS production

and development of diabetic complications in cell lines and animal models (Brownlee [26]). Figure 2.3 represents the overview of the molecular mechanisms implicated in the development of diabetic complications. Brownlee and coworkers showed that mitochondrial ROS leads to single-strand breaks in the DNA. This activates poly(ADP-ribose) polymerase (PARP) which makes polymers of ADP-ribose. Activated PARP leads to deactivation of glyceraldehyde 3-phosphate dehydrogenase (GAPDH), an enzyme in the glycolysis pathway. Reduced activity of GAPDH leads to accumulation of intermediate products of the glycolysis and activates all four major pathways of diabetes complications, namely, polyol pathway, hexosamine pathway, PKC, and AGE pathway.

In this chapter, we reviewed literature to establish the causal role of imbalanced production of ROS or OS in the development of hyperglycemia-mediated diabetic complications. We also evaluated literature on the current glycemic goals suggesting the need for personalisation of diabetes treatment. **The rest of the thesis describes evolution of an idea about how OS can be utilised in predicting the personalised glucose targets.** We hope that the concepts described in this chapter would be helpful in understanding the reasoning behind our personalisation algorithm to follow.

Chapter 3

Population study design and preliminary data analysis

3.1 Introduction

The redox homeostasis or optimal ROS level inside the cell is regulated by the balance between pro-oxidant and antioxidant mechanisms. In diabetes this balance can not be sustained, leading to excessive accumulation of ROS and enhanced OS (Halliwell [93]). As described in Chapter 2 (see Section 2.3), OS markers hold crucial information regarding the progression of diabetes due to their central position in hyperglycemia-mediated development of PDCs. On the one hand, changes in the GS may be directly reflected in changes in the OS. On the other hand, OS is causally involved in the pathophysiology of PDCs. The causal role of OS in the development of PDCs implicates it in defining what should the optimal glucose control be. An optimal glucose control would be that which would minimise OS sufficiently such that this would augment antioxidant status of the cell and further reduce the rate of development of PDCs. In order to achieve this (that is defining optimal glucose targets), first, we need to ask: which OS marker can be utilised **to track the progression of diabetes?**

OS markers broadly fall into two categories: (a) molecules involved in the antioxidant

defence of the cell (e.g. glutathione, vitamin E, C and enzymes like superoxide dismutase, catalase, glutathione reductase), and (b) cell molecules which show oxidative damage (e.g. markers of DNA, protein and lipid damage). Hyperglycemia is known to be associated with elevated levels of lipid peroxidation marker like thiobarbituric acid (TBARS) (Augustin *et al.* [94]) and secondary end-products of lipid peroxidation like 8-epi-prostaglandin F2 (8-epi-PGF2α) isoprostane (Sampson *et al.* [95]). 8-epi-PGF2α is considered as a direct, sensitive biomarker of membrane lipid-peroxidation (Kaviarasan *et al.* [96]). The diabetic state is associated with lowered antioxidant defence state molecules like vitamin C (Iino *et al.* [97]), vitamin E (Lonn *et al.* [98]) and glutathione (Lagman *et al.* [99]). Enzymes involved in the OS regulation are also used to measure OS state. There are a plethora of studies which have looked at activities of enzymes like superoxide dismutase (SOD), catalase, glutathione peroxidase and glutathione reductase in the diabetic state (Akkus *et al.* [100]; Bhatia *et al.* [101]; Song *et al.* [102]).

A point worth noting is that although the literature is replete with studies showing association of different OS markers with the diabetic state, no OS marker has been established to classify diabetes. One important aspect is that we lack population studies which monitor longitudinal changes in the OS state of a diabetic patient, which could in principle be used to classify diabetes using OS.

The present thesis work is based on an interventional trial performed on newly-diagnosed Indian type 2 diabetes patients. Prof Saroj Ghaskadbi from Savitribai Phule Pune University shared this dataset with us. An interesting feature of this study is that patients were kept on antidiabetic treatment for about two months and ten OS markers were **longitudinally** measured at the intervals of 0-week, 4-weeks and 8-weeks. The details of the study design and blood sample collection are provided in Section 3.2.

In this chapter, our objective is to identify which OS marker can be used to monitor diabetes progression. The longitudinal aspect of the study design would help us decipher (a) how rapidly a given OS marker varies in response to changes in the GS over the short study period of 8 weeks, and (b) whether changes in an OS marker delineate a diabetic state from

the non-diabetic state. These two features give insight about which OS marker is suitable for monitoring diabetes progression. We first summarise data analysis carried on different OS variables serially measured in newly-diagnosed Indian diabetic patients at the intervals of 0, 4, and 8 weeks. Specifically, we studied trends in the OS variables in response to GS. We observed that markers of glutathione metabolism respond rapidly to the antidiabetic treatment compared to other OS variables.

3.2 Population study design and sample collection

3.2.1 Subject information

The clinical trial was performed on newly-diagnosed type 2 diabetic patients (n=54) attending the Diabetes Unit, KEM Hospital, Pune for the period of 2 months. Two criteria were used to define the diabetic status of an individual, namely, (a) fasting blood glucose >6.9 mmol/L and (b) glycated haemoglobin (HbA_{1c}) >6.5% (47.5 mmol/mol). The non-diabetic control group (n=50) was comprised of individuals from academic institutions in Pune. Non-diabetic status was defined by (a) fasting blood glucose <6.9 mmol/L and (b) HbA_{1c} <6.5% (47.5 mmol/mol). The anthropomorphic details of the study subjects (age, BMI and gender) are provided in the Appendix Section 5.1. The population study followed a longitudinal interventional design in which diabetic subjects were kept on the antidiabetic drug treatment for about two months and their fasting blood samples were collected at the interval of 0, 4 and 8 weeks. Similarly, fasting blood samples of non-diabetic subjects were also collected and processed for further biochemical measurements. The details of the drug treatment are provided in the Appendix Section 5.2. Diabetic patients were instructed on physical exercises and diet and advised to avoid the use of oral antioxidants and multi-vitamin supplements. Subjects with/having (a) a recent cardiovascular event and heart disease (b) clinical infection and inflammation (c) excessive alcohol intake (d) chronic smoking habit (e) malignant disease and pregnant women were removed from the study protocol. Finally, written consents were taken from all the study subjects and study design was approved by the Institutional

Ethical Committee, KEM Hospital and Research Centre, Pune.

3.2.2 Sample preparation

Fasting blood samples were used for the measurements of biochemical components. The details of the biochemical measurements of remaining physiological markers are provided in Acharya *et al.* [28]. We briefly discuss biochemical assays used to measure blood components. Plasma was separated by spinning down the sample volume at 4000 rpm for 10 minutes. Further, buffy coat was removed, and blood erythrocytes (RBCs) were washed thrice with cold saline. A 50% hemolysate was prepared by adding ice-cold ultrapure water to the RBCs (MilliQ plus reagent grade; Millipore, Bedford, MA) and stored at -80. HbA1c levels were measured using was measured by using an HPLC cation exchange column on D10 HbA1c analyser (Bio-Rad Laboratories, Hercules, CA). GOD-PAP (glucose oxidase Peroxidase) method was used to measure plasma glucose concentrations using auto-analyzer (Hitachi 902, Japan). Total free glutathione, GSH_t (reduced (GSH) and oxidised (GSSG) forms of glutathione) was measured according to the method of Akerboom and Sies [103]. Plasma insulin levels were measured using ELISA-based insulin measurement kits obtained from Mercodia (Uppsala, Sweden).

3.3 Statistical methods

3.3.1 Percent relative measures of changes in the mean and standard deviation of diabetic stress variables with respect to the non-diabetic group

To compare the mean (standard deviation (sd)) values over the diabetic population relative to the mean (standard deviation) of the corresponding non-diabetic group, we computed a percent relative mean (sd) difference given by the formula(s):

$$\text{Percent relative mean difference} = \frac{\text{mean(Diabetic group) - mean(Non-diabetic group)}}{\text{mean(Non-diabetic group)}} \times 100$$

$$\text{Percent relative sd difference} = \frac{\text{sd(Diabetic group)- sd(Non-diabetic group}}{\text{sd(Non-diabetic group)}} \times 100$$

Positive (negative) percent relative values indicate difference is higher (lower) with respect to non-diabetic group.

3.3.2 Bootstrap estimates of confidence interval (CI) for reporting sample mean values to account for small study size

To obtain confidence in stating mean and standard error around the mean value, we bootstrapped over the non-diabetic and diabetic values obtained for each of the physiological markers measured during the study period. Ten thousand datasets were simulated by sampling with replacement from the values measured for each physiological marker for each of the 3 visits. For each simulated dataset, a mean value was calculated. This procedure generated distribution of 10000 simulated sample means. This distribution of simulated sample means was used to obtain mean and standard error around the mean for a given physiological marker. This standard error was used to obtain normal and percentile-based CI around the mean considering 95% confidence level. These CIs were reported along with the sample mean±se values. We also compared the CI for the difference of means between the two groups to be compared using the bootstrap algorithm. In almost all the cases where comparisons were made, they match up with the CI obtained from Student's t-test. So we have reported CI from the Student's t-test along with the *p-values* obtained using confidence level, $\alpha = 0.05$. All the calculations were performed using statistical software package R (version 2.14.1).

3.4 Results

3.4.1 Preliminary analysis of OS markers revealed rapid recovery in the markers of glutathione metabolism

Acharya *et al.* previously studied serial changes in the OS biomarkers in newly diagnosed diabetic patients [28]. In all, seventeen physiological markers were studied in response to variations in the glycemic load over the period of 2 months. These biomarkers were roughly divided into following categories: (1) OS defence markers: glutathione, glutathione reductase, glutathione peroxidase, superoxide dismutase, catalase, bilirubin and uric acid. (2) Lipid profile markers: cholesterol, triglycerides and high density lipoproteins (3) Cell damage markers: protein carbonyls, protein sulfhydryls and TBARs (4) Kidney and liver function markers: creatinine, glomerular filtration rate, alanine aminotransferase (ALTKE) and aspartate aminotransferase (ASTKE). Among the above mentioned markers, OS defence markers and cell damage markers are the ten OS biomarkers studied. Plasma glucose, insulin and glycosylated haemoglobin (HbA_{1c}) were measured along with the mentioned biomarkers, at the intervals of 0 week (visit 1), 4 weeks (visit 2) and 8 weeks (visit 3). The measurement units for all the biomarkers are provided in the Appendix Section 3.2.

To quantitatively compare changes in stress variables in the diabetic state with respect to the non-diabetic state, percent relative mean and standard deviation difference were calculated for all stress variables (see Statistical Section 3.3.1). Table 3.1 gives an account of percent relative mean and standard deviation difference for all of the stress variables studied. As mentioned earlier, relative mean values indicate changes between the first and third visits in diabetic patients when glucose levels were therapeutically controlled. Further, scatter-histograms were used to reveal trend between glucose and stress variables, across three visits.

Among the OS defence markers, glutathione, glutathione reductase, glutathione peroxidase, superoxide dismutase and catalase showed a low relative mean value compared to corresponding non-diabetic values in the first visit (Table 3.1). By the third visit, relative

mean differences were found to increase, indicating a shift towards the physiologically healthy ranges (as expressed by the non-diabetic group). On the contrary, bilirubin and uric acid levels were higher in the first visit and lowered by the third visit.

Increased levels of protein carbonyls and decreased levels of protein sulfhydryls represent protein damage inside the cell due to OS. Table 3.1 shows high (low) relative mean difference value for protein carbonyls and TBARs (protein sulfhydryls) in the first visit indicating OS damage. By the third visit, relative mean difference value for protein carbonyls and TBARs was well below half the relative mean difference value in the first visit. This indicates a strong sensitivity of protein carbonyls and TBARs to the glucose control in the diabetic group. However, proteins sulfhydryls did not show such sensitivity in the third visit (Table 3.1).

Other physiological parameters like lipid profile markers and kidney and liver function markers were also studied for their changes with respect to the glycemic changes. Lipid profile markers cholesterol and triglycerides showed a high relative mean value compared to the corresponding non-diabetic values in the first visit and decreased by third visit (Table 3.1). Hence cholesterol and triglycerides, but not lipoproteins, can be treated as useful correlates of glucose control in diabetic patients. Kidney and liver function markers, ASTKE and ALTKE did not show much change in the relative percent mean from first visit to third visit. The other two markers, creatinine and glomerular filtration rate, showed improvement over the study period. However, the difference between the first and third visit is well below 15% (Table 3.1). Therefore, it can be inferred that kidney and liver function markers are less sensitive to glucose changes in the diabetic group, over three visits.

HbA_{1c} is a measure of chronic levels of glucose in the blood. Since the half-life of HbA_{1c} is about six weeks, the HbA_{1c} values in the third visit reflect a cumulative glucose control over eight weeks of therapy. Table 3.1 shows a high relative mean difference value for HbA_{1c} in the first visit which is lowered by about half by the third visit.

Overall, all the OS markers showed some improvement over the study period in diabetic patients (Acharya *et al.* [28] and Table 3.1) We used scatter-histograms to eyeball whether

	First visit		Third visit	
	Mean (%)	Stdev.* (%)	Mean (%)	Stdev. (%)
OS defence markers				
Glutathione	-83	-63	-61	-59
Glutathione reductase	-26	18	-17	-9
Glutathione peroxidase	-63.4	-39	-7.73	18
Superoxide dismutase	-10	-37.2	-7.4	-3.15
Catalase	-21	-30	-10	-10
Bilirubin	27.2	11	5.44	-13
Uric acid	21.9	38	-4.2	-20
Lipid profile markers				
Cholesterol	15.2	9.3	0.42	-9.3
High density lipoproteins	-6.2	-1	-10.4	3
Triglycerides	70.4	90	40.5	80
Cell damage markers				
Protein carbonyls	83	14	32	7.1
Protein sulfhydryls	-47.1	5.8	-31.6	-12
TBARs	33.7	87	4.38	37
Kidney and liver markers				
Creatinine	-0.2	-17	-9.5	-21
Glomerular filtration rate	-9.5	-16	2	-6.4
ASTKE	-13.6	-8	-18.4	-1
ALTKE	9.6	-2.9	4.6	11
Glycosylated hemoglobin	75.7	250	38.2	75
Glucose	114.8	493	70.4	370

Table 3.1: Percent relative mean and standard deviation (Stdev.) difference for diabetic stress variables compared to non-diabetic values. Data adapted from Acharya JD *et al.* [28].

changes in the stress variables over the 8 weeks are sufficient to distinguish individuals based upon their diabetic status (see Appendix Section 3.6.1 for scatter-histograms of all the biomarkers). Scatter-plot represents serial variation in the biomarker values across the three visits, and histograms show corresponding shifts in the fitted distributions of the biomarker over the three visits. We noticed that markers of the glutathione metabolism specially GSH_t and GPx showed "marked" improvement before and after antidiabetic therapy. For instance, Figures 3.1 and 3.2 show scatter-histograms of GSH_t against plasma glucose for non-diabetics and diabetics, respectively. The glutathione histograms depict serial changes over the 8 weeks in the GSH_t distributions. The first visit diabetic mean±se glutathione value (140±16) was much lower when compared to the mean±se glutathione value of the non-diabetics (859±3). After controlling glucose levels in diabetic patients, glutathione levels showed an upward shift with the mean±se value of 334±18. Further, the diabetic scatterplot revealed that the first (0 week) and third visit (8 weeks) glutathione levels can be roughly demarcated at around GSH_t value of 200 (nM/ml) (see Figure 3.2). Similarly, Figures 3.3 and 3.4 show scatter-histograms of non-diabetic and diabetic GPx activity levels over the three visits. GPx activity was rapidly increased over the 8 weeks study period in response to antidiabetic treatment. In the first visit, diabetic GPx activity levels were low with the mean±se value of 0.07±0.00. Over the study period, diabetic GPx activity improved with the mean±se value of 0.179±0.006 (Figure 3.4) slowly approaching the non-diabetic GPx range (see Figure 3.3). Moreover, a clear distinction between 0 week and 8 weeks GPx activities can be assigned near GPx activity level of 0.11 (U /mg of protein)(see Figure 3.4).

Among several physiological markers studied, scatter-histograms of GSH_t and GPx revealed that individuals need not only be classified based on GS but along the stress variable axis as well. Therefore, we inferred that the markers of glutathione metabolism, specially GSH_t and GPx can be used to distinguish diabetic state from the non-diabetic state.
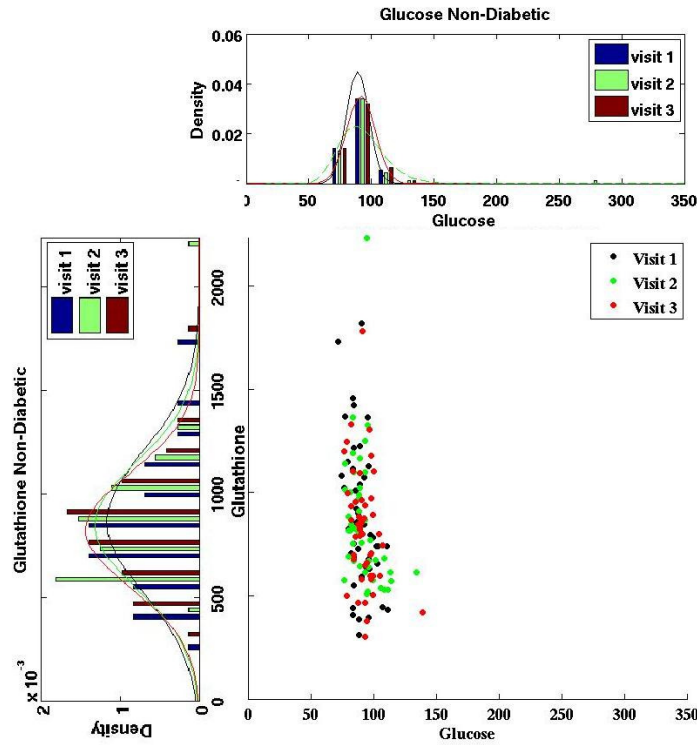
Figure 3.1: Scatter-histogram of glutathione versus glucose for non-diabetics. Non-diabetic glucose levels show physiologically normal range of 80-120 with overall mean±se of 91±2 over three visits. Non-diabetic glutathione is normally distributed with mean±se of 859±3 over the three visits.
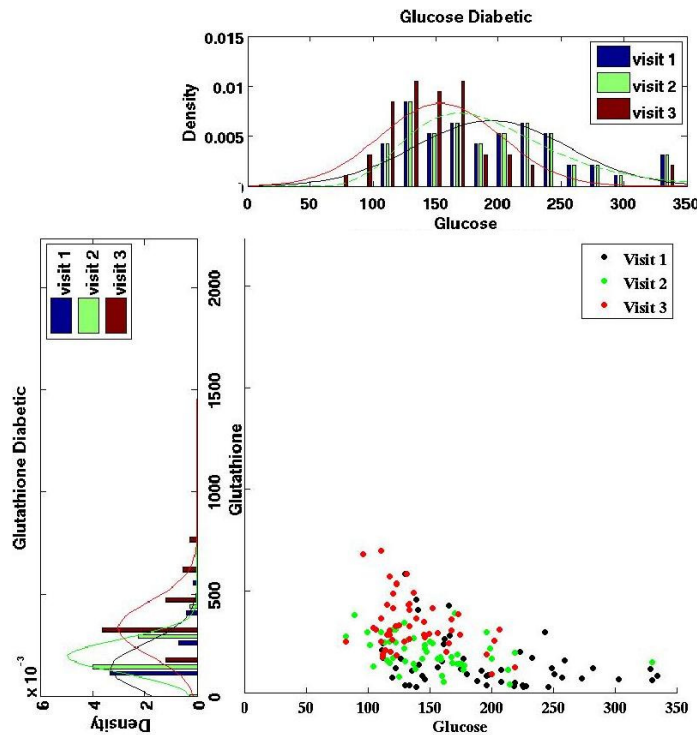
Figure 3.2: Scatter-histogram of glutathione versus glucose for diabetics. The scatter plot shows glucose range between 70-350 in the first visit. In the first visit, mean±se values for glucose and glutathione are 194±3 and 140±16, respectively. By the third visit, mean±se value for glucose was reduced to 153±2 and glutathione mean±se value was increased to 334±18.
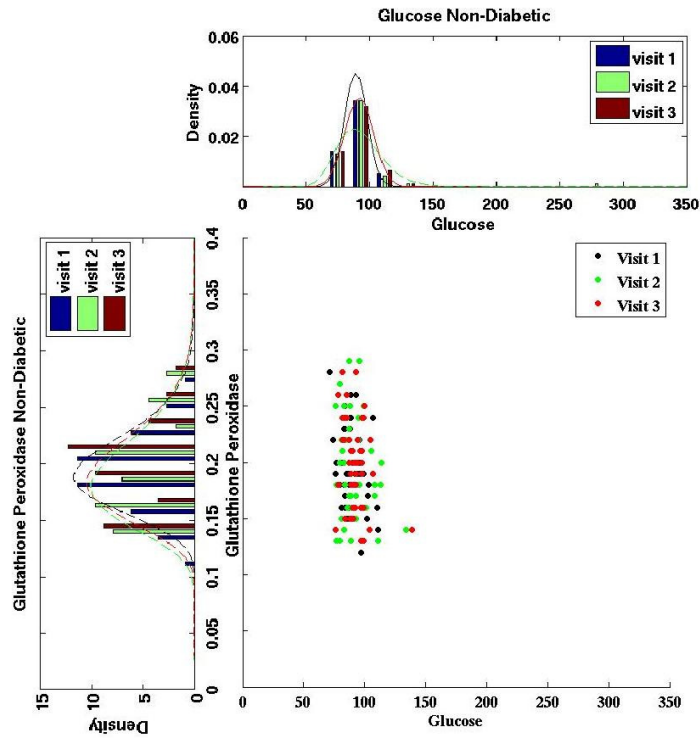
Figure 3.3: Scatter-histogram of glutathione peroxidase versus glucose for non-diabetics. Non-diabetic glutathione peroxidase activities range between 0.1-0.3, with mean±se value of 0.194±0.003 over the three visits.
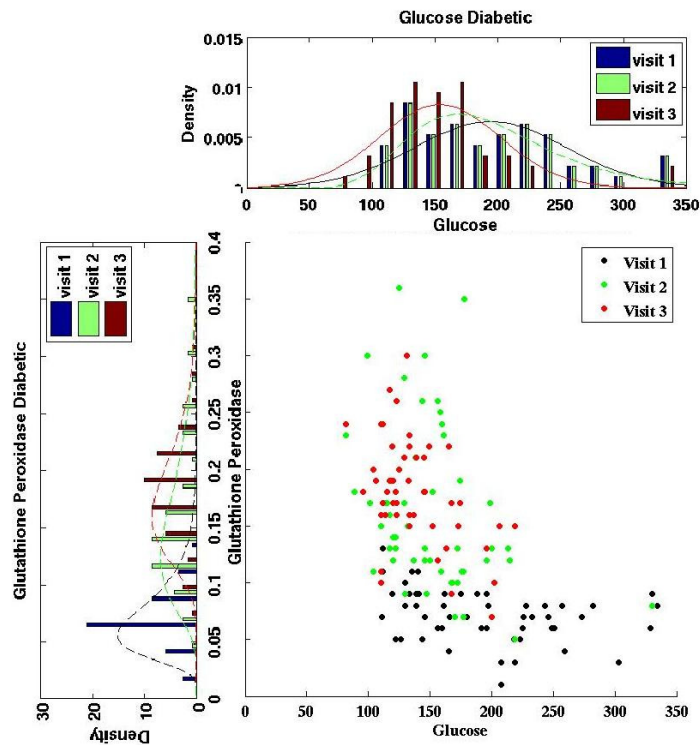
Figure 3.4: Scatter-histogram of glutathione peroxidase versus glucose for diabetics. In the first visit, mean±se glutathione peroxidase activity is 0.07±0.003. By the third visit, glutathione peroxidase activity showed considerable increase with the mean±se value of 0.179±0.006.

3.5 Discussion

In this chapter, we examined which OS marker can be suitably used to monitor diabetes progression along with glucose. We used the dataset on newly-diagnosed diabetic patients who were kept on glucose control treatment for about two months and serially tracked changes in the OS. We were specifically interested in how rapidly a given OS marker varies in response to changes in the GS. We also evaluated whether the diabetic profile was distinctly different from the non-diabetic profile for a given OS marker using scatter-histograms (see scatter-histograms for all the variables in the Section 3.6.1). We showed that among almost 12 markers of OS studied, markers of glutathione metabolism respond rapidly to antidiabetic treatment. Further, these markers show distinct diabetic and non-diabetic ranges (for instance see scatter-histograms of GSH_t and GPx), unlike other markers, followed in the study.

We note that markers of glutathione metabolism may show significant variation over the short study period of 8-weeks, while other OS markers may hold important clinical information over longer study periods.

3.6 Appendix

3.6.1 Scatter-histograms of OS markers

Scatter-histograms of all the physiological biomarkers are provided for the reference for all the three visits, with visit 1, 2 and 3 stand for 0-week, 4-weeks and 8-weeks, respectively.

We asked whether serial changes in the biomarkers over the 8 weeks is sufficient to distinguish individuals based upon their diabetic status. In other words, we enquired whether a distinct clustering would emerge based upon the distribution of data points on the scatterplot. Corresponding histograms represent changes in the fitted distributions over the study period. The bootstrapped mean±se values are provided for the comparison for each visit.

Biomarker	Biochemical measurement Unit
Glutathione	nM/ml
Glutathione reductase	U/mg protein
Glutathione peroxidase	U/mg protein
Superoxide dismutase	U/mg protein
Catalase	U/mg protein
Bilirubin	mg%
Uric acid	mg%
Cell damage markers	
Protein carbonyls	nmole/mg protein
Protein sulfhydryls	nmole/mg protein
TBARs	nmole MDA/L
Lipid profile markers	
Cholesterol	mmol/L
High density lipoproteins	mmol/L
Triglycerides	mmol/L
Kidney and liver markers	
Creatinine	umol/L
Glomerular filtration rate	ml/min/m^2
ASTKE	U/mg protein
ALTKE	U/mg protein
Glycosylated hemoglobin	%
Glucose	mg/dL

Table 3.2: Biochemical units of the biomarkers followed in the study period. Units obtained from Acharya *et al.* [28].
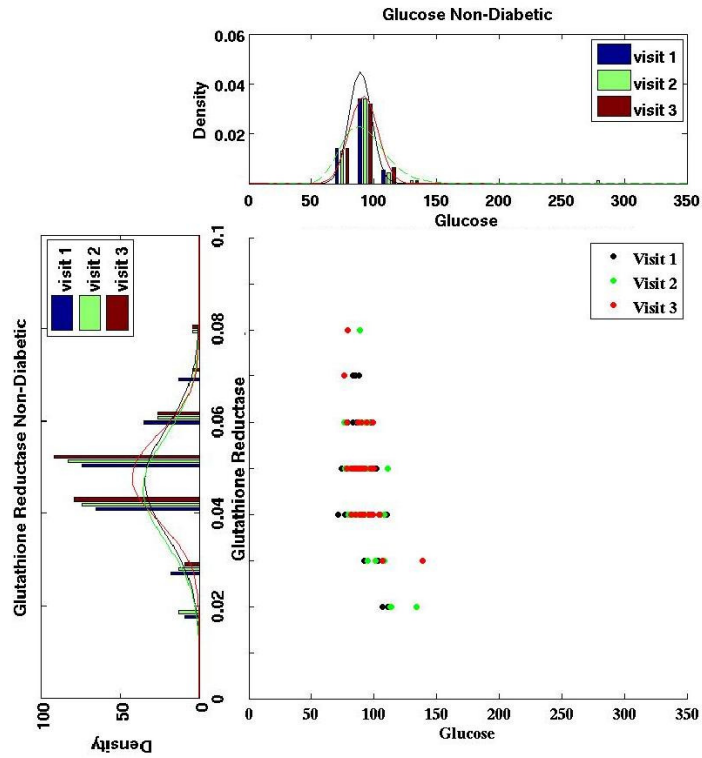
Figure 3.5: Scatter-histogram of glutathione reductase versus glucose for non-diabetics. Glutathione reductase activities range between 0.02-0.08, with mean±se value of 0.049±0.001 over the three visits.
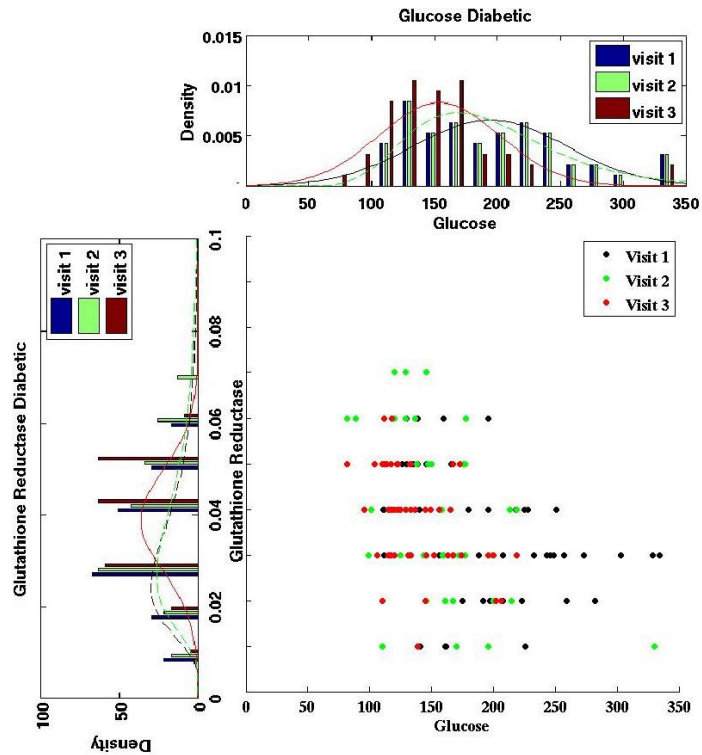
Figure 3.6: Scatter-histogram of glutathione reductase versus glucose for diabetics. In the first visit, mean±se glutathione reductase activity is 0.034±0.001. By the third visit, glutathione reductase activity did not show much change with the mean±se value of 0.038±0.001.
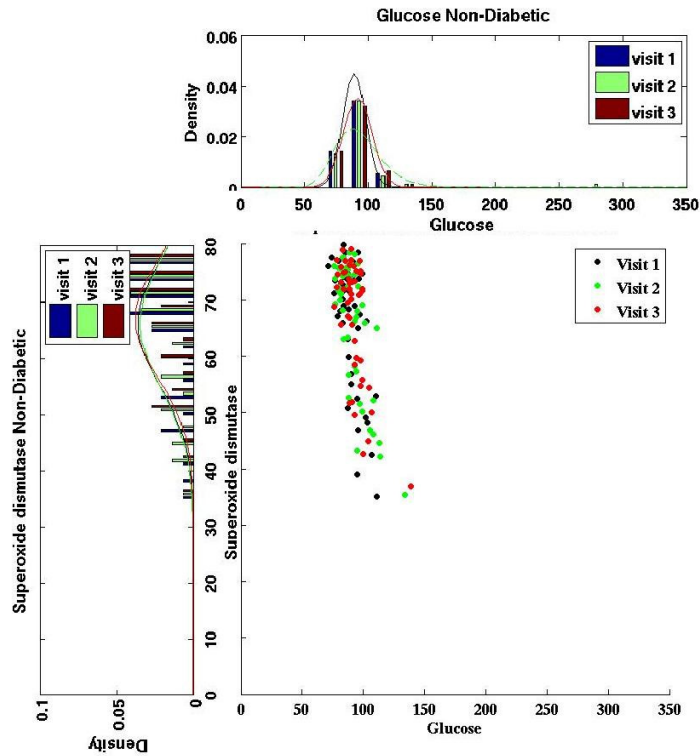
Figure 3.7: Scatter-histogram of superoxide dismutase activity versus glucose for non-diabetics. Non-diabetic glutathione peroxidase activities range between 35-80, with mean±se value of 0.194±0.003 over the three visits.
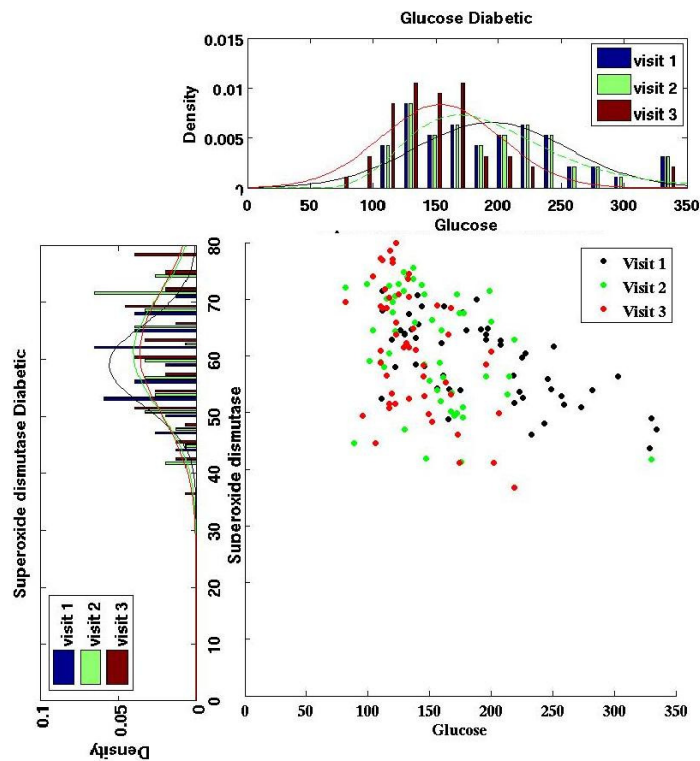
Figure 3.8: Scatter-histogram of superoxide dismutase activity versus glucose for diabetics. In the first visit, mean±se glutathione peroxidase activity is 0.07±0.003. By the third visit, glutathione peroxidase activity showed considerable increase with the mean±se value of 0.179±0.006.
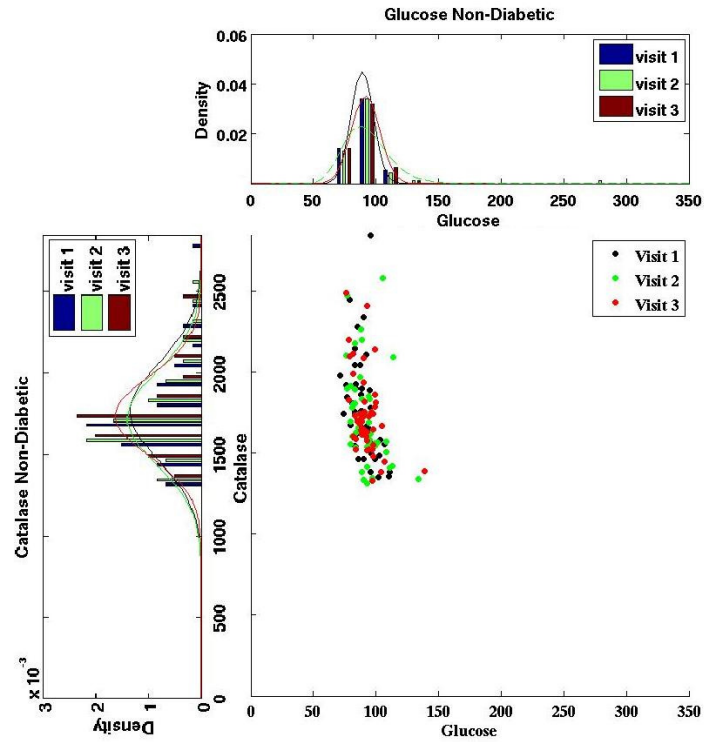
Figure 3.9: Scatter-histogram of catalase activity versus glucose for non-diabetics. Non-diabetic catalase activities range between 1300-2700, with mean±se value of 1743±29 over the three visits.
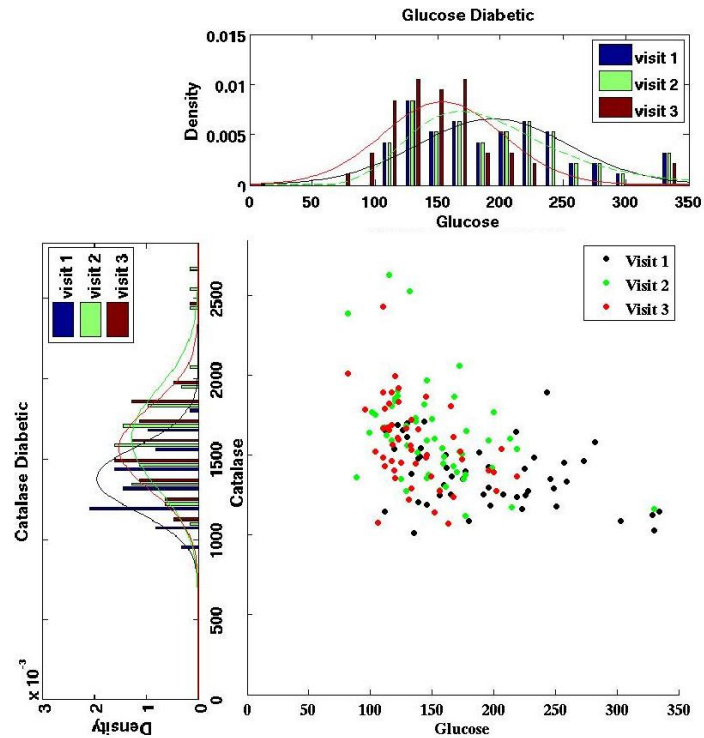
Figure 3.10: Scatter-histogram of catalase activity versus glucose for diabetics. In the first visit, mean±se catalase activity is 1376±27. By the third visit, catalase activity showed considerable increase with the mean±se value of 1567±36.
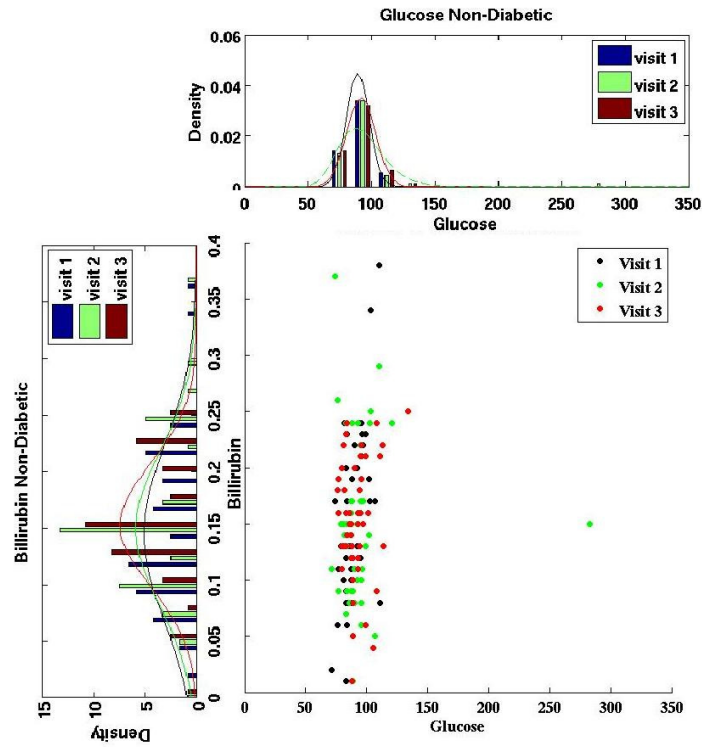
Figure 3.11: Scatter-histogram of bilirubin activity versus glucose for non-diabetics. Non-diabetic bilirubin levels range between 0.01-0.4, with mean±se value of 0.147±0.007 over the three visits.
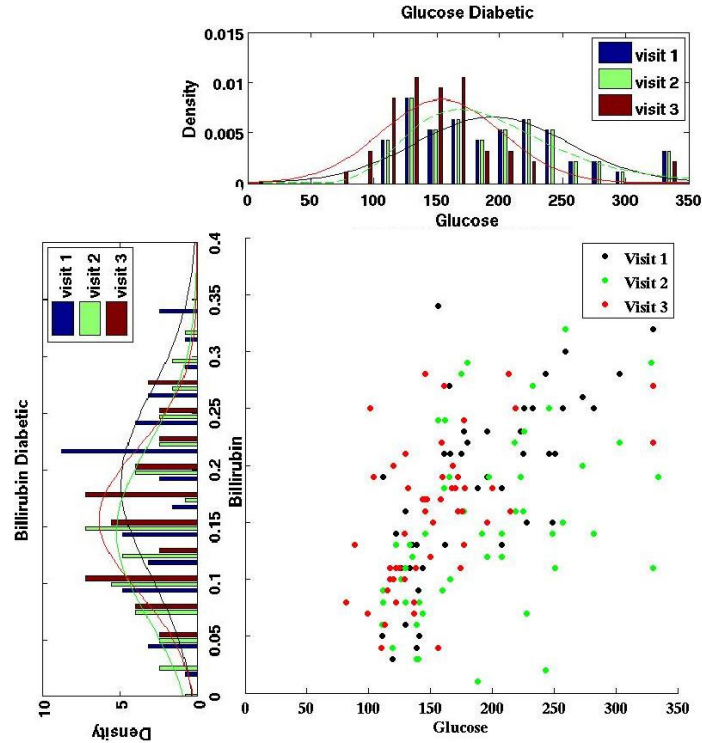
Figure 3.12: Scatter-histogram of bilirubin levels versus glucose for diabetics. In the first visit, diabetic mean±se bilirubin level was 0.187±0.01. By the third visit, bilirubin levels decreased to mean±se value of 0.155±0.008.
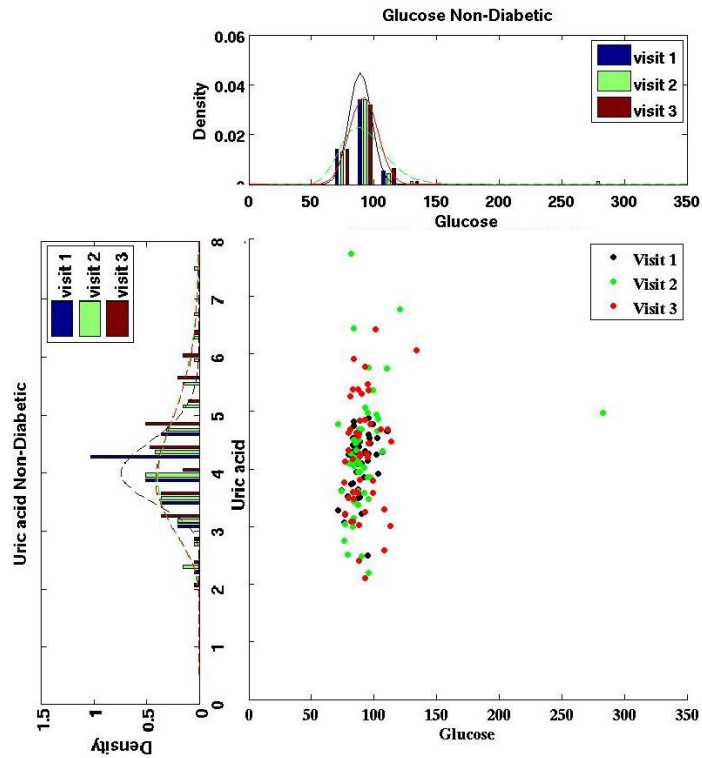
Figure 3.13: Scatter-histogram of uric acid levels against glucose for non-diabetics. Non-diabetic uric acid levels range between 2.0-8.0, with mean±se value of 4.18±0.08 over the three visits.

Figure 3.14: Scatter-histogram of uric acid levels against glucose for diabetics. In the first visit, mean±se diabetic uric acid level was 5.1±0.1. By the third visit, uric acid levels show slight decrease with the mean±se value of 4.0±0.09.
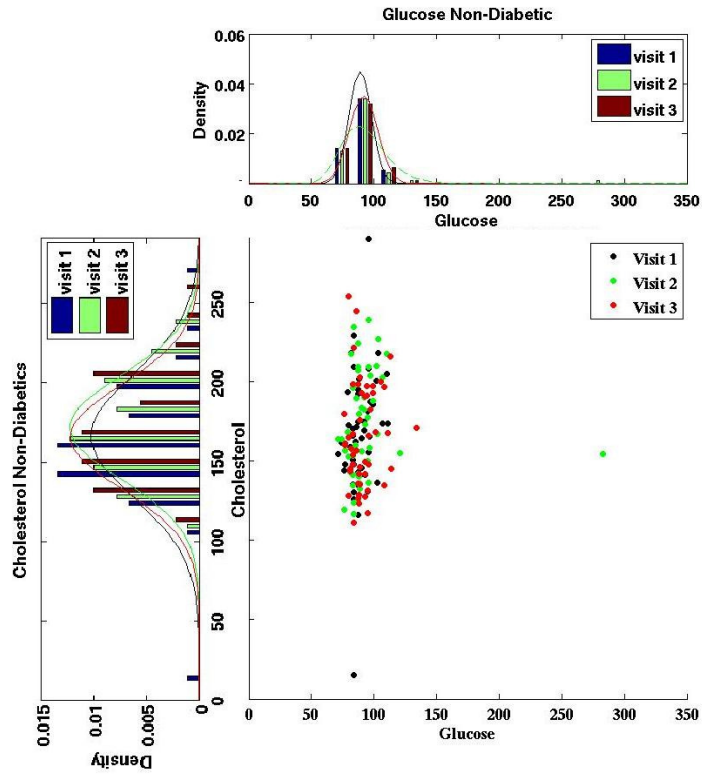
Figure 3.15: Scatter-histogram of cholesterol levels against glucose for non-diabetics. Non-diabetic cholesterol levels range between 110-290, with mean±se value of 169.3±3.6 over the three visits.
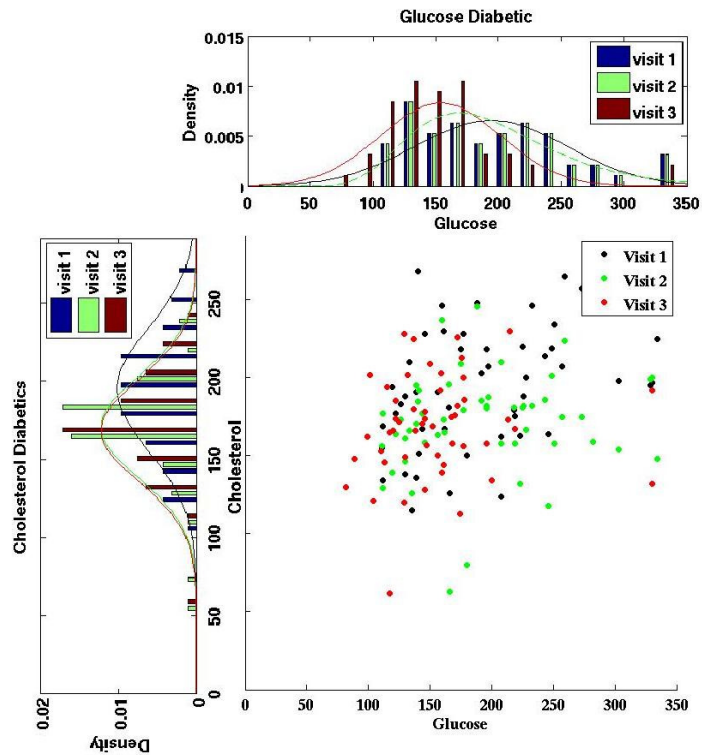
Figure 3.16: Scatter-histogram of cholesterol levels against glucose for diabetics. In the first visit, mean±se diabetic uric acid level was 195±5.4. By the third visit, cholesterol levels show slight decrease with the mean±se value of 168.5±4.5.
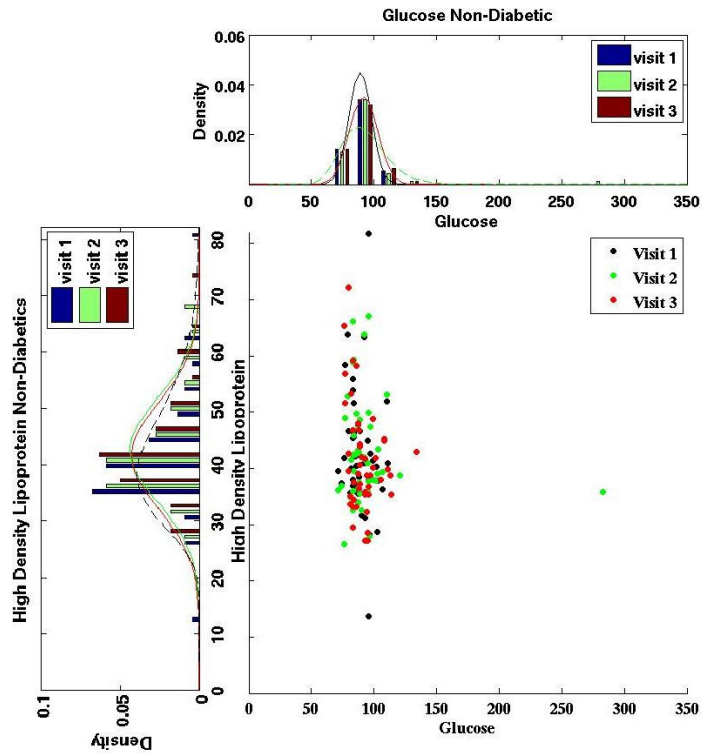
Figure 3.17: Scatter-histogram of high density lipoproteins levels against glucose for non-diabetics. Non-diabetic high density lipoproteins levels range between 12-82, with mean±se value of 42.4±1.0 over the three visits.
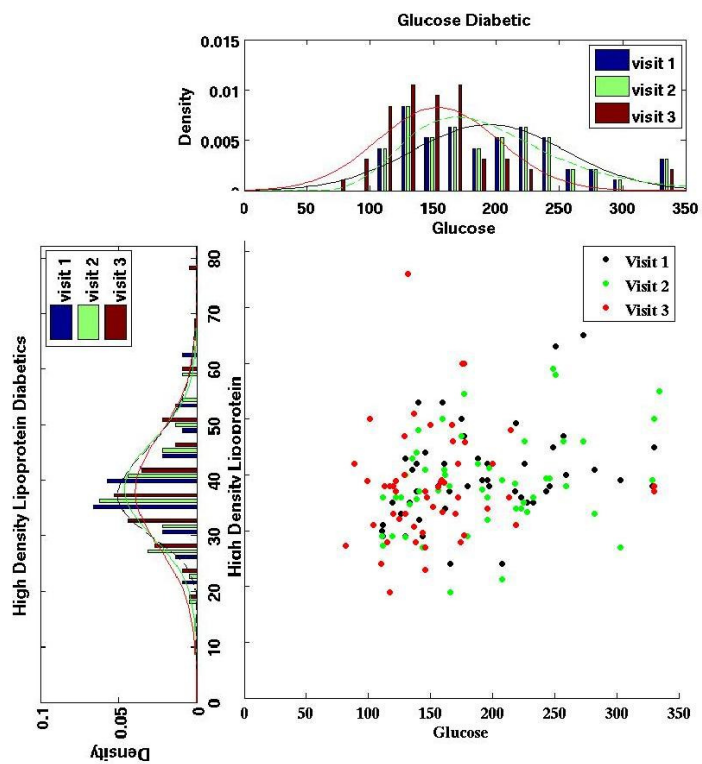
Figure 3.18: Scatter-histogram of high density lipoproteins levels against glucose for diabetics. In the first visit, mean±se diabetic high density lipoproteins level was 39.8±1.2. By the third visit, cholesterol levels show a little change with the mean±se value of 38.0±1.4.
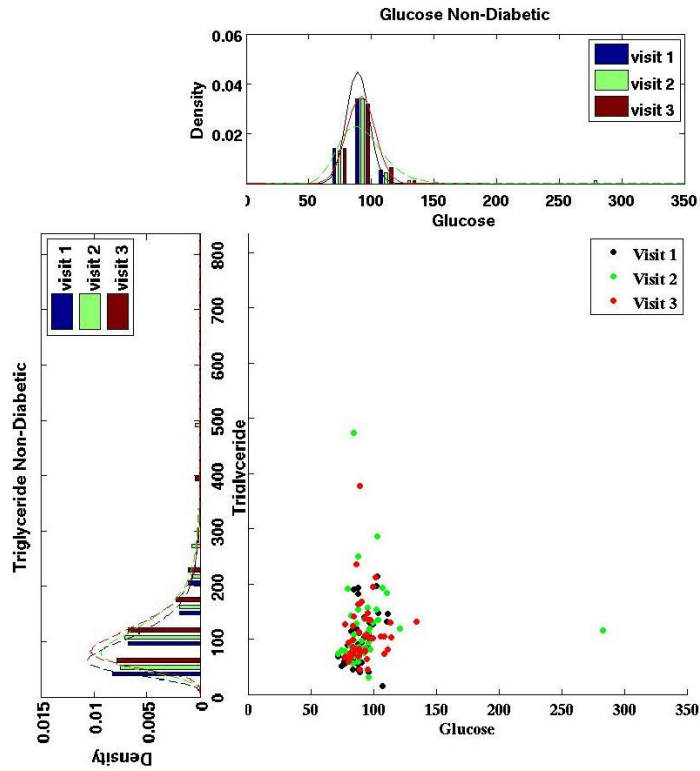
Figure 3.19: Scatter-histogram of triglyceride levels against glucose for non-diabetics. Non-diabetic triglyceride levels range between 10-490, with mean±se value of 42.4±1.0 over the three visits.
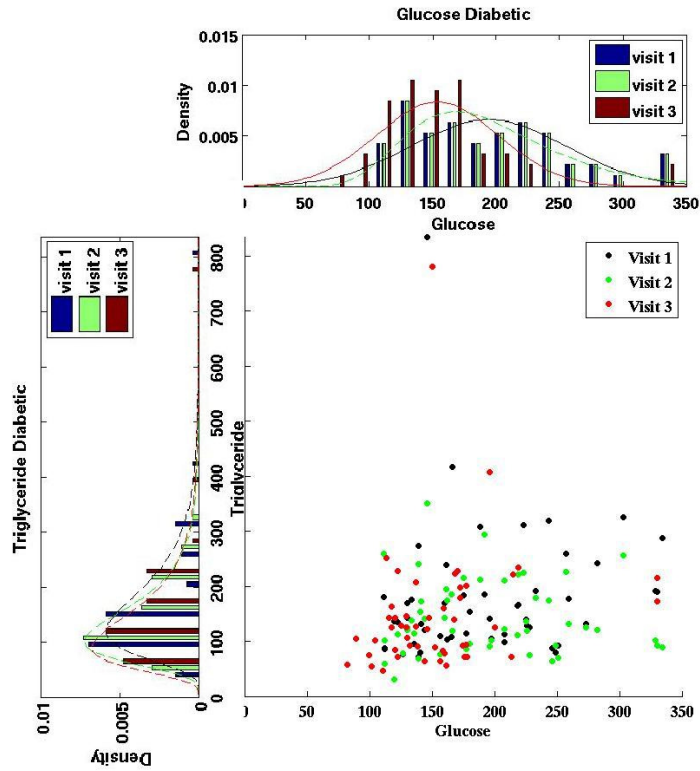
Figure 3.20: Scatter-histogram of triglyceride levels against glucose for diabetics. In the first visit, mean±se diabetic triglyceride level was 39.8±1.2. By the third visit, triglyceride levels show a little change with the mean±se value of 38.0±1.4.
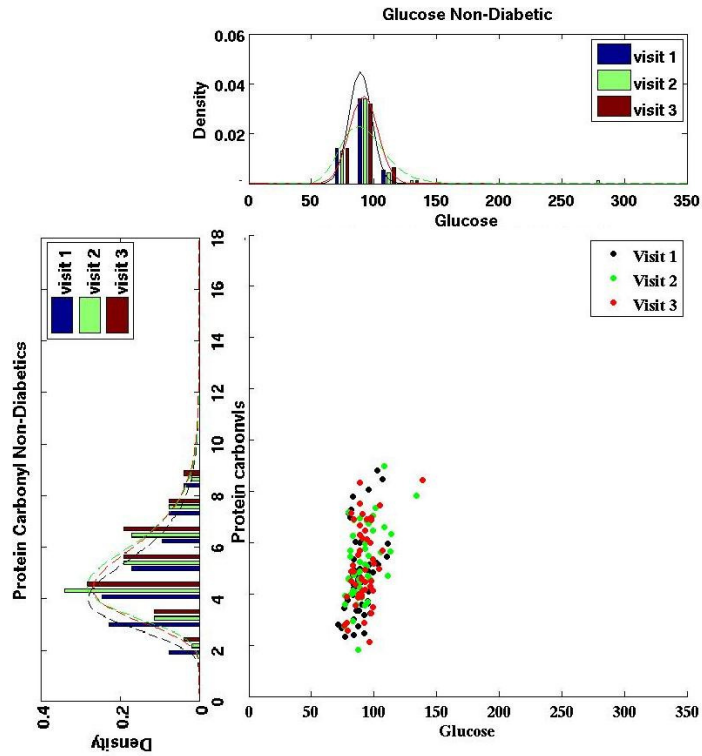
Figure 3.21: Scatter-histogram of protein carbonyl levels against glucose for non-diabetics. Non-diabetic protein carbonyl levels range between 2-10, with mean±se value of 4.9±0.1 over the three visits.
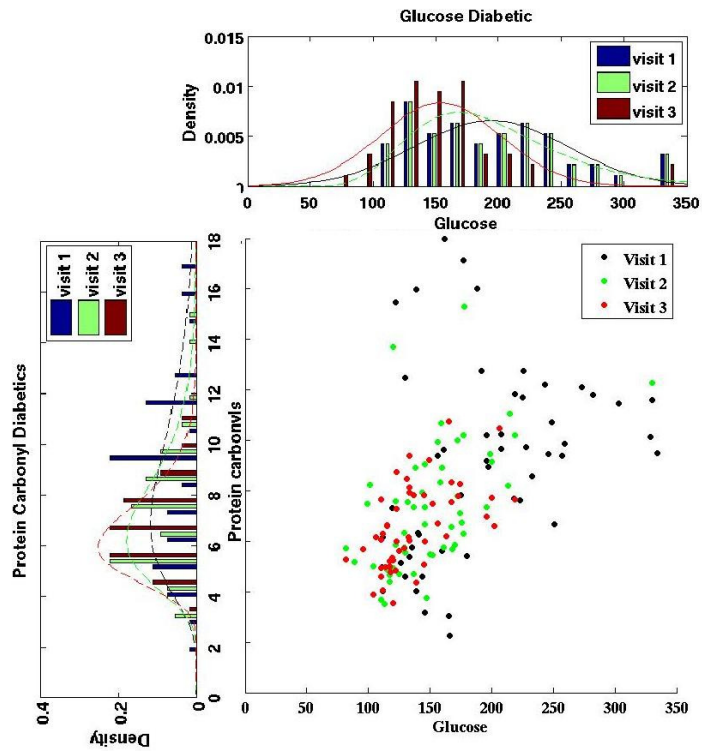
Figure 3.22: Scatter-histogram of protein carbonyl levels against glucose for diabetics. In the first visit, mean±se diabetic protein carbonyl value was 9.0±0.5. By the third visit, protein carbonyl levels reduced to the mean±se value of 6.5±0.2.
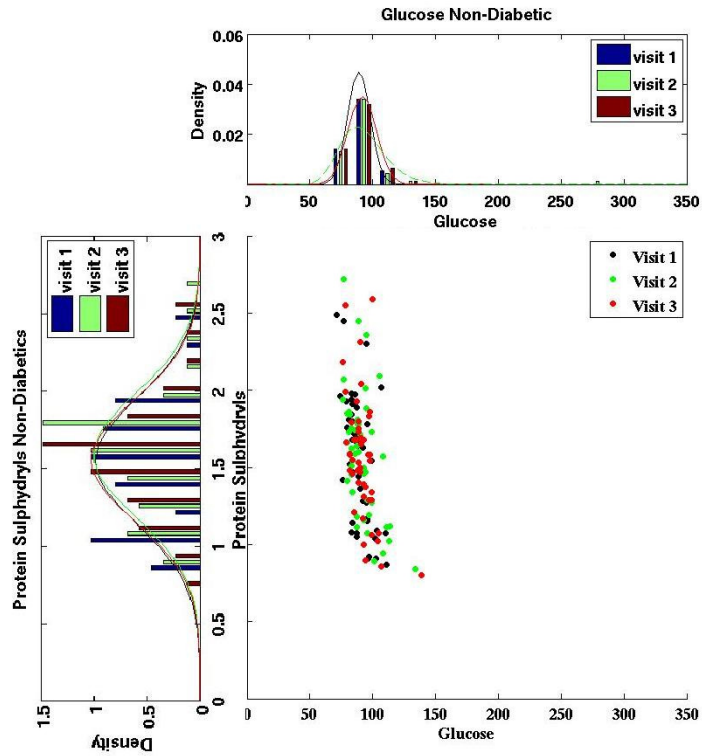
Figure 3.23: Scatter-histogram of protein sulfhydryl levels against glucose for non-diabetics. Non-diabetic protein sulfhydryl levels range between 0.7-2.7, with mean±se value of 1.56±0.04 over the three visits.
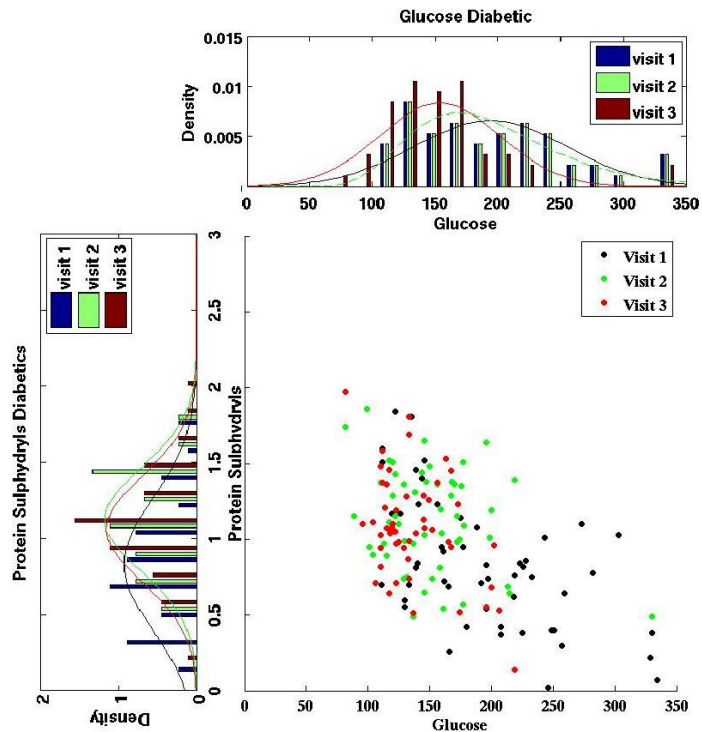
Figure 3.24: Scatter-histogram of protein sulfhydryl levels against glucose for diabetics. In the first visit, mean±se diabetic protein sulfhydryl value was 0.82±0.05. By the third visit, protein sulfhydryl levels improved a little to the mean±se value of 1.07±0.04.
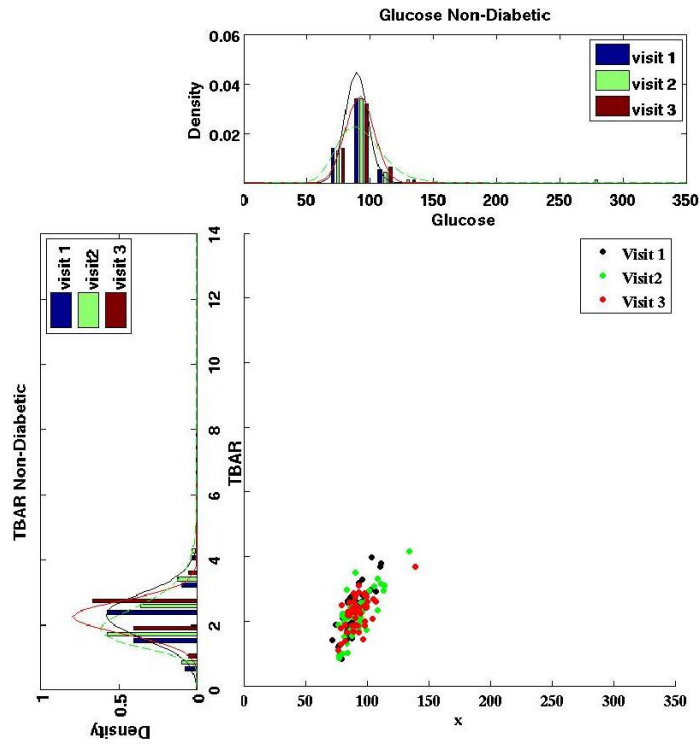
Figure 3.25: Scatter-histogram of TBARs levels against glucose for non-diabetics. Non-diabetic TBARs levels range between 0.4-4.0, with mean±se value of 2.23±0.07 over the three visits.
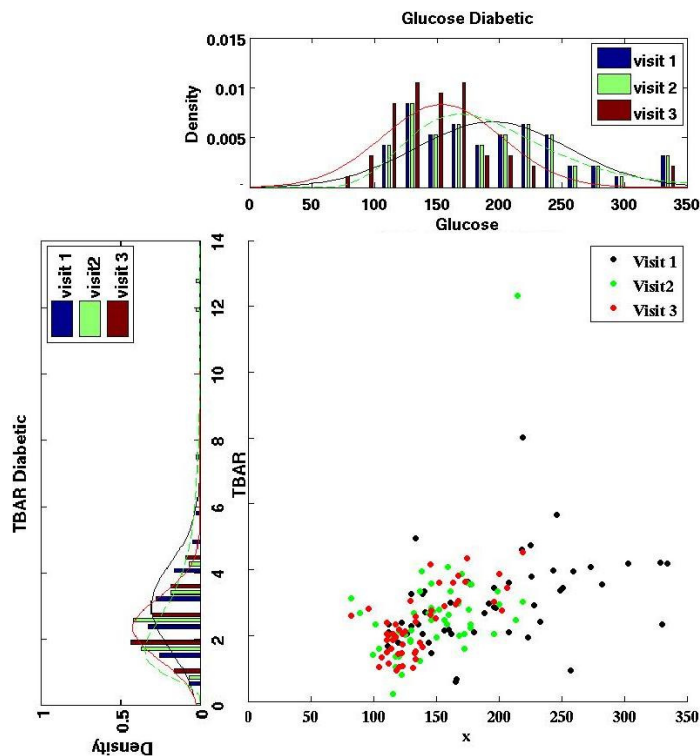
Figure 3.26: Scatter-histogram of TBARs levels against glucose for diabetics. In the first visit, mean±se diabetic TBARs value was 3.0±0.2. By the third visit, TBARs levels reduced to the mean±se value of 1.07±0.04.
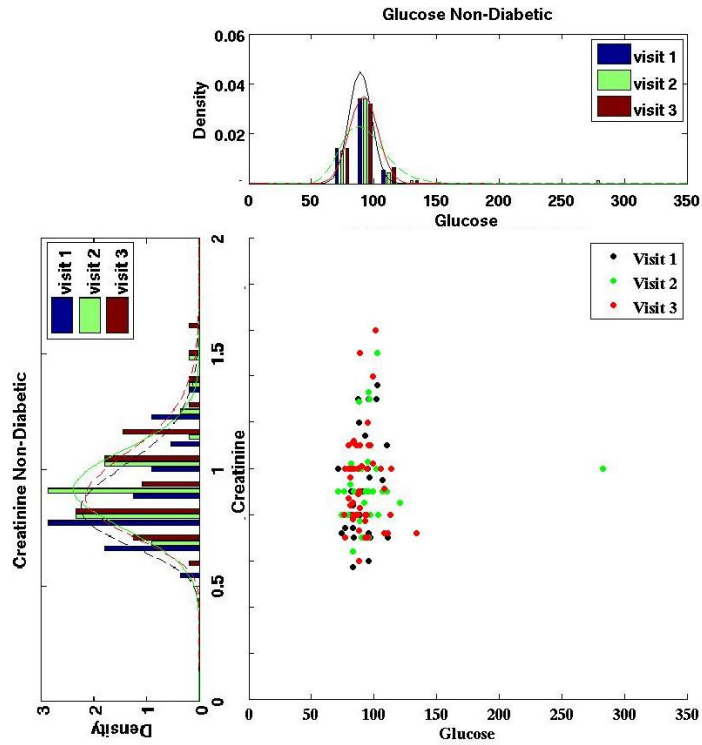
Figure 3.27: Scatter-histogram of creatinine levels against glucose for non-diabetics. Non-diabetic creatinine levels range between 0.5-1.5, with mean±se value of 0.90±0.0 over the three visits.
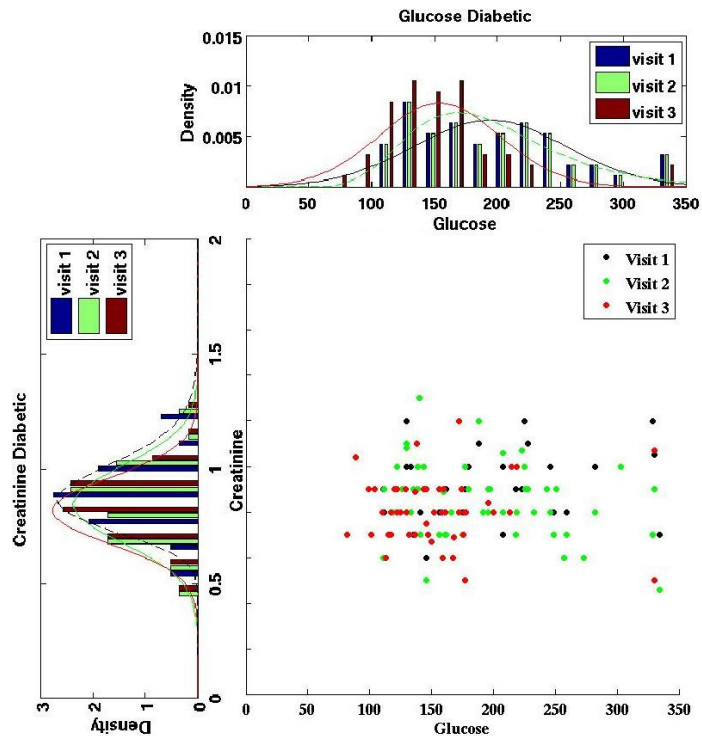
Figure 3.28: Scatter-histogram of creatinine levels against glucose for diabetics. In the first visit, mean±se diabetic creatinine value was 0.9±0.0. By the third visit, creatinine levels reduced to the mean±se value of 0.81±0.1.
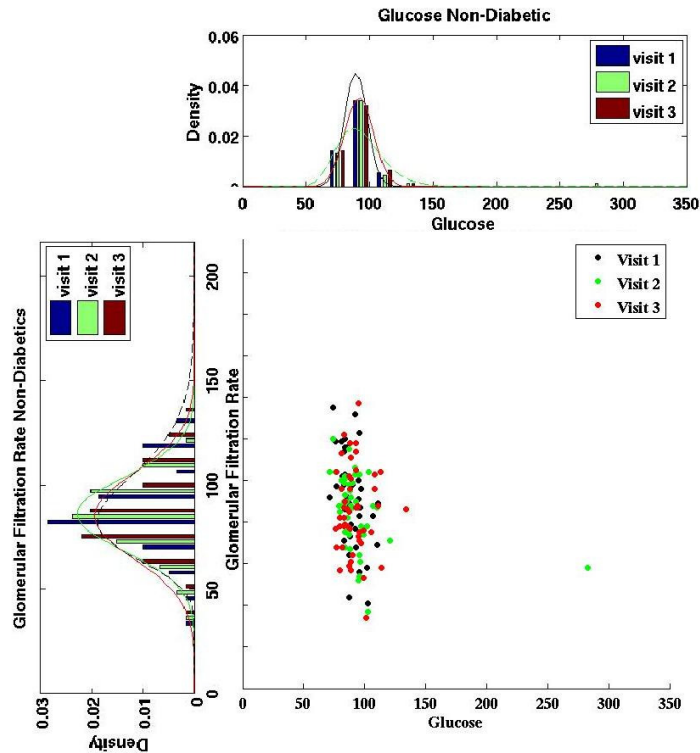
Figure 3.29: Scatter-histogram of glomerular filtration rate against glucose for non-diabetics. Non-diabetic glomerular filtration rate ranges between 30-150, with mean±se value of 88.3±2.0 over the three visits.
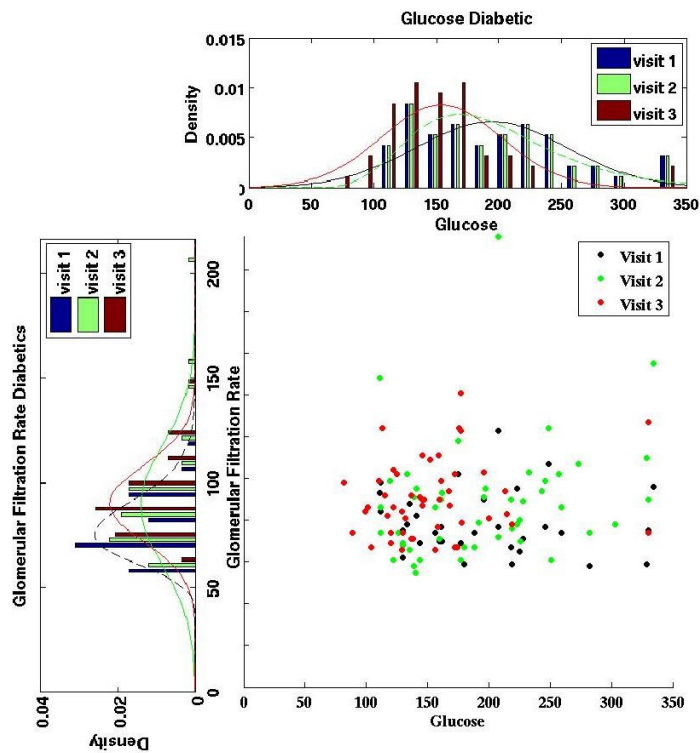
Figure 3.30: Scatter-histogram of glomerular filtration rate against glucose for diabetics. In the first visit, mean±se diabetic glomerular filtration rate was 80.0±2.3. By the third visit, glomerular filtration rate improved to the mean±se value of 90.1±2.5.
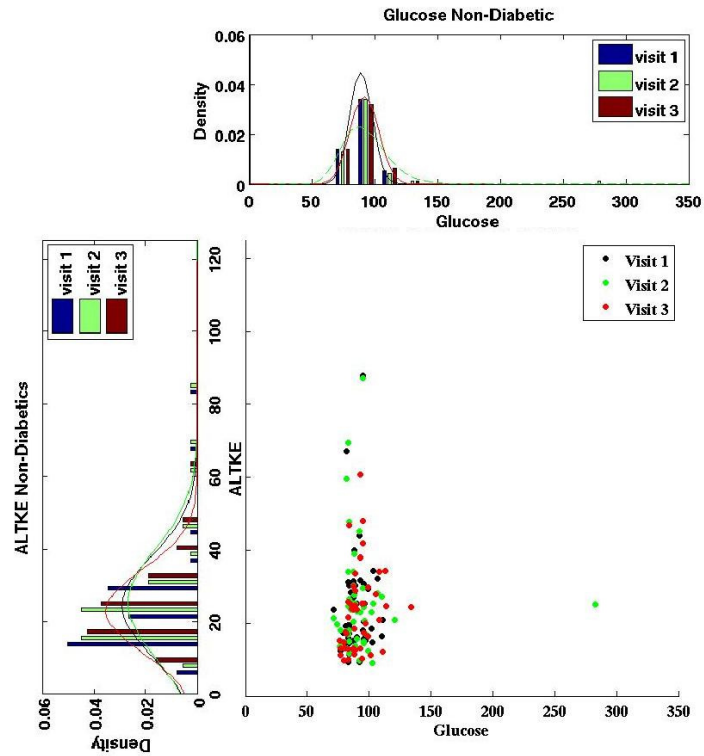
Figure 3.31: Scatter-histogram of ALTKE against glucose for non-diabetics. Non-diabetic ALTKE ranges between 10-90, with mean±se value of 24.8±1.4 over the three visits.
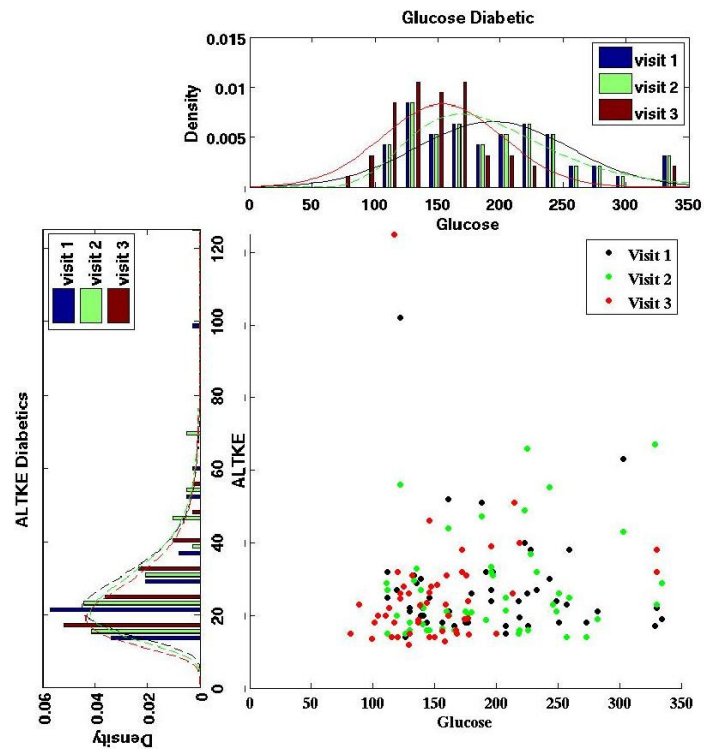
Figure 3.32: Scatter-histogram of ALTKE against glucose for diabetics. In the first visit, mean±se diabetic ALTKE was 27.2±2.0. By the third visit, ALTKE remained unchanged with the mean±se value of 26.0±2.3.
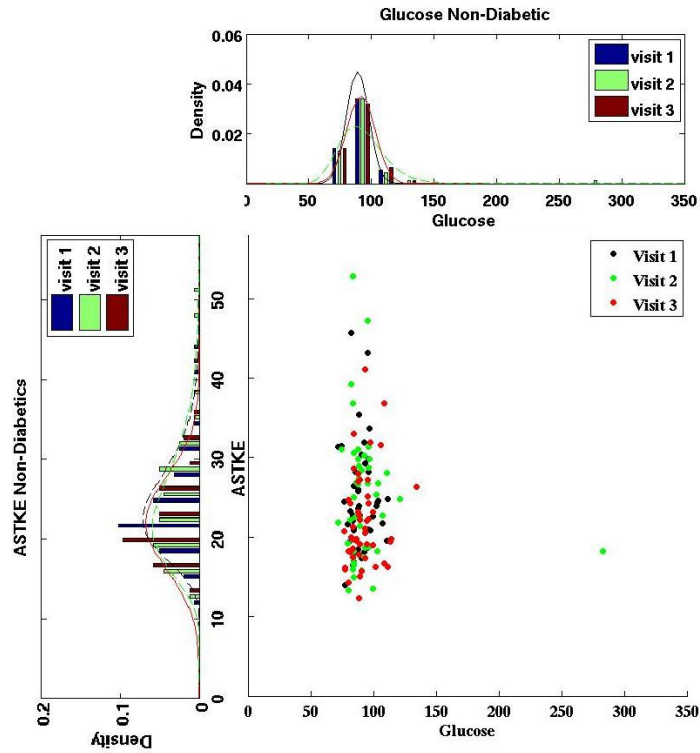
Figure 3.33: Scatter-histogram of ASTKE against glucose for non-diabetics. Non-diabetic ASTKE ranges between 12-52, with mean±se value of 24.5±0.7 over the three visits.

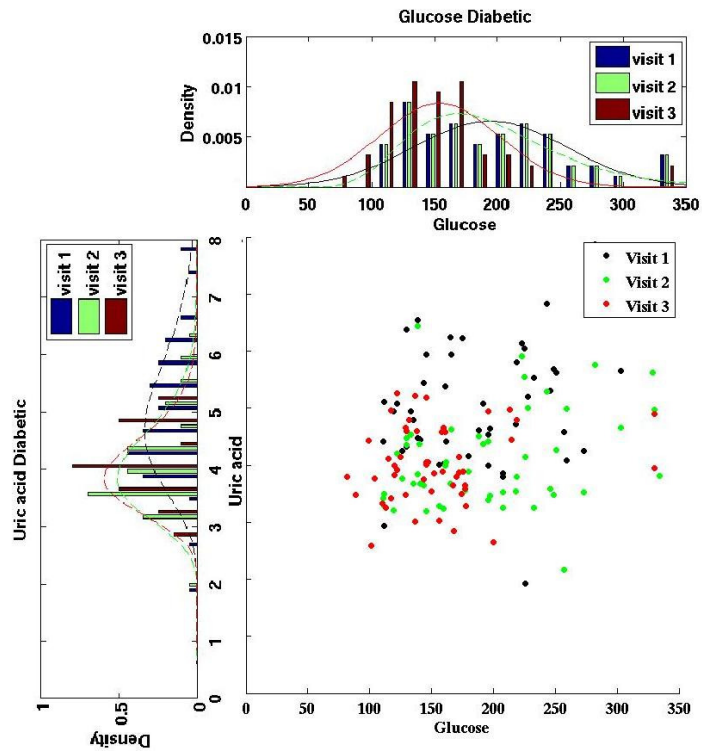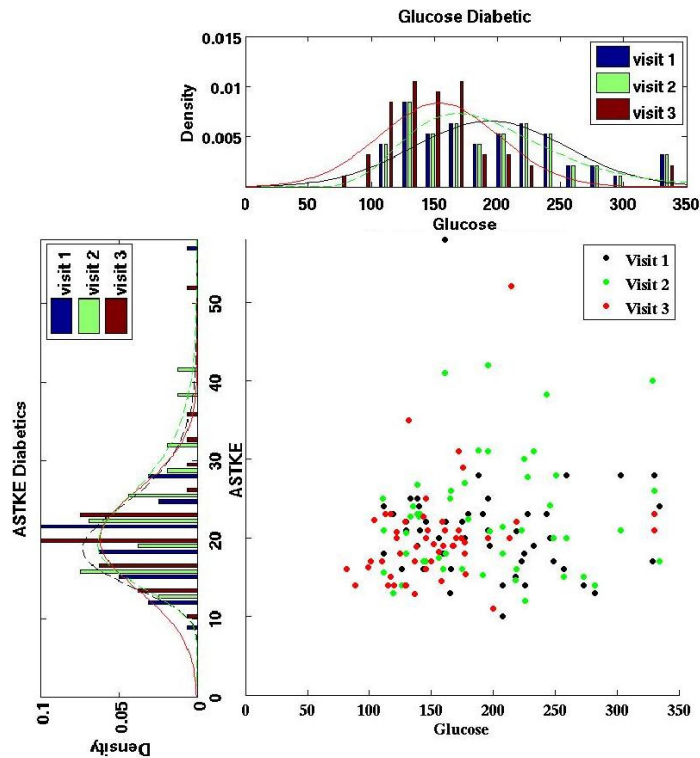**Figure 3.34:** Scatter-histogram of ASTKE against glucose for diabetics. In the first visit, mean±se diabetic ASTKE was 21.2±0.9. By the third visit, ASTKE did not change much with the mean±se value of 20.0±0.9.

Chapter 4

Blood glutathione accurately classifies diabetic states

4.1 Introduction

In Chapter 3, we studied how several OS parameters vary in response to antidiabetic treatment in diabetic patients. In particular, we showed that markers of glutathione metabolism recover quickly over the short study period of 8-weeks (see Chapter 3, Section 3.4.1). We decided to study variation in glutathione metabolism in response to glucose control in greater detail.

Glutathione (GSH_t) is an endogenous antioxidant buffer of the cell, which exists as a redox couple: in reduced (GSH) and oxidised disulfide (GSSG) form. Glutathione is primarily involved in maintaining the appropriate redox status of the cell, by scavenging free radicals produced due to energy metabolism (Scholz *et al.* [104]; Grant [105]). It is also known to play an essential role in DNA synthesis and repair, cell differentiation and proliferation, iron metabolism, and nitric acid cycle (Prasad *et al.* [106]; Atakisi *et al.* [107]; Kumar *et al.* [108]; Shelly [109]). Undoubtedly hampered glutathione metabolism might be reflected as a systemic response to the diseased state. For instance, GSH/GSSG ratio is routinely used as a measure of redox status and known to be altered in clinical conditions like

neurodegenerative disorders, cancer and diabetes (Jones [110]; Owen and Butterfield [111]). These studies suggest that glutathione is an excellent OS marker *in vivo* (Jones *et al.* [112]).

Most importantly, the role of glutathione metabolism is well established in the context of the development of hyperglycemia-mediated PDCs. Hyperglycemia leads to mitochondrial overproduction of ROS *via* TCA cycle; which takes toll on glutathione and other antioxidant systems of the cell (Goh and Cooper [83]; Peppa *et al.* [113]; Stirban *et al.* [114]). A large body of clinical evidence shows that diabetic state is associated with the lowered blood glutathione levels (Thornalley *et al.* [115]; Samiec *et al.* [116]; Dincer *et al.* [117]; Nwose *et al.* [118]) and reduced GSH synthesis rates (Tachi *et al.* [119]; Murakami *et al.* [120]; Whillier *et al.* [121]). The central role of GSH metabolism in the regulation of glucose metabolism can be studied using GSH infusion studies in diabetic patients: GSH infusion readily improved GSH synthesis rates, glucose homoeostasis and reduces PDCs (Paolisso *et al.* [122]; De Mattia *et al.* [123]; Marfella *et al.* [124]). Sekhar *et al.* showed that infusion of amino acids cysteine and glycine, which are precursors of GSH synthesis, not only restored the GSH synthesis rates but also showed reduction in the oxidative damage markers [125]. **Therefore, it is important to ask: if GSH metabolism plays such a crucial role in the regulation of glucose metabolism, how it can be utilised in the diagnosis and treatment of diabetes?**

In this chapter, we, first analyse whether reduction in hyperglycemia is associated with concomitant improvement in the diabetic status, as measured by Homeostasis Model Assessment (HOMA) indices: measures of insulin sensitivity and β-cell dysfunction (see Section 4.5.3 for more details). We show that improvement in the β-cell dysfunction is associated with improved GSH_t levels in diabetic patients. Then, we sought to explore the relationship between GSH_t and HbA_{1c} in greater detail. We specifically ask: whether GSH_t levels are sufficient to define diabetes and hence might be useful in tracking the progression of diabetes? To establish that GSH_t can be used to classify diabetes, we perform a hierarchical cluster analysis on the GSH_t values pooled from non-diabetic subjects and diabetic patients at 0 and 8-weeks. We show that GSH_t levels alone can be used to classify individuals from

diabetic to non-diabetic state. We propose that GSH_t can be an excellent OS marker in monitoring and diagnosis of the diabetic status.

Parts of this work have been previously published in Kulkarni *et al.* [126]. The figures and tables in this chapter are reproduced under the creative commons attribution license.

4.2 Statistical methods

4.2.1 Bootstrap estimates of confidence interval for reporting sample mean values to account for small study size

The CIs were reported along with the sample *mean* $\pm$ *sd* values as described in Chapter 3, Section 3.3.2. The comparison between the sample means was also performed as described in Section 3.3.2.

4.2.2 Multiple linear regression of GSH_t against age and BMI

OS is an important factor influencing the process of aging (Finkel and Holbrook [127]; Kregel and Zhang [128]). Therefore, age is an important confounding factor while interpreting changes in the OS as a function of GS. Since the non-diabetic and diabetic groups were not age-matched as a part of the study design, we imposed age-matching by dividing study subjects into two age groups: below and above age 40. Multiple linear regression of GSH_t against age and BMI were performed within the age groups to confirm the absence of confounding effects (see Section 4.5.4 for more information). For between-group comparisons, Student's t-test was used with the p-value calculations at the 95% level of significance. Statistical package R was used to perform the computations and data analysis.

4.2.3 Cluster Analysis of GSH_t values

A hierarchical cluster analysis was conducted on the GSH_t values pooled from non-diabetic subjects and diabetic patients at 0 and 8-weeks. Euclidean distance measure was used to produce the distance matrix, and Ward's method was used to perform hierarchical cluster

analysis using built-in functions linkage() and dendrogram() in MATLAB.

4.3 Results

4.3.1 Antidiabetic treatment reduces plasma glucose levels, however plasma insulin levels remain unchanged in diabetic patients over the study period

Acharya *et al.* conducted an interventional study on newly-diagnosed diabetic patients to control hyperglycemia using antidiabetic drug treatment (see Appendix Section 5.2 for more information on the drug treatment details) [28]. Diabetic plasma glucose levels were expected to reduce over the study period due to antidiabetic drug treatment. Figure 4.1a shows serial changes in the mean plasma glucose levels in diabetic patients at 0-week (D0), 4-weeks (D4), 8-weeks (D8) and compared with the non-diabetic plasma glucose values pooled from 0-week and 8-weeks (ND). Antidiabetic treatment was found to reduce glucose levels significantly in diabetic patients with mean±sd (bootstrapped CI for the mean) of 10.6 ± 3.4 (9.6, 11.5) at D0 to 7.6 ± 1.7 (7.1, 8.1) at D8. However, D8 glucose values were still higher compared to the ND glucose levels with mean±sd (bootstrapped CI for the mean) being 4.92 ± 0.42 (4.8, 5.0).

We also studied changes in the diabetic plasma insulin levels over the study period. Figure 4.1b represents serial variation in the mean plasma insulin levels in diabetic patients. Plasma insulin levels show considerable variation within the D0, D4 and D8 groups. Also, mean insulin levels were not changed significantly over the study period. The $mean \pm sd$ (with corresponding bootstrapped CI for the mean) value for plasma insulin levels in diabetic patients at D0 being 11.5 ± 8.2 (9.35, 13.7) and 12.3 ± 8.9 (9.9, 14.7) at D8. However, D8 insulin levels were found to be notably higher compared to the ND insulin levels; indicating that diabetic patients were hyperinsulinemic compared with non-diabetic subjects (Figure 4.1b).

(a) Mean plasma glucose

(b) Mean plasma insulin
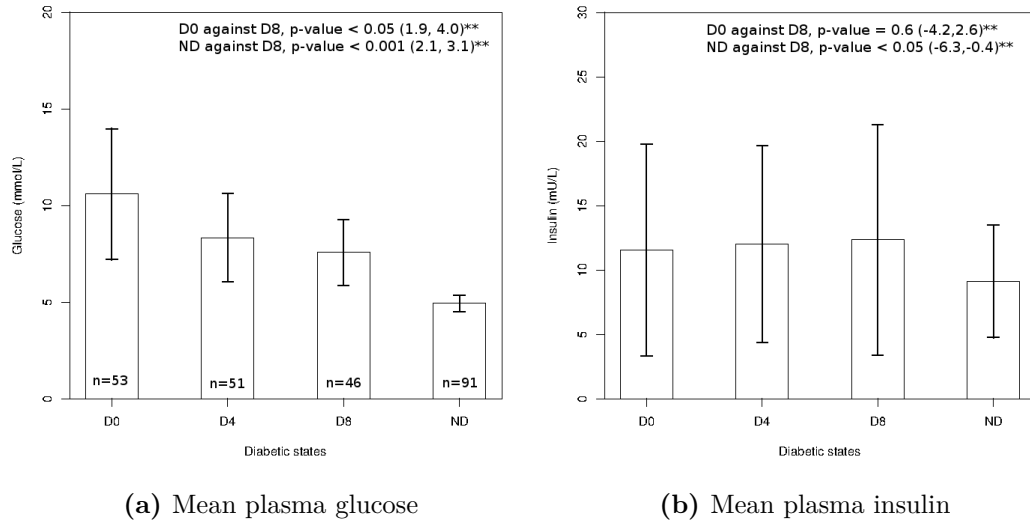
Figure 4.1: Serial change in the average plasma glucose (figure 4.1a) and insulin levels (figure 4.1b) levels in diabetics kept on the antidiabetic treatment for 8 weeks. D0: Diabetic values at 0 week (n=53); D4: Diabetic values at 4 week (n=51), D8: Diabetic values at 8-weeks (n=46) and ND: Non-diabetic values at 0 and 8 weeks (n=92). Figure 4.1a shows serial changes in mean±sd (bootstrapped CI for the mean) values of plasma glucose corresponding to D0, D4, D8 and ND. ND values lie in the physiological range of 4.92±0.4 (4.84, 5.0). The D0, D4 and D8 values being 10.6 ± 3.4 (9.6, 11.5), 8.3 ± 2.3 (7.7, 9.0) and 7.6 ± 1.7 (7.1, 8.0), respectively. Comparison of the mean plasma glucose at D0 and D8 shows statistical significance, with *p-value*<0.001 with CI for the difference between the means of (35.6,73.8). Also, the difference between D8 and ND plasma glucose values was significantly higher with *p-value*<0.001, CI for the difference between the means=(39.0, 57.3). Figure 4.1b shows serial changes in mean±sd (bootstrapped CI for the mean) values of plasma insulin corresponding to D0, D4, D8 and ND being 11.5 ± 8.2 (9.4, 13.7), 12.0 ± 7.6 (10.0, 14.0), 12.3 ± 9.0 (10.0, 14.7) and 9.1 ± 4.4 (8.23, 10.0), respectively. There is, however, a slight increase in the insulin secretion at D8, comparison of means between D0 and D8 was not statistically significant, with *p-value*=0.6, CI for the difference between the means=(-4.2,2.6). However, insulin levels at ND were found to be marginally but significantly lower compared to D8 with *p-value*<0.05, CI for the difference between the means=(-6.3,-0.4).

4.3.2 Antidiabetic treatment significantly improves β-cell function but not insulin sensitivity in diabetic patients

Insulin resistance and impaired insulin secretion along with hyperglycemia are the salient features of the type 2 diabetes. Enhanced glucose levels are known to aggravate insulin resistance and hamper insulin secretion. Homeostatic Model Assessment (HOMA) indices, namely, HOMA2-IR and HOMA-%B, are popularly used in the clinical trials as surrogate measures of insulin sensitivity and insulin secretion (or β-cell dysfunction), respectively. We used HOMA2-IR and HOMA-%B indices of the study subjects to observe the impact of antidiabetic drug treatment on the improvement of diabetic status. For more information about calculations of HOMA indices refer to Appendix Section 5.3.

Mechanistically, a reduction in hyperglycemia is expected to decrease IR and improve β-cell dysfunction. Figures 4.2a and 4.2b show serial changes in the mean-HOMA2-IR and mean-HOMA-%B against diabetic states in study subjects, respectively. Mean-HOMA2-IR was found to be lowered in diabetic patients over the study period with mean±sd (with corresponding bootstrapped CI for the mean) of 2.1±1.4 (1.7, 2.5) at D0 compared to 2.0±1.3 (1.63, 2.37) at D8. However, this IR improvement was not statistically significant (Figure 4.2a). On the contrary, insulin secretion as measured by HOMA-%B was found to be significantly improved after the antidiabetic treatment (mean±sd (with corresponding bootstrapped CI for the mean) for D8 mean-HOMA-%B being 75.4±52.6 (60.6, 90.2) against D0 mean-HOMA-%B of 45.6± 33 (36.7, 54.5); Figure 4.2b). On an average, HOMA-%B shows an inverse relationship with the glycemic status. Thus, antidiabetic treatment improves β-cell function but not insulin sensitivity.

4.3.3 Improvement in the β-cell function is correlated with increased GSH_t levels in diabetics over the study period

Overproduction of mitochondrial ROS is a key mechanism through which hyperglycemia leads to PDCs (Brownlee [26]; Giacco and Brownlee [27]). Therefore, restoration of GS would be expected to restore oxidative imbalance at least partially, and improve diabetic

(a) HOMA2-IR against glucose   **(b)** HOMA-%B against glucose
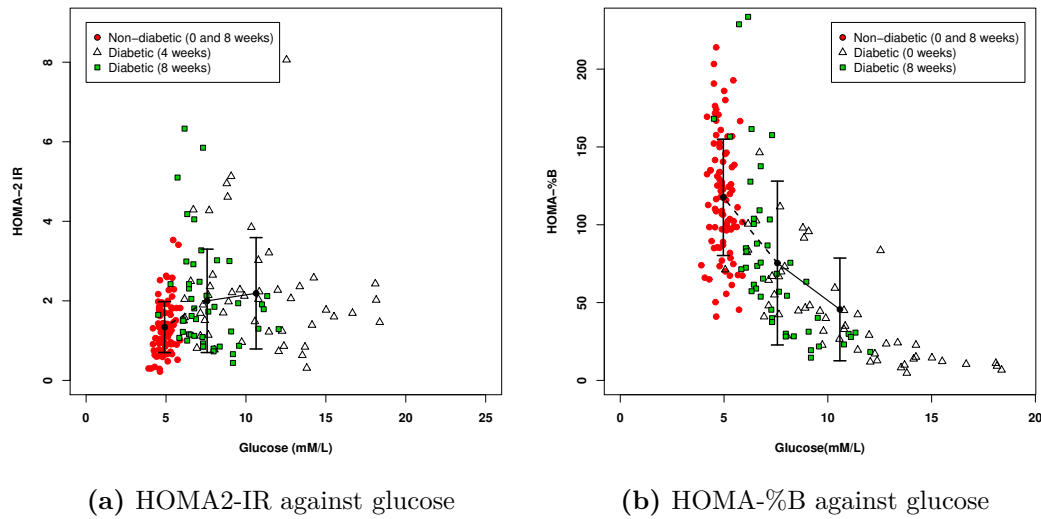
Figure 4.2: Serial changes in the average HOMA2-IR (Figure 4.2a) and HOMA-%B (Figure 4.2b) against plasma glucose for diabetics kept on antidiabetic treatment. Red filled circle: ND at 0 and 8 weeks (n=92); Open triangles: D0 (n=53); Green filled rectangles: D8 (n=47). The bold line indicates serially observed change in the diabetic HOMA scores from D0 to D8, while the dotted line shows projection to the asymptotic values of ND HOMA scores, if diabetic patients were to continue on the therapy for longer time period. Figure 4.2a shows average reduction in HOMA2-IR values from D0 (2.13 ± 3.7, (1.7,2.5)) to D8 (2.0 ± 1.3, (1.6,2.4)), although not significant (*p-value* $= 0.6$, CI for the difference between the means being (-0.67,0.4)). Figure 4.2b shows that HOMA-%B scores were significantly improved after therapy with mean$\pm$sd (bootstrapped CI for the mean) values being 45.6 ± 33 (36.7,54.6) at D0 to 75.4 ± 52.6 (60.6,90.2) at D8 (*p-value*<0.05, CI for the difference between the means being (12.0,47.5)). The ND mean$\pm$sd (bootstrapped CI for the mean) values for HOMA2-IR (1.34 ± 0.64 (1.21,1.47)) and HOMA-%B (118 ± 37.6 (110,125)) are provided for the reference. Figure 4.2a is reproduced from Kulkarni *et al.* [126], published as Figure S12 in the Supplementary information.

(a) HOMA2-IR against GSH_t **(b)** HOMA-%B against GSH_t
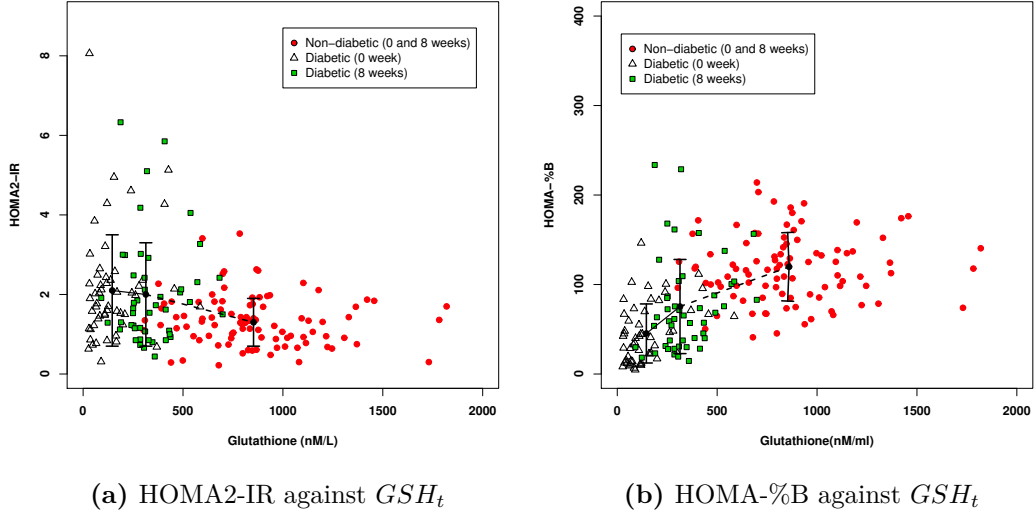
Figure 4.3: Serial changes in the mean-HOMA2-IR (Figure 4.3a) and mean-HOMA-%B (Figure 4.3b) against GSH_t in study subjects. Red filled circle: ND at 0 and 8 weeks (n=92); Open triangles: D0 (n=53); Green filled rectangles: D8 (n=47). The bold line indicates serially observed change in the diabetic HOMA scores from D0 to D8, while the dotted line shows projection to the asymptotic values of ND HOMA scores, if diabetic patients were to continue on the therapy for longer time period. Reduction in the glycemic load was reflected in the serial mean-GSH_t levels. The mean±sd (bootstrapped CI for the mean) GSH_t values for D0, D8 and ND being 145 ± 122 (112,179), 341 ± 134 (302,379) and 860 ± 311 (797,922), respectively. The mean±sd (bootstrapped CI for the mean) values for HOMA scores was provided in the Figure 4.2. Figure 4.3b is reproduced from Kulkarni *et al.* [126], published as Figure S13 in the Supplementary Information.

status. To enquire whether OS improvement is also associated with improvement in the diabetic condition, we correlated HOMA scores with the GSH_t , as a measure of OS. Figure 4.3b shows that HOMA-%B but not HOMA2-IR is positively correlated with GSH_t (Figure 4.3b). In fact, HOMA2-IR as a function of GSH_t remained unchanged over the study period (Figure 4.3a). Based on our analysis we propose that glucose intervention may alleviate diabetic status via improving OS (as measured in terms of GSH_t).

4.3.4 GSH_t shows age-dependence in non-diabetic individuals but not in diabetic patients

We observed that the age-groups of non-diabetic subjects and diabetic patients were significantly different (see Appendix Section 4.5.1, Table 4.1). Age-matched grouping was required to compare the non-diabetic and diabetic OS with respect to GS. We performed a linear regression of GSH_t against age in non-diabetic and diabetic subjects (Figure 4.4). We found that GSH_t showed dependence on age in non-diabetic subjects (Figure 4.4a), but not in diabetic patients (Figure 4.4b). Further, we noticed that non-diabetic GSH_t levels show two distinct clusters above and below 40 age-groups (Figure 4.4a). Therefore, we divided non-diabetic and diabetic subjects in above and below 40 age-groups, based on approximate age-matching with non-diabetic clusters. Also, we found that within the above 40 age-group, GSH_t levels were not dependent on age, BMI or gender (see Appendix Section 4.5.4, Table 4.3). However, age-dependence was observed in the non-diabetic below 40 age-group (see Appendix Section 4.5.4, Table 4.4). Therefore, GSH_t cluster-analysis is presented for above 40 age-group. The GSH_t cluster-analysis details for below 40 age-group are provided in the Appendix Section 4.5.6.

4.3.5 GSH_t is a classifier of diabetic states in the above 40 age-group

Hyperglycemia is known to be associated with lower GSH_t levels in diabetic patients. Therefore, systematic reduction in the HG is expected to relieve OS and improve GSH_t levels concomitantly. To establish whether OS improves with the antidiabetic treatment, we correlated GSH_t with HbA_{1c} of non-diabetic subjects (ND: 0 and 8-weeks) and diabetic patients from before therapy 0 week (D0) and after 8-weeks of antidiabetic treatment (D8). Figure 4.5 shows a cluster-histogram of GSH_t against HbA_{1c} for ND, D0 and D8 for the above 40 age-group. HbA_{1c} reflects fluctuations in the glucose load over the period of past three months and, therefore, considered as a stable marker of GS. ND HbA_{1c} values were found to lie between standard non-diabetic HbA_{1c} range of 30-47.3 (mmol/mol), with the $mean \pm sd$ (bootstrapped CI for the mean) of 40±4 (38,42). After 8-weeks of antidiabetic treatment,

59
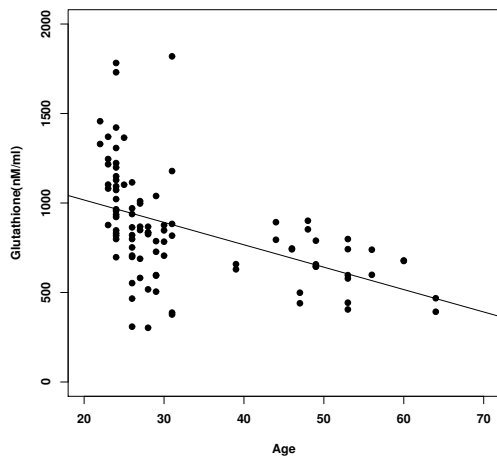
(a) GSH_t against Age, Non-diabetics
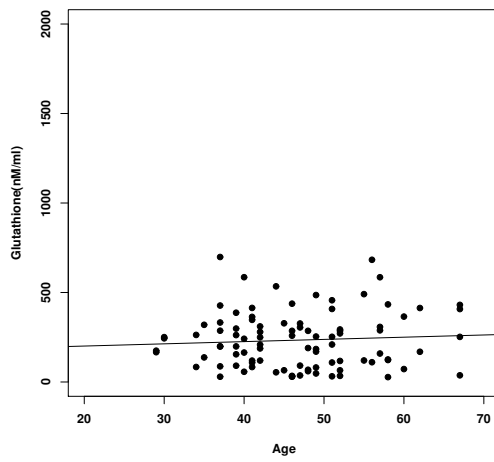
(b) GSH_t against Age, Diabetics

Figure 4.4: Linear regression of GSH_t against age in non-diabetics (n=94) and diabetic (n=98) subjects taken over 0 and 8 weeks. Figure 4.4a shows that GSH_t levels were affected due to aging in non-diabetics. The regression equation for this relationship being $GSH_t = 1267 - 12.5 \times$age (*p-value* <0.001). On the other hand, GSH_t levels in diabetics were not dependent on age. The regression equation for this relationship being $GSH_t = 176 - 1.2 \times$age, with the *p-value* = 0.4. Figure 4.4a is reproduced from Kulkarni *et al.* [126], published as Figure S14 in the Supplementary Information.

diabetic HbA_{1c} values showed a downward shift in the $mean \pm sd$ (bootstrapped CI for the mean) from 86.3±23.8 (79,94) at D0 to 60.7±11 (57.5,64) at D8. D0 HbA_{1c} values showed a wider distribution with the range of 52-150, which reduced to 44-83 after 8 weeks. The concomitant changes were noticed in the GSH_t distributions. At the beginning at D0, the GSH_t levels had narrow distribution range of 27-585 (nM/ml) with the $mean \pm sd$ (bootstrapped CI for the mean) of 124 ± 121 (90, 163) which shifted upwards to $mean \pm sd$ (bootstrapped CI for the mean) of 342 ± 123 (308, 381) and the wider GSH_t range of 122-682 at D8. The ND GSH_t distribution was ahead of D8 with $mean \pm sd$ (bootstrapped CI for the mean) of 657 ± 156 (595, 719) with a wide range of 392-900. The additional information about the approximately fitted distributions shown in Figure 4.5 is given in the Appendix Section 4.5.5, Table 4.5.

To use a biomarker to monitor disease progression, it should track pathogenesis of the disease. In other words, it should be able to classify individuals based on the distinct disease states. We used GSH_t levels from above and below 40 age-groups to establish whether, GSH_t levels are sufficient to define diabetic states, along with the GS markers. Our analysis on the population histograms showed that there is a clear distinction of different diabetic states with respect to GSH_t levels. To establish this demarcation quantitatively, we performed a cluster analysis on the GSH_t values, pooled from ND, D0 and D8 (Figure 4.5). Interestingly, we found that three distinct GSH_t clusters emerge out of the analysis corresponding to the respective diabetic state, namely, 0-220 (nM/ml) correspond to D0; 220-480 (nM/ml) corresponding to D8 "recovery phase" and 480-1000 (nM/ml), the ND band. Cluster analysis suggests that GSH_t classification follows the diabetic classification based on fasting glucose ranges and hence GSH_t can be used to classify individuals based on their diabetic state. We speculate that GSH_t ranges can be an excellent tracker of diabetes progression.

We also analysed GSH_t values in the below 40 age-group. However, due to few data points in the diabetic group (n=11), the results were not conclusive. Nevertheless, the below 40 age-group cluster analysis is described in Appendix Section 5.6.
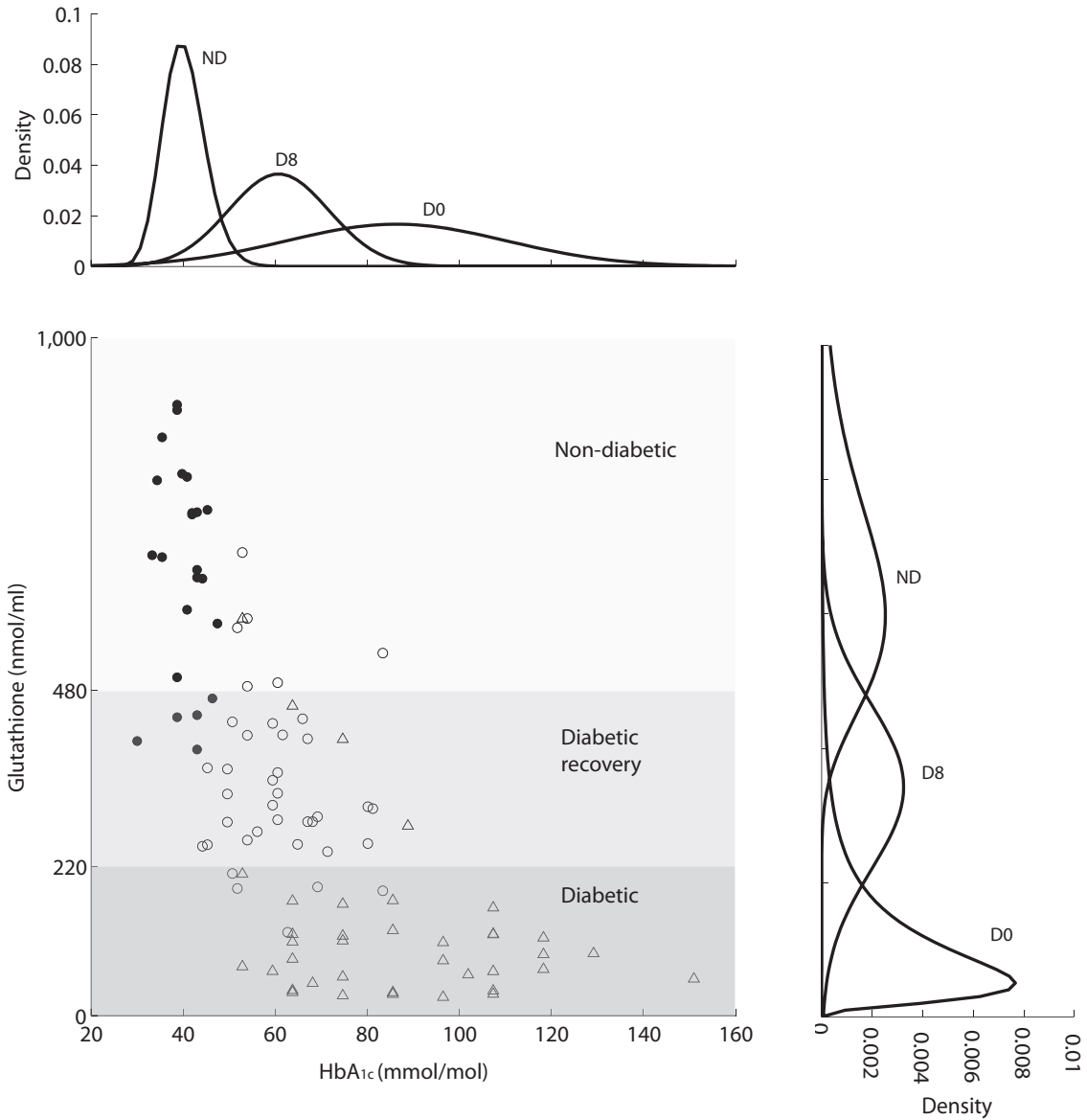
Figure 4.5: Cluster analysis of GSH_t values pooled together from ND, D0 and D8, above 40 age group. ● : ND (n=23), ○ : D0 (n=38), △ : D8 (n=38). Three distinct classes of GSH_t (nM/ml) emerge out of the cluster analysis: Diabetic phase corresponding to D0 (0-220); Diabetic recovery phase corresponding D8 (220-480) and non-diabetic phase corresponding to ND (480-1000). The corresponding histograms represent fitted distributions to HbA_{1c} and GSH_t. The estimated parameter values for the approximately fitted distributions are given in the Appendix Section 4.5. Figure reproduced from Kulkarni *et al.* [126], published as Figure 2 in the paper.

4.4 Discussion

In this chapter, we correlated blood GSH_t levels with the glycemic marker HbA_{1c} in the diabetic patients. We explored in detail whether GSH_t levels can predict the diabetic status of an individual, independent of the plasma glucose or HbA_{1c} levels. We performed hierarchical cluster analysis on GSH_t levels pooled from non-diabetic and diabetic at 0 and 8-weeks time points. We found that following GSH_t ranges emerge out of the cluster analysis: (1) 0-220 (nM/ml): poor antioxidant defence associated with the newly diagnosed diabetic state (2) 220-480 (nM/ml): diabetic recovery phase after antidiabetic treatment and (3) 480-1000 (nM/ml): normoglycemic state of non-diabetics. Interestingly, this GSH_t based classification matches with the glucose based diabetic classification. In other words, we showed that GSH_t could be used to classify individuals with diabetic status independent of glucose levels. So far, only plasma glucose and HbA_{1c} have been used to track the progression of diabetes. Based on our results, we propose that blood GSH_t can be used to monitor the diabetes progression along with glucose.

An important aspect that emerges out of this analysis is how the age of an individual can be utilised in proposing diabetes diagnosis. We noted two observations regarding age-dependence and GSH_t levels in the study population (see Figure 4.4): (a) GSH_t does not show age-dependence in diabetic conditions (b) Diabetic and non-diabetic GSH_t levels differ significantly. Since, age is an important confounding factor in comparing the OS state of diabetic and non-diabetic individuals; we need to account for the effect of age on the GSH_t levels for the sake of comparison. There are two possible ways to account for age while comparing non-diabetic and diabetic GSH_t levels. One is doing age-correction collectively on ND, D0 and D8 GSH_t values, using multiple linear regression. However, since the groups were not age-matched as a part of the study design, this wouldn't give an exact idea about age-correction that should be imposed while comparing two groups. Also, we think this would make an erroneous change in the diabetic GSH_t values. Therefore, we preferred age-matching over age-correction while doing cluster-analysis. We divided both non-diabetic

and diabetic groups in above and below 40 age-groups for cluster-analysis. Above 40 age-group shows interesting GSH_t ranges as associated with diabetic states. However, below 40 age-group didn't show GSH_t ranges mostly due to lack of enough data points (see Appendix Section 4.5.6, Figure 4.6). Nevertheless, this analysis demonstrates a possibility that different clustering schemes would evolve based on the ageing status. Our population study, albeit with small sample size, calls for the large longitudinal population studies to decipher agewise GSH_t ranges associated with progression of diabetes stages.

We found that glucose control leads to improvement in the β-cell dysfunction but not insulin sensitivity (see Figure 4.2). HOMA indices make use of fasting glucose and insulin values to calculate HOMA2-IR and HOMA-%B scores. In our population study, we observed that fasting insulin values remain almost unchanged over the study period in diabetic patients (see Figure 4.1b). Therefore, changes in HOMA-%B can be mostly attributed to the reduction in the fasting glucose values and not insulin levels. On the other hand, HOMA2-IR scores remain unchanged in diabetic patients. One reason might be the action of drugs used for diabetes treatment. Almost 60% of the diabetic patients were given gliptins to control blood glucose. Gliptins typically act through altering gluconeogenesis in the liver and improving insulin secretion in the pancreas. We infer that the reduction in the plasma glucose levels would be mostly due to altered liver glucose output, and there may not be substantial contribution from the changes in the IR. We also noticed that improvement in the HOMA-%B scores was found to be positively correlated with GSH_t levels (see Figure 4.3b). Whether, enhancement in HOMA-%B and GSH_t levels are two independent effects of the glucose control or OS causally influences HOMA-%B scores is not clear. However, GSH infusion studies in diabetics and also in non-diabetics showed an overall improvement in the glucose homoeostasis and insulin secretion Paolisso *et al.* [122]; De Mattia *et al.* [123]; Marfella *et al.* [124]). Hence, plausibility that OS is a causal link through which glucose control improves diabetic status may not be denied.

The systematic increase in the erythrocyte GSH_t levels corresponding to reduced glycemic load indirectly suggests that GSH synthesis capacity is still retained in diabetic patients. For

instance, Whillier *et al.* used diabetic RBCs to show that activity of the enzyme GSH synthetase is retained in the diabetic state. This would have a major implication from the clinical perspective [121]. Reducing glycemic load is one way to improve GSH turnover. Another way would be supplementation of amino acids essential for GSH synthesis, which would aid in reducing DC rate.

Our study speculates that the GSH_t ranges could be a useful way to define on an average how much OS control needs to be enforced for controlling diabetes progression. Further, tracking GSH_t as a marker of OS might be useful to account for age-dependent metabolic changes in the diabetes management.

4.5 Appendix

4.5.1 Anthropomorphic characteristics of the non-diabetic subjects and diabetic patients

In the non-diabetic group, two subjects were removed: Case 14 developed diabetes during the study period and Case 16 was removed due to missing data. Five diabetic patients were removed due to missing data points either in glucose and GSH_t (Cases 5,8,53) or BMI (Cases 42,48). Anthropomorphic characteristics of 48 non-diabetic subjects and 49 diabetic patients are given in the Table 4.1.

Characteristic		Non-diabetic	Diabetic
Gender	Female	23	22
	Male	25	27
Age	Mean $\pm$ Std. Dev.	32.8 $\pm$ 11.78	47.8 $\pm$ 10.5
	Range	22-64	29-76
BMI	Mean $\pm$ Std. Dev.	23.75 $\pm$ 3.2	26.0 $\pm$ 3.6
	Range	16.8-33.3	20.3-41.6

Table 4.1: Summary of anthropomorphic characteristics: gender,age and BMI of study subjects. Table 4.1 is reproduced from Kulkarni *et al.* [126], published as Table S1 in the Supplementary Information.

4.5.2 Details of the antidiabetic drug treatment given to diabetic patients

Details of the antidiabetic medication given to 48 diabetic patients over the period of 8-weeks are given in the Table 4.2.

Drug treatment	Number of diabetics
DPP-4 inhibitor	28
Biguanide	10
Biguanide and sulphonamides	10

Table 4.2: Summary of the antidiabetic drug treatment. Out of 48 diabetics, 58% received DPP-4 inhibitor or gliptin treatment, 21% were given biguanide drug treatment and remaining 21% were kept on combination of biguanides and sulphonamides. Table 4.2 is reproduced from Kulkarni *et al.* [126], published as Table S2 in the Supplementary Information.

4.5.3 Details of the calculation of HOMA2-IR and HOMA-%B scores

Insulin sensitivity is defined as the whole-body glucose uptake rate in the presence of insulin. Defronzo *et al.* [40], developed a method in 1979 to measure insulin sensitivity. This method is called as "glucose-clamp" method. An artificial hyperinsulinemic condition is maintained in the study subject and glucose is infused so as to retain particular plasma glucose level in the blood. Insulin sensitivity is defined by the glucose infusion rate which is required to maintain particular plasma glucose levels in the blood. For example, if a person is insulin resistant, the whole body glucose uptake rate would be reduced. Therefore, lower glucose infusion rates will be required to maintain desired plasma glucose levels, contrary to a person who is relatively less insulin resistant. This method is considered as the "Gold-standard"for measurement of insulin sensitivity. However, it is labour-intensive and tedious to put into practice, especially for large clinical trials. Therefore, several surrogate insulin sensitivity indices were developed which make use of fasting plasma glucose and insulin values to predict insulin resistance in the body (Muniyappa *et al.* [129]). Of the several surrogate indices, HOMA indices are popularly used in the clinical trials. They are found to be highly correlated with the results of glucose clamp method (Matthews *et al.* [130]; Levy *et al.* [131]; Bonora *et al.* [132]). HOMA2-IR is a surrogate index for whole body insulin sensitivity and HOMA-%B is used

to predict β-cell functionality.

HOMA (now designated HOMA2-IR) was originally a simple formula that was a product of the two quantities fasting plasma glucose and fasting plasma insulin given by [133],

$$HOMA = \frac{FPG \times FPI}{405}, \tag{4.1}$$

where FPG is expressed in mg/dL and FPI in mU/L.

Levy *et al.* proposed a modified version of HOMA, for which an online HOMA2-IR and HOMA-%B calculator is available on the University of Oxford, Clinical Trial Unit webpage [131]. We used this online HOMA2-IR and HOMA-%B calculator to obtain HOMA scores of study subjects and used the as surrogate measures of insulin sensitivity and β-cell dysfunction in our analysis.

4.5.4 Multiple linear regression of GSH_t dependence on Age and BMI in above-40 and below-40 age groups

Non-diabetic subjects and diabetic patients were divided into two age-groups: above and below age 40. Multiple linear regression was performed to assess within group age and BMI dependence on GSH_t levels in non-diabetics as well as diabetic group.

We observed that within the above-40 age group, GSH_t was not influenced by age or BMI (Table 4.3). However, age-dependence was observed in non-diabetic subjects below-40 age group (Table 4.4). Therefore, age and BMI can be removed as confounding factors while interpreting cluster analysis results for above-40 age group, but not for below-40 age group.

4.5.5 Additional statistical details pertaining to Figure 4.5.

Table 4.5 gives details of the fitted distributions along with mean±sd values obtained for fitted curves for GSH_t and HbA_{1c} histograms in the Figure 4.5. Each populations were *approximately* fitted either to a normal or log-normal distribution as indicated. Parameters of the normal and log-normal distributions (mean and standard deviation) were obtained in MATLAB using the functions *normfit()* and *lognfit()*, respectively. The Shapiro-Wilk test

Non-diabetics		
Predictor variable	**Coefficient**	**p-value**
Intercept	1021	0.122
BMI	10.47	0.58
Age	-12.5	0.18
Diabetics		
Predictor variable	**Coefficient**	**p-value**
Intercept	111.5	0.6
BMI	-3.76	0.62
Age	2.16	0.34

Table 4.3: Multiple linear regression of 0-week GSH_t with Age and BMI, in non-diabetics (n=23) and diabetics (n=38) above age 40. Both age and BMI are not significant predictors of GSH_t within non-diabetic and diabetic groups, as shown by corresponding *p-values*. Table 4.3 is reproduced from Kulkarni *et al.* [126], published as Table S3 in the Supplementary Information.

for normality and q-q plots were used to confirm the normality. The distributions given are approximations, standard Student's t-test was used for the comparative purpose and bootstrapped CI intervals were provided wherever required.

Cluster analysis was performed as described in the statistical methods section 4.2.3.

Table 4.6 shows distribution of ND, D0 and D8 percentages observed in each cluster. In cluster 1: 22% of the values correspond to D0, 71% correspond to D8 and remaining 8% correspond to ND. Cluster 2 contains 13% of the GSH_t values corresponding to D8 and 34% corresponding to D0, but there are no ND values. Cluster 3 comprised of 78% ND, 3% D0 and 16% of D8.

4.5.6 Cluster analysis results of GSH_t values for diabetics and non-diabetics below age 40

We performed a heirarchical cluster-analysis on GSH_t values pooled from ND, D0 and D8 in below age 40 (Figure 4.6).

Table 4.7 shows the $mean \pm sd$ of GSH_t and HbA_{1c} of each of the populations, diabetic and non-diabetic, at 0 and 8-weeks, below 40 age-group. Each population was fitted either to a normal or log-normal distribution as indicated. The Shapiro-Wilk test for normality
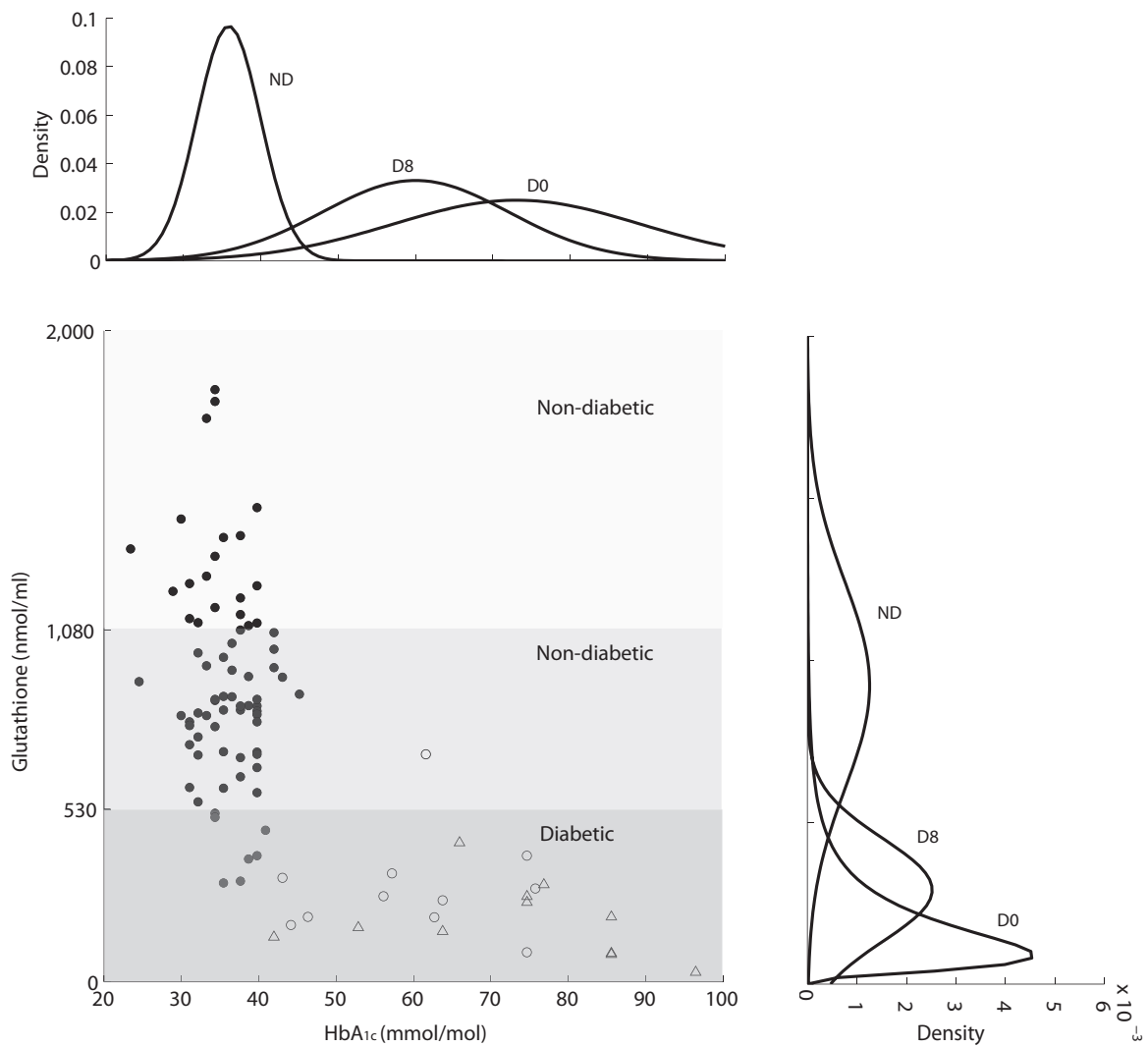
Figure 4.6: Cluster analysis of GSH_t values pooled together from non-diabetics and diabetics at 0 and 8-weeks, below age 40. • : non-diabetics 0 and 8-weeks (n=72), ∘ : diabetics 0-week (n=11), △ : diabetics 8-weeks (n=11). Three clusters emerged out of the cluster analysis. Unlike the cluster analysis for the age group above 40, below 40 GSH_t values do not show separation within diabetic groups at 0 and 8-weeks. However, non-diabetic below 40 age group is separated into two clusters. Figure 4.6 is reproduced from Kulkarni *et al.*, Supplementary Information [126], earlier published as Figure S1 in the Supplementary Information.

Diabetics		
Predictor variable	**Coefficient**	**p-value**
Intercept	111.5	0.6
BMI	-3.76	0.62
Age	2.16	0.34
Non-diabetics		
Predictor variable	**Coefficient**	**p-value**
Intercept	1779	0.001
BMI	18.3	0.29
Age	-47.1	0.009

Table 4.4: Multiple linear regression of 0-week GSH_t with age and BMI, in non-diabetics (n=36) and diabetics (n=11) below age 40. In both groups, BMI is not significant predictor of GSH_t . However, age predicts GSH_t in non-diabetics, but not in diabetics. Table 4.1 is reproduced from Kulkarni *et al.* [126], published as Table S4 in the Supplementary Information.

and q-q plots were used to confirm the normality. Parameters of the normal and log-normal distributions (mean and standard deviation) are obtained in MATLAB using the functions *normfit()* and *lognfit()*, respectively.

Table 4.8 shows statistics of a hierarchical cluster analysis performed on the below 40 age-group non-diabetic and diabetic GSH_t values pooled from 0 and 8-weeks. Euclidean distance measure was used to produce the distance matrix and Ward's method was used to perform hierarchical clustering. In cluster 1, 60% of the values correspond to non-diabetics, 9% correspond to 8-week diabetics but no 0-week diabetics. Cluster 2 corresponds to only 30% of the all non-diabetics. Cluster 3 contains 10% correspond to 0-week diabetics, 91% diabetics at 8-weeks and 78% of the non-diabetics.

	Fitted distribution	Mean	Standard deviation
GSH_t **(nmol/ml)**			
Non diabetic	Log-normal	620.9	157.6
Diabetic 0 week	Log-normal	121.0	108.9
Diabetic 8 weeks	Normal	342.4	123
HbA_{1c} **(mmol/mol)**			
Non diabetic	Log-normal	36.8	4
Diabetic 0 week	Normal	86.3	23.8
Diabetic 8 weeks	Normal	60.7	10.9

Table 4.5: Mean and standard deviation values corresponding to normal or log-normal probability density curves fitted to GSH_t and HbA_{1c} levels of non-diabetics and diabetics shown in the Figure 4.5. Table 4.5 is reproduced from Kulkarni *et al.* [126], published as Table S5 in the Supplementary Information.

	ND(0 and 8-weeks)	D0	D8
Cluster 1	5	3	27
Cluster 2	0	34	5
Cluster 3	18	1	6

Table 4.6: A hierarchical cluster analysis performed on GSH_t values of non-diabetics (n=23) , diabetics at 0 week (n=38) and diabetics at 8 weeks (n=38) showed 3 clusters emerging from the data. For instance, cluster 1 is comprised of 3 diabetics at 0-week, 27 diabetics from 8-weeks and 5 non-diabetic subjects. Table 4.6 is reproduced from Kulkarni *et al.* [126], published as Table S6 in the Supplementary Information.

	Fitted distribution	Mean	Standard deviation
GSH_t **(nmol/ml)**			
Non diabetic	Normal	922.0	317.0
Diabetic 0 week	Log-normal	195.0	166.0
Diabetic 8 weeks	Normal	290.0	158.0
HbA_{1c} **(mmol/mol)**			
Non diabetic	Normal	35.8	4.1
Diabetic 0 week	Normal	73.0	15.9
Diabetic 8 weeks	Normal	60.0	12.0

Table 4.7: Mean and standard deviation values corresponding to normal or log-normal probability density curves fitted to GSH_t and HbA_{1c} levels of non-diabetics and diabetics below age 40. Table 4.7 is reproduced from Kulkarni *et al.* [126], published as Table S7 in the Supplementary Information.

	Non-diabetics (0 and 8 weeks)	Diabetics (0 week)	Diabetics (8 weeks)
Cluster 1	43	0	1
Cluster 2	22	0	0
Cluster 3	7	11	10

Table 4.8: A hierarchical cluster analysis performed on GSH_t values of non-diabetics (n=72) 0 and 8 weeks together, diabetics at 0 week (n=11) and diabetics at 8 weeks (n=11) showed 3 clusters emerging from the data. Table 4.8 is reproduced from Kulkarni *et al.* [126], published as Table S8 in the Supplementary Information.

Chapter 5

A physiological model of the OS response to GS in diabetic patients

5.1 Introduction

Mitochondrial overproduction of ROS is a **unifying** mechanism of the hyperglycemia-mediated development of PDCs (see Chapter 2, Section 2.3). A schematic representation of the role of OS in the development of PDCs is depicted in Figure 5.1. The theory suggests a plausible approach to reduce progression of diabetes: controlling OS internally using antioxidants is to reduce PDCs.
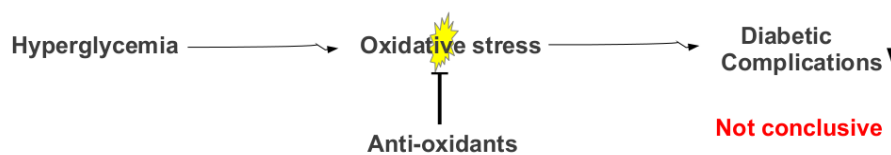
Figure 5.1: A schematic representation of OS as a central causal link in the hyperglycemia-mediated development of PDCs. Therefore, direct intervention of OS using antioxidant molecules is expected to reduce the rate of diabetic complications.

Several nonenzymatic systemic antioxidant molecules have been used to establish the role of OS in the development of diabetic vascular disorders. These antioxidant molecules include fat soluble vitamins C, E and A, vitamins of B-complex group (B1, B2, B6 and B12), trace

elements like copper, zinc and selenium, α-lipoic acid, co-enzyme Q10 (CoQ10), carotenoids, and cofactors like folic acid, uric acid, albumin, N-acetylcysteine and glutathione. Of these, vitamin E, C and α-lipoic acid are the most sought after antioxidant molecules for diabetes treatment. Vitamin C, E and α-lipoic supplementation in diabetic rats has shown to reduce or prevent rate of development of retinopathy or retinal abnormalities (Di Leo *et al.* [134]; Kowluru *et al.* [135]), nephropathies (Kedziora-Kornatowska *et al.* [136]), neuropathy (Johansen *et al.* [30]) and overall improvement in OS. α-lipoic acid has been especially proven to be useful in the treatment of diabetic animal models of neuropathy and nephropathy (Oyenihi *et al.* [137]; Shay *et al.* [138]).

The utility of antioxidants in clinical trials is inconclusive

Results of these animal studies when translated into clinical trials have, however, not turned out to be conclusive (Golbidi *et al.* [139]). Some of the trials involving a small number of patients and short study duration showed favourable outcomes. For example, combined therapy of Vitamin C and E supplementation has been shown to reduce urinary albumin excretion rate (Gaede *et al.* [140]). Vitamin E dose of 1000 IU/day showed promising results to normalise retinal and renal functions in diabetic patients (Bursell *et al.* [141]). A beneficial effect of the oral antioxidant Raxofelast was observed in diabetic patients in which it improved OS status measured in terms of lipid peroxidation marker: 8-epi-PGF2α (Chowienczyk *et al.* [142]). However, large clinical trials conducted based on small studies have failed to show a decisive role of antioxidants. The Heart Outcome Prevention Evaluation (HOPE) study, carried out on 3,654 diabetic patients for on an average of 4.5 years, showed none or neutral effect of vitamin E supplementation on cardiovascular disorders and nephropathies (Lonn *et al.* [98]). Millen *et al.* Another large-scale study showed that there is no significant association between vitamin E supplementation and diabetic vascular complications (Millen *et al.* [143]). Among other antioxidants, use of α-lipoic acid as an antioxidant has shown some promise in the treatment of diabetic nephropathies and is currently under investigation (Poh and Goh [144]; Hector *et al.* [145]). These clinical studies suggest that although experimentally OS has been implicated in the diabetic pathophysiology, and theoretically OS can be looked

like a lucrative target for controlling diabetes, **its utility is restricted by the lack of quantitation, which would help in designing how much and how long OS should be controlled with respect to GS.**

Since OS may not be regulated effectively using antioxidants, instead of controlling OS internally, we propose to monitor OS along with GS, as diabetes treatment progresses (see Figure 5.2). Hyperglycemia is known to produce enhanced levels of ROS in PDCs. Therefore, it is expected that controlling hyperglycemia would relieve OS, and since OS is causally involved in the development of PDCs, controlling OS will reduce the rate of PDCs. Thus, if variation in OS with respect to changes in the GS can be captured quantitatively, this could help us in predicting optimal glucose control in a personalised manner. An optimal glucose control would be that by which OS is maximally controlled, and therefore would reduce development of PDCs.
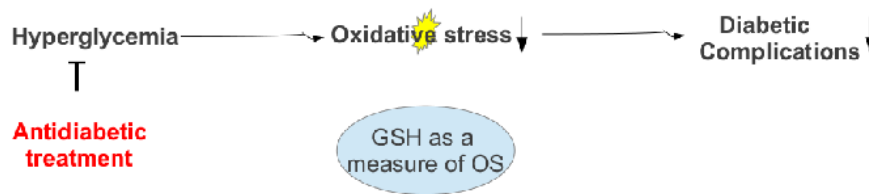
Figure 5.2: Monitoring OS status of an individual to define personalised glucose targets in diabetic patients. An optimal glucose control would be that by which OS is maximally controlled, and therefore would reduce development of PDCs.

The present chapter describes a minimal mathematical model of glutathione-glucose physiology to capture the **non-linear inverse** relationship between OS and GS for an individual. A minimal model is characterised by three parameters, namely, G_{tot}: the maximal GSH_t pool achieved by a diabetic patient when glucose is lowered to the normoglycemic range; v: glucose threshold at which GSH_t is half-maximal and k: the slope determining parameter of the curve (see Section 5.2 for logic and assumptions of the model and Appendix Section 5.5.1 for the model derivation). The model is fitted to four GSH-glucose pairs: 0, 4 and 8 weeks GSH-glucose values of an individual diabetic patient and an age-adjusted nondiabetic GSH-glucose pair computed for a given diabetic patient (see Section 5.3 for the calculations).

Therefore, the modelling process implicitly incorporates age of an individual. The parameter values vary for each diabetic patient, thereby capturing individual variation. We discuss the robustness of the curve fitting procedure accounting for the daily variation in GSH and glucose values. Finally, the utility of the model in predicting personalised glucose targets is illustrated by two case studies.

This work is previously published as Kulkarni *et al.* [126]. The figures and tables used in this chapter are reproduced under the creative commons attribution license.

5.2   A minimal mathematical model

5.2.1   Logic and assumptions of the model

Human clinical trials consistently show that hyperglycemia is associated with reduction in the blood GSH levels. As described in Chapter 2, we support this observation by showing that GSH levels are inversely related to HbA_{1c} levels in diabetic patients kept on an antidiabetic treatment. However, the essence of this argument is deeper than showing a qualitative inverse relation between the OS-GS axis; for instance what would be the quantitative relationship between OS and GS? Can we extrapolate from the existing observation and predict the functional relationship between the two variables? To address this question in depth, we argued in the following manner: Before therapy GSH_t levels in the newly-diagnosed diabetic patients were found to lie in the narrow band of 0-220 (nM/ml). Since diabetic patients were not exposed to any anti-diabetic treatment before the clinical trial, the 0-week GSH_t values can be considered as the lowest possible steady-state levels achieved due to prolonged uncontrolled hyperglycemia. Therefore, we inferred that there would be lower asymptotic GSH_t levels corresponding to the hyperglycemic end. On the other hand, there would be a physiological upper asymptote above which GSH_t levels may not rise in a normoglycemic state. Therefore, we proposed that GSH_t levels as a function of GS of an individual would have a **nonlinear, saturating, reversible** relationship, at least in the initial phase of diabetic recovery.

A minimal model is proposed based on GSH-glucose physiology to capture the inverse relationship between the OS and GS. Figure 5.3 portrays a simple schematic of GSH-glucose biochemistry. Excessive glucose metabolism generates superoxide radicals via TCA cycle in the mitochondrial electron transport chain. Excess superoxide radicals get converted into hydrogen peroxide (H2O2), after reacting with water molecule. Inside the cell, glutathione exists as reduced (GSH) and oxidised (GSSG) forms. GSH scavenges H2O2 generated from the energy metabolism, and produces GSSG and water molecule in the enzymatic process. This reaction is catalysed by the enzyme glutathione peroxidase (GPx). In turn, glutathione reductase (GR) converts GSSG back into the GSH utilising reducing equivalent NADPH. Following assumptions were made while putting up the minimal model:
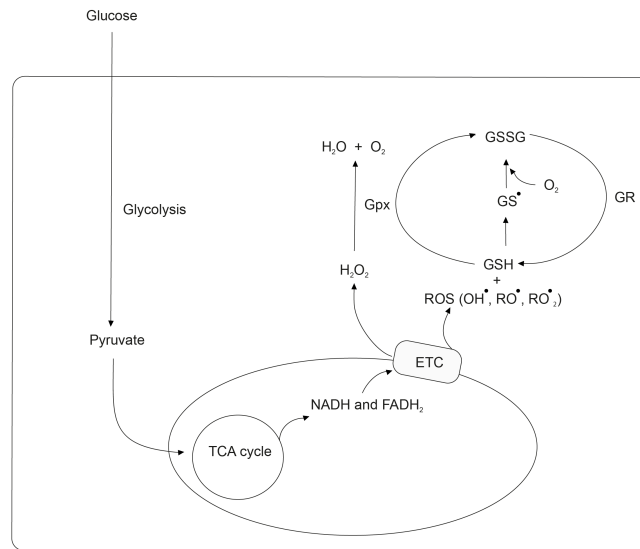
Figure 5.3: A simple underlying physiology of glutathione-glucose metabolism. ROS produced due to glucose metabolism is scavenged by reduced form of GSH and it gets converted into GSSG *via* the enzyme (glutathione peroxidase) GPx. GSH pool is replenished by the enzymatic action of glutathione reductase (GR). This figure is reproduced from Kulkarni *et al.* [126], published as Figure 1 in the paper.

1. Total free glutathione GSH_t, made up of GSH + GSSG, is conserved over the study period.

2. Plasma glucose would act as a proxy for the hydrogen peroxide, as it would represent

OS state of an individual

3. Glutathione peroxidase reaction would follow a Michaelis-Menten kinetics, with GSH and glucose as substrates

4. The conversion of GSSG to GSH by GR would have Michaelis-Menten kinetics, but it is assumed that NADPH, another substrate of the enzyme does not limit the rate of the reaction.

5. Almost more than 90% of the erythrocyte GSH_t pool is comprised of reduced form of the glutathione. Therefore, GSH is used as an approximation of measured GSH_t values in diabetic patients.

The rate of change of reduced form of the glutathione (GSH) is given by the Equ.(5.1). The net change in the GSH pool is due to the rate at which GSH utilised due to glucose metabolism (as a proxy for OS state inside the erythrocyte) and the rate at which GSH is produced from the oxidised form of the glutathione (GSSG). The detailed derivation and mathematical aspects of the Equ.(5.1) are provided in the Appendix section 5.5.1.

$$\frac{d[GSH]_b}{dt} = \frac{v(G_{tot} - [GSH])}{k + (G_{tot} - [GSH])} - \frac{[Glucose][GSH]}{k + [GSH]}. \tag{5.1}$$

The steady-state expression between GSH and glucose was derived by setting Equ.(5.1) = 0. The steady-state expression is a Goldbeter-Koshland (GK) functional form with nonlinear decreasing saturating relationship given by the Equ.(5.2). (see Appendix section 5.5.1 for

detailed derivation of the GK functional form).

$$GSH(Glu) = \frac{-(v \cdot G_{tot} - v \cdot k - Glu \cdot k - G_{tot} \cdot Glu) - \sqrt{\begin{array}{l} v^2 \cdot G_{tot}{}^2 + v^2 \cdot k^2 + k^2 \cdot Glu^2 \\ +Glu^2 \cdot G_{tot}{}^2 + 2 \cdot Glu^2 \cdot k \cdot G_{tot} \\ -2 \cdot G_{tot}{}^2 \cdot Glu \cdot v + 2 \cdot k^2 \cdot v \cdot Glu \\ +2 \cdot v^2 \cdot k \cdot G_{tot} - 4 \cdot Glu \cdot G_{tot} \cdot v \cdot k \end{array}}}{2 \cdot (Glu - v)}.$$

(5.2)

The Equ.(5.2) is characterised by three parameters: G_{tot}: the maximal total GSH pool for a diabetic patient; v: the threshold glucose value for which GSH is half-maximal and k: the slope parameter of the curve. The GK functional form was used to obtain individual diabetic fits.

5.2.2 Curve fitting procedure

Four GSH-glucose data points were used for each diabetic patient to obtain the fit: 0, 4 and 8-weeks GSH-glucose pairs and fourth non-diabetic GSH-glucose data point adjusted according to the age of a diabetic individual. In Chapter 2, we showed that GSH shows age-dependence in non-diabetic individuals (see Section 3.3, Figure 5a, Chapter 2). The regression between non-diabetic GSH against age was used to obtain age-adjusted non-diabetic GSH pool as the fourth point (see Equ.(5.3) for the reference). Age-adjusted GSH value was paired with the mean non-diabetic glucose value of 4.8 mM/L.

$$GSH = 1267 - 12.5 \times Age$$

(5.3)

GSH-glucose data points and GK functional form were provided as inputs to the *optim()* function in statistical software package R. Internally, Nelder-Mead algorithm was used to optimise the function and obtain parameters for each fitted OS-GS trajectory. The plotting of the curves and statistical analysis was performed in R.

5.3 Results

5.3.1 Minimal model captures unique GSH_t-glucose dose-response for each diabetic patient

We used steady-state GK functional form to fit diabetic GSH_t-glucose dose-response curves (Equ.5.2). Age-dependence on the OS is implicitly defined in the curve fitting procedure. In that, the asymptotic maximal GSH_t level for each diabetic patient would correspond to age-matched non-diabetic GSH_t value. We could fit 34 out of 49 diabetic dose-responses (Figure 5.4, without age-grouping). Above and below 40 age-group curves are provided separately for the reference in the Appendix section 5.5. The grey lines on the background show individual diabetic fits. The individualised diabetic curves along with parameter values are provided in the Appendix section 5.5.3. The solid black line is the population-averaged curve (PAC) computed over 34 fitted lines. Each curve is characterised by three parameter values, namely, G_{tot}: The maximal GSH_t pool for each diabetic individual; v: the threshold glucose value corresponding to half-maximal GSH_t levels and k: the slope parameter which would define steepness of the curve.

The PAC is parameterized by mean±sd of G_{tot}: 728 ± 128, v:7.5 ± 1.1 and k: 43.7 ± 40. The GSH_t shows *a biphasic graded response* to glucose therapy: hyperglycemia is associated with lower GSH_t levels, transiting to normoglycemic regimen associated with maximal GSH_t values. *Hyperglycemia to normoglycemia shift corresponds with a switch in the OS status* at an inflection point v (7.5 mM L) -the threshold glucose level at which GSH_t is half-maximal, denoted by the black dot on the PAC. The red portion of the black curve is the steepest region of the curve. It is a transition phase between hyperglycemia and normoglycemia. We call it as an "inflection region". The interesting feature emerged out of curve fitting is that the "pre-diabetic" zone as defined ADA (5.5-6.9 mmol/L) and WHO (6.1-6.9 mmol/L) overlaps with the upper portion of the inflection region. The individuals having pre-diabetic glucose values have a higher risk of developing diabetes and associated comorbodities. We infer that corresponding GSH values in this zone are deteriorated from the healthy GSH
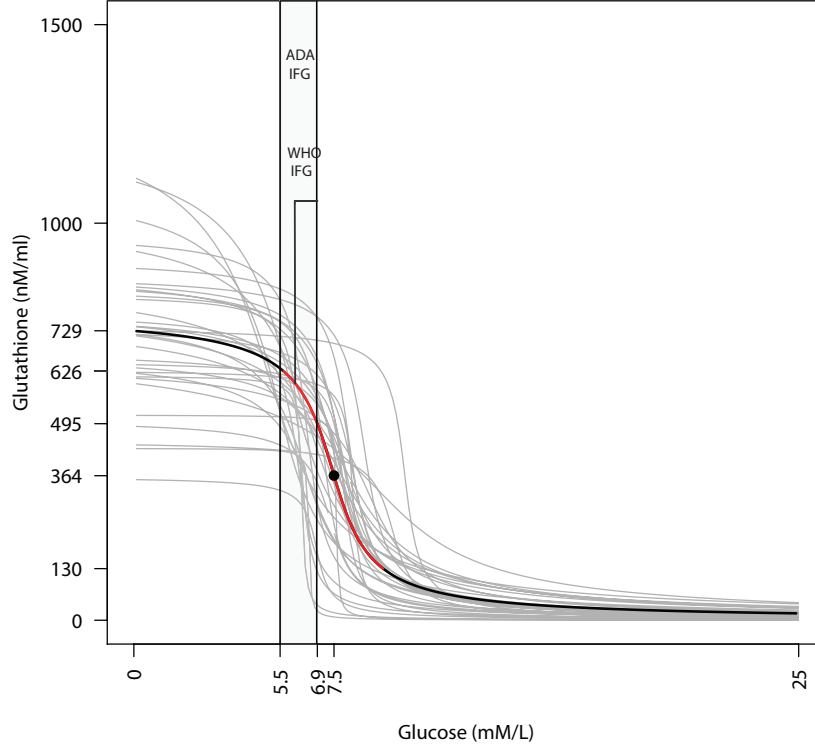
Figure 5.4: The GSH_t response to glycemic therapy is unique for each diabetic patient. The thin grey lines in the background are the individual dose-responses of diabetic patients captured using minimal model (n=34 out of 49). The bold black curve is the population-averaged profile taken over 34 curves. The black dot on the curve is the "inflection point" (glucose threshold $v = 7.5$mM/L), at which GSH_t is half-maximal. The G_{tot} for the average profile is 728 nM/ml and characterised by a slope parameter $k = 43.7$. The transition phase between hyperglycemia and normoglycemia is marked by a red portion, called as "inflection region" (roughly about $\frac{v}{4}$ around the inflection point). Interesting feature of the curve is that "impaired fasting glucose" (IFG) or "pre-diabetic" glucose range defined by ADA (5.5-6.9 mmol/L) and WHO (6.1-6.9 mmol/L), overlay the upper portion of the inflection region. Also, the after therapy 8-weeks GSH_t levels (220-480 nM/ml) occupy the lower portion of the inflection region. This figure is reproduced from Kulkarni *et al.* [126], published as Figure 3 in the paper.

levels. *Therefore we reinterpret "pre-diabetes" in terms of OS as GSH range between maximal and half-maximal GSH levels.* We postulate that individuals having GSH values in this zone would have a higher risk of developing full-blown diabetes. This has important implication for the personalised diabetes therapy. *Since OS may not be controlled precisely using antioxidant treatment; we propose to control glucose well below v, the inflection point, so that diabetic patient would get maximum benefit out of diabetes treatment in terms of improvement of OS status.*

On the other hand, we also found that 8-weeks diabetic GSH_t levels lie in the lower portion of the inflection zone. According to our hypothesis, the optimal glucose control would be when their GSH_t levels improve enough to lie in the "pre-diabetes" region. Individual diabetic curves show considerable deviation from the population curve and have unique parameter values which can be utilised in the personalisation of diabetes treatment.

5.3.2 Robustness of the curve fitting procedure

We fitted individual diabetic GSH_t-glucose dose-responses using minimal model. However, it is hard to determine whether the fitted trajectory would depict the actual GS-OS relationship. In other words, it is important to verify whether small perturbations around the GSH_t-glucose time points affect the curve fitting procedure. For instance, Blanco *et al.* [146] showed that there is around 15% diurnal variation in the blood GSH_t levels. Similarly, single time point reading of plasma glucose may not reflect an average change in the GS. Two approaches were used to account for these variations in the GSH_t and glucose levels.

HbA_{1c} converted glucose values

Selvin *et al.* [147] in 2010 performed a clinical trial on diabetic patients and showed that baseline HbA_{1c} is associated with development of diabetes and further PDCs. HbA_{1c} reflects net glycemic load in the blood over the period of past three months and not affected due to fluctuations in the daily glucose levels. Therefore, HbA_{1c} is considered as a stable marker of GS, contrary to plasma glucose which varies daily depending upon food intake. We used
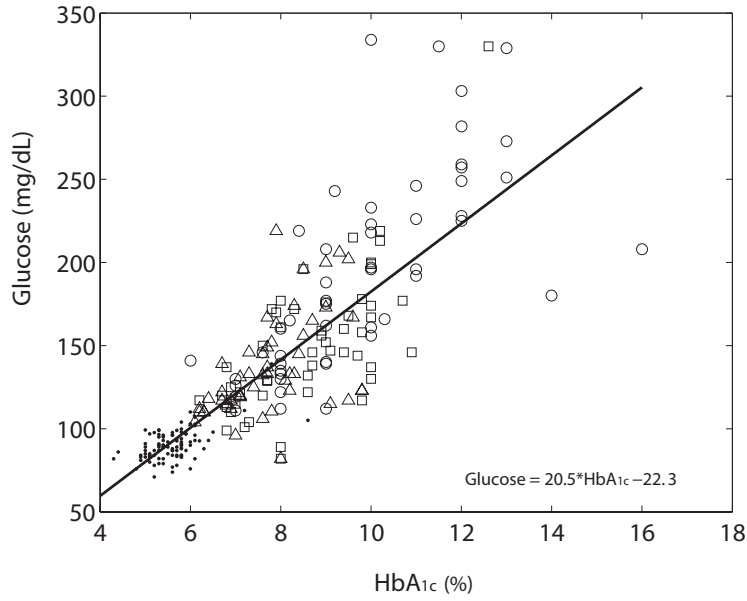
Figure 5.5: A linear regression between HbA_{1c} against plasma glucose. Fasting glucose and HbA_{1c} values taken from • : Non-diabetic (n=98, pooled from 0 and 8-weeks); ○: Diabetics 0-week (n=51); □: Diabetics 4-weeks (n=51); △: Diabetics 8-weeks (n=51). This equation is used to convert HbA_{1c} into a glucose value for model fitting. This figure is reproduced from Kulkarni *et al.* [126], published as Figure S28 in the supplementary information.

HbA_{1c} converted glucose values to obtain the OS-GS fits in diabetic patients. A linear regression (Figure 5.5) between HbA_{1c} against glucose was used to derive the conversion equation (Equ.5.4).

$$Glucose = 20.5 HbA_{1c} - 22.3 \tag{5.4}$$

For each diabetic patient, HbA_{1c} values at 0, 4 and 8-weeks were converted into glucose and utilised in the curve fitting procedure.

Simulations with variations around GSH_t levels

To account for the standard error around the GSH_t time point, we simulated curve fitting procedure considering a diurnal variation in GSH levels. The diurnal variation in GSH and GSSG is estimated to be approximately 15-30 % (Blanco *et al.* [146]; Chakravarty and Rizvi [148]). Briefly, a random number generator was used to generate a new GSH_t value
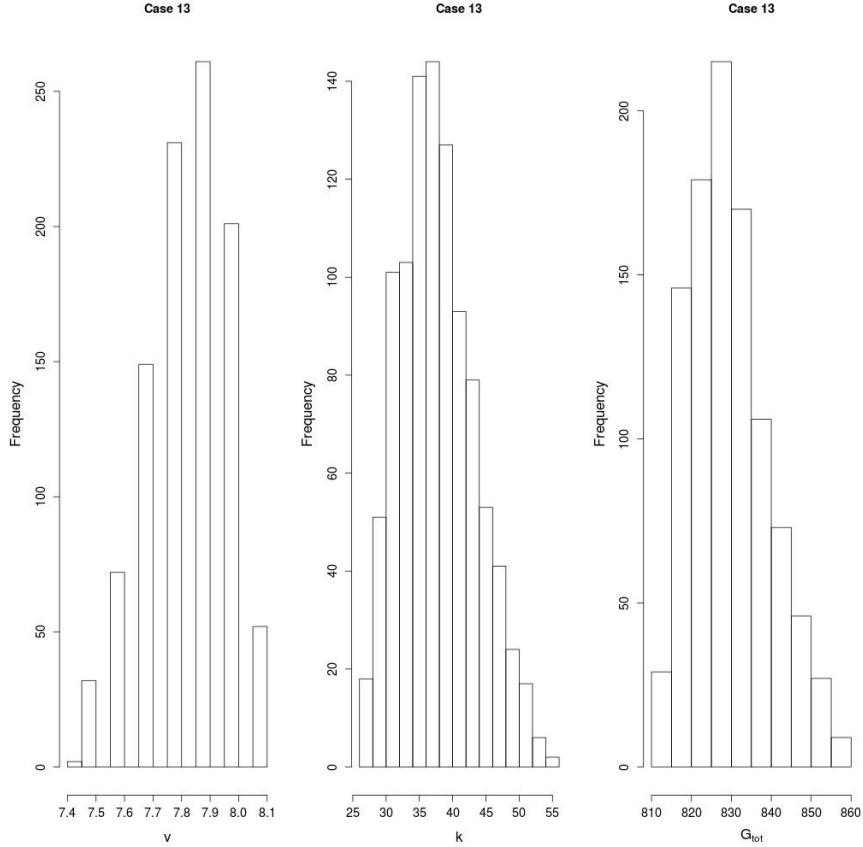
Figure 5.6: Distributions of v, k and G_{tot} for Case 13 assuming an error in the measured GSH. GSH measurements at the 0, 4 and 8-weeks values were randomly varied up to 15%; 1000 curve fitting procedures were done and 1000 parameter datasets were generated. The $mean \pm sd$ for v, k and G_{tot} across these 1000 computations are 7.8 ± 0.1, 37.7 ± 5.6 and 829 ± 9, respectively. This figure is reproduced from Kulkarni *et al.* [126], published as Figure S29b in the supplementary information.

considering 15-30% variation around the given GSH value. Parameter values were obtained by fitting the model to the simulated GSH time points. Thousand such parameter sets were generated using simulated curve fitting procedure. We describe two case studies; with 15% (Case 13) and 30% (Case 15) variation around the measured GSH_t value. Figures 5.7 and 5.6 show simulated distributions of the parameters k, v, and G_{tot} obtained for Case 13 and Case 15, respectively.

We observed that in the Case 13 with 15% variation in the GSH values, the predicted glucose threshold v wouldn't vary more than 1.2%. In fact, even with 30% variation in
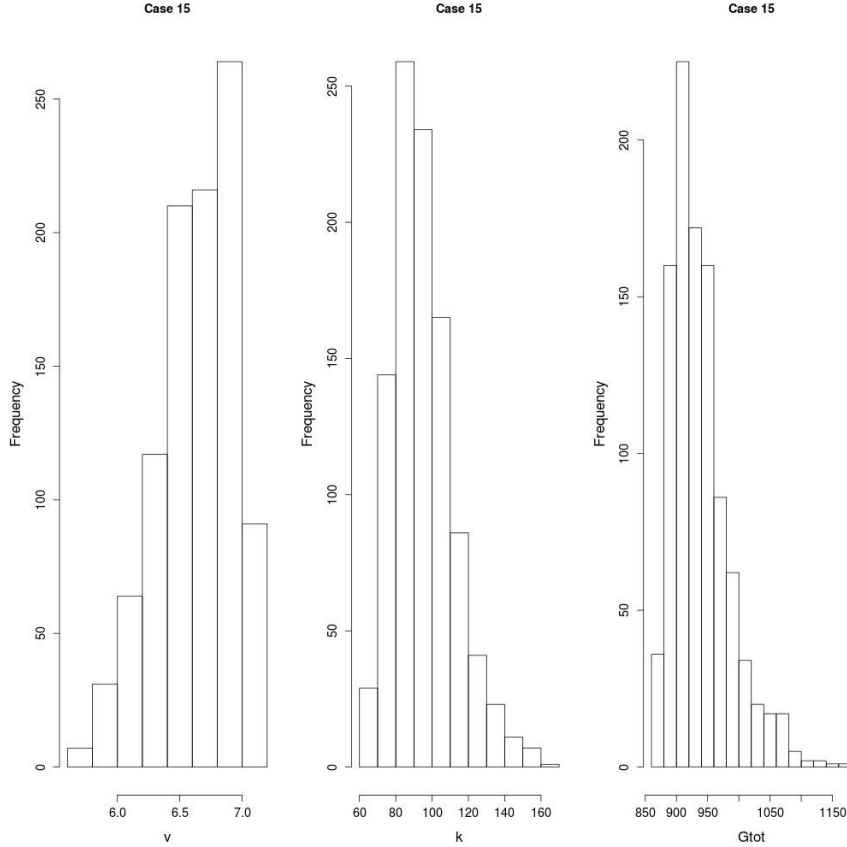
Figure 5.7: Distributions of v, k and G_{tot} for Case 15 assuming an error in the measured GSH. GSH measurements at the 0, 4 and 8-weeks values were randomly varied up to 30%; 1000 curve fitting procedures were done and 1000 datasets were generated. The $mean \pm sd$ for v, k and G_{tot} across these 1000 computations are 6.6 ± 0.3, 95.3 ± 16.7 and 938 ± 46, respectively. This figure is reproduced from Kulkarni *et al.* [126], published as Figure S29a in the supplementary information.

the Case 15, there would be only 4.5% variation in the predicted glucose threshold values. Therefore, the curve fitting is robust and predicted glucose control levels wouldn't be affected by GSH variation. Similarly, predicted G_{tot} pools show less than 5% variation in both the cases (1% for Case 13 and 4.9% for Case 15). The slope parameter k shows a variation of an order of magnitude of ten higher than v and G_{tot} (14.8% for Case 13 and 17% for Case 15). This may slightly change the recovery trajectory but not the predicted glucose target. Hence, we conclude that the overall curve-fitting procedure is robust towards daily variation in GSH levels.
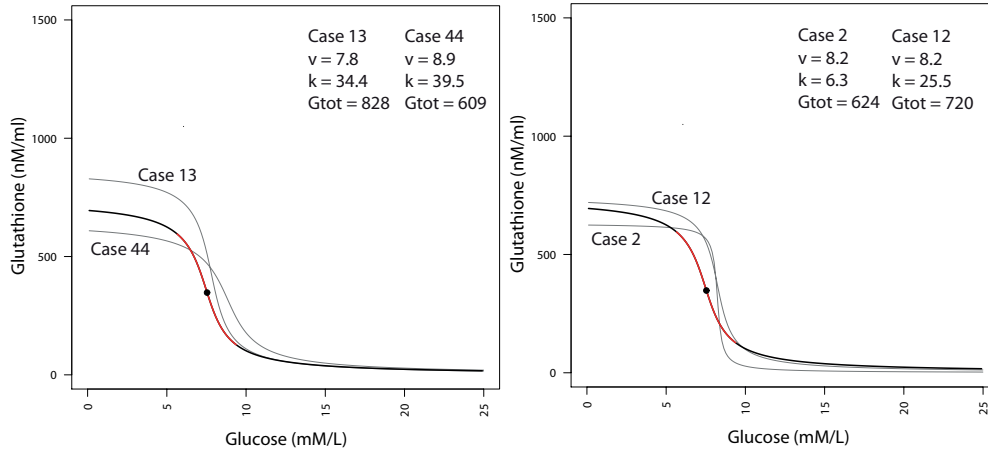
Figure 5.8: GSH-glucose dose-responses are unique for each diabetic individual. Left panel compares two cases (Cases 13 and 44) with similar *k's* but with distinct *v's*. On the other hand, right panel compares two cases (Cases 2 and 12) having same *v's* but differ in their slope parameter value, *k*. All the four cases have different predicted glucose targets as discussed in the Section 5.3.3. This figure is reproduced from Kulkarni *et al.* [126], published as Figure 4 in the paper.

5.3.3 Personalised glucose targets: clinical perspective

Individual GSH-glucose dose-responses differ for each diabetic patient (see grey lines in the background of Figure 5.4). We interpret personalised glucose targets in terms of the OS in the following manner: GSH levels along with glycemic markers would be monitored for two months at the intervals of 0, 4, and 8 weeks. An algorithm given by minimal model would be used to obtain the dose-response curve for a diabetic patient, which is characterised by a threshold glucose parameter *v*. We hypothesise that the optimal glucose target would be to lower glucose well below *v*, such that a diabetic patient would obtain a maximal benefit in terms of improved GSH pools. Furthermore, we speculate that monitoring OS along with the GS would help in predicting better glucose targets, for instance, whether glucose therapy should be intensified or lowered depending upon whether maximal GSH pool is attained or not. We illustrate the clinical implications of this by considering two cases studies; particularly comparing patients having similar *k's* but different *v's* (left panel of Figure 5.8) and patients having same threshold glucose value *v's* but differ in their slope parameters *k's* (right panel of the Figure 5.8).

86

Cases 13 and 44 in the left panel of Figure 5.8 have similar slopes k but differ in their threshold glucose values, v. Also, Case 44 has lowered $G_{tot} = 609$ value compared with Case 13 $G_{tot}= 828$. Accordingly, Case 44 diabetic would need to reduce glucose just below v=8.9mM/L to reach maximal GSH pools. But Case 13 patient would need to take glucose therapy little longer to reduce the glucose below v =7.8 mM/L. We note that in both these Cases 13 and 44, the optimal glucose targets are much higher than imposed standard glucose control regimen (HbA_{1c} <6.5%), and much flexible glucose control is possible. On the contrary to left panel, the right panel shows Cases 2 and 12 with same glucose threshold $v =$ 7.2 but differ in their slope parameter value, k. Therefore, we conclude that despite having same v values, Case 12 slowly reaches to maximal GSH pool (k=25.5) and thus would need longer glucose control compared to Case 2 which has steeper trajectory with k=6.3.

To sum up, OS-GS trajectory is dynamically regulated by a combination of slope parameter, maximal GSH pool and threshold glucose value; and accordingly, glucose targets can be defined in a personalised manner.

5.4 Discussion

In this chapter, we discussed a minimal mathematical model to obtain individualised OS-GS trajectories in diabetic patients. We could fit around 70% (34 out of 49 diabetic patients) GSH_t-glucose dose-responses. Individual OS-GS trajectories are provided in the Appendix Section 5.5.3). The minimal model captured variations in individual responses to glucose control treatment. We showed that these individual responses could be characterised by three parameters, namely, G_{tot}: maximal GSH_t pools inside the cells; v: threshold glucose value when GSH_t is half-maximal; k: slope parameter of the curve. We proposed that this feature be used in clinical setting to predict optimal glucose target in personalised manner (see Figure 5.8). **We speculate that threshold glucose value (v) is the optimal glucose control for a diabetic patient.** A stepwise algorithm based on the minimal model which can be implemented in a clinical setup is provided in Figure 5.9.

We found that in around 30% of the patient cases, meaningful fits could not be obtained.

**Algorithm for predicting personalised glucose targets using the
GSH-glucose minimal model**

Step 1 : Monitor diabetic patients for 2 months and measure their plasma HbA1c, plasma
Glucose and total glutathione levels at the intervals of 0, 4 and 8 weeks.

Step 2 : Obtain *HbA1c* converted glucose values, as explained in Section 5.3.2,
using Eq. 5.4.

Step 3 : Plot the graph of GSH against converted glucose values. The age-adjusted
GSH-glucose pair would be obtained using Eq. 5.3 (Section 5.2.2).

Step 4 : Use the steady-state Goldbeter-Koshland functional form (Section 5.2.1, Eq. 5.2)
to obtain the parameters of the models, namely, *v* (the threshold glucose value),
k (the slope parameter) and *Gtot* (maximal GSH pool).

Step 5 : The prediction of the model is controlling glucose levels well below the threshold
glucose value (*v*) is the personalised glucose target for that patient.

Figure 5.9: A stepwise algorithm based on the GSH_t -glucose minimal model to obtain the
personalised glucose target for a diabetic patient.

In these patients, GSH_t levels have not shown concomitant changes with respect to glucose control, and therefore, fitting procedure failed to obtain the fit. (for example see Case 17 in the panel figure 5.13; Case 21 in the panel figure 5.14; Cases 50-52 in the panel figure 5.19). There are a couple of interesting cases where the interpretation of the fits would be difficult. For example, in Case 22 (panel figure 5.14) and Case 28 (panel figure 5.15), the GSH levels by 8-weeks are already higher or near to the age-adjusted nondiabetic GSH levels. In these cases, curve passed through a single point and predicted glucose threshold values v are relatively higher. Therefore, our minimal model predictions can be verified and testable in diabetic patients. However, a shortcoming is the fewer number of time points (n=4) per diabetic patient used in this population study. This might be a limitation in having better predictive power in the model. Higher number of data points would also be useful in building complex models which would be closer to the underlying physiology. Nonetheless, **an important feature of our work is the introduction of a novel strategy to incorporate OS markers in the diabetes treatment and the predictive power can be improved by collecting a higher number of time points**. We hope that this small longitudinal clinical trial might turn out to be a starting point for larger clinical trials which would add confidence in the data interpretation.

Instead of strict glucose regimens, current approaches in the antidiabetic treatments suggest the need for personalised glucose targets (see Section 2.2.1). In this chapter, we proposed a simple quantitative algorithm to capture OS-GS trajectory, thereby predicting personalised glucose targets for type 2 diabetic patients. We emphasise on having *optimal* rather than strict or even standard glucose control, based on the OS of an individual. The flexible glucose control may raise a concern regarding consistently higher glucose levels in patients over the long time periods. For example, as discussed in the Section 5.3.3, Figure 5.8, the predicted glucose targets might be higher than the standard glucose targets; outside of the "pre-diabetic" zone. This may cause persistent hyperglycemia and eventually increase PDCs rate, as suggested by the theory. We argue that, however, maintaining OS well below threshold glucose v, may be sufficient to relieve the stress and most importantly side-effects of

the drug therapy can be reduced, especially in the elderly patients. The corollary prediction would be to maintain "pre-diabetic" OS levels by GSH or amino acid supplementation, to monitor its effect on long-term development of PDCs.

In our modelling study, we assumed that the GSH_t (GSH + GSSG) is conserved over the study period. However, since almost 90% of the GSH_t is made up of GSH, the Eq. 5.2 actually assumed to represent GSH_t rather than GSH. The model predicts that when glycemic stress is low, GSSG pool is high and as glycemic stress is reduced GSSG pool is reduced and simultaneously GSH pool increases over the study period. This is in contradiction to the fact that at any given instance, most of the GSH_t pool is composed of GSH and less than 10% of the GSSG pool. Therefore, our model doesn't account for changes in the GSSG pool and in fact overpredicts the GSSG pool. It also suggests that increases in the GSH pool (over the study period) is due to complex processes like exporting GSSG out of the cell and may be processes affecting GSH synthesis which may play an important role in maintaining erythrocytic GSH pool (Reed *et al.* [32]; Raftos *et al.* [33]). We note that despite the availability of kinetic data on individual enzymes of the GSH metabolism and diabetic erythrocytes, we do not have a comprehensive model of diabetic GSH-glucose metabolism. In other words, there is scope to improve the existing minimal model to incorporate complex interactions and make more meaningful predictions.

In conclusion, we propose that longer time courses of GSH and glucose in diabetic patients would be useful in building complex models of GSH-glucose metabolism in future. We hope that our minimal model would be a beginning towards that endeavour.

5.5   Appendix

5.5.1   Derivation of the steady-state solution of the minimal GSH-glucose model

The minimal model for the antioxidant action of GSH, as described in the Section 5.2, is to assume a ROS-dependent interconversion between the reduced (GSH) and oxidized

form (GSSG). This derivation of the GSH-glucose minimal model appears in Kulkarni *et al.* [126], published in the supplementary information (Section 5.1). We include it here for completeness. Taking the simplifying assumption is that cellular ROS is roughly proportional to the blood glucose concentration, $[ROS] = \beta[Glucose]$: using Michaelis-Menten kinetics for the forward and backward reactions, we have

$$\frac{d[GSH]_c}{d\tau} = \frac{v_1([G_{tot}]_c - [GSH]_c)}{k^\star + ([G_{tot}]_c - [GSH]_c)} - \frac{v_2\beta[Glucose][GSH]_c}{k^\star + [GSH]_c}, \tag{5.5}$$

where $[Glucose]$ is the plasma glucose concentration, $[G_{tot}]_c$ is the maximal value of total cellular GSH, $[GSH]_c$ is cellular $[GSH]$ and $[GSSG]_c = [G_{tot}]_c - [GSH]_c$ is cellular $[GSSG]$. v_1 and v_2 represent maximal enzymatic reaction rates for the enzymes GR and GPx, respectively. Here we have taken the same Michealis-Menten constant, k, for both, forward and backwards reactions; this simplification is used to avoid overfitting the data. Introducing the rescaled variables $v = \frac{v_1}{v_2\beta}$ and $t = v_2\beta\tau$, we get

$$\frac{d[GSH]_c}{dt} = \frac{v([G_{tot}]_c - [GSH]_c)}{k^\star + ([G_{tot}]_c - [GSH]_c)} - \frac{[Glucose][GSH]_c}{k^\star + [GSH]_c}. \tag{5.6}$$

Notice that the equation Eq. (5.6) is in terms of cytosolic GSH variables. Clinically, however, the measurements are most readily collected from the blood. We thus have to transform cytosolic variables to plasma variables. Reed et al. [32] describe a detailed mathematical model of GSH metabolism; they show that, to first order, plasma GSH varies in proportion to cellular GSH, that is, $[GSH]_c \approx \alpha[GSH]_b$, where $[GSH]_b$ is blood GSH. Moreover, they demonstrate that this relationship is valid even as OS varies, and it is valid between diabetics and healthy persons, see Fig. 6 in [32]. Eq. (5.6) can therefore be written in terms of plasma GSH as

$$\alpha\frac{d[GSH]_b}{dt} = \frac{v([G_{tot}]_c/\alpha - [GSH]_b)}{k^\star/\alpha + ([G_{tot}]_c/\alpha - [GSH]_b)} - \frac{[Glucose][GSH]_b}{k^\star/\alpha + [GSH]_b}. \tag{5.7}$$

Thus the equation for $[GSH]_b$, in terms of the quantities $G_{tot} = [G_{tot}]_c/\alpha$ and $k = k^\star/\alpha$, is

$$\alpha \frac{d[GSH]_b}{dt} = \frac{v(G_{tot} - [GSH]_b)}{k + (G_{tot} - [GSH]_b)} - \frac{[Glucose][GSH]_b}{k + [GSH]_b}. \tag{5.8}$$

Setting

$$\frac{d[GSH]_b}{dt} = 0, \tag{5.9}$$

the steady state expression of $[GSH]_b$ as it varies with $[Glucose]$ is thus obtained as

$$\frac{v(G_{tot} - GSH)}{k + (G_{tot} - GSH)} - \frac{Glu \cdot GSH}{k + GSH} = 0 \tag{5.10}$$

where we have dropped the square brackets and subscript for simplicity and abbreviated $[Glucose]$ as Glu. Thus, we have the following implicit relation between GSH and Glu:

$$v(G_{tot} - GSH) \cdot (k + GSH) - Glu \cdot GSH \cdot (k + (G_{tot} - GSH)) = 0. \tag{5.11}$$

By rearranging the terms in Eq. (5.11) we get,

$$(Glu - v) \cdot GSH^2 + (v \cdot G_{tot} - v \cdot k - Glu \cdot k - G_{tot} \cdot Glu) \cdot GSH + k \cdot v \cdot G_{tot} = 0. \tag{5.12}$$

This is a quadratic equation that can be solved for GSH in terms of glucose: its physically relevant solution is the Golbeter-Koshland formula [149]:

$$GSH(Glu) = \frac{-(v \cdot G_{tot} - v \cdot k - Glu \cdot k - G_{tot} \cdot Glu) \pm \sqrt{\begin{array}{c}(v \cdot G_{tot} - v \cdot k - Glu \cdot k - G_{tot} \cdot Glu)^2 \\ -4 \cdot k \cdot v \cdot G_{tot}(Glu - v)\end{array}}}{2 \cdot (Glu - v)}$$

$$\tag{5.13}$$

Or, equivalently, expanding the square term inside the square root we get the following from:

$$GSH(Glu) = \cfrac{-(v \cdot G_{tot} - v \cdot k - Glu \cdot k - G_{tot} \cdot Glu) - \sqrt{\begin{matrix} v^2 \cdot G_{tot}{}^2 + v^2 \cdot k^2 + k^2 \cdot Glu^2 \\ +Glu^2 \cdot G_{tot}{}^2 + 2 \cdot Glu^2 \cdot k \cdot G_{tot} \\ -2 \cdot G_{tot}{}^2 \cdot Glu \cdot v + 2 \cdot k^2 \cdot v \cdot Glu \\ +2 \cdot v^2 \cdot k \cdot G_{tot} - 4 \cdot Glu \cdot G_{tot} \cdot v \cdot k \end{matrix}}}{2 \cdot (Glu - v)}.$$

(5.14)

This is the GSH-glucose minimal model that the data is fit to.

Note that the equation is parameterized by the three quantities, v, k and G_{tot}, that will vary from individual to another. We have the following physical interpretations of these parameters:

1. Notice that if we set $Glu = 0$ in Eq. (5.10), $GSH = G_{tot}$ satisfies the equation. That is, G_{tot} can be interpreted as the maximal value of total cellular GSH at low glucose.

2. Taking $Glu = v$ in Eq. (5.10) we find $GSH = G_{tot}/2$. Thus v is the threshold glucose value for which GSH is half-maximal.

3. Taking logarithms in Eq. (5.10) and differentiating, and taking the limits $GSH \to G_{tot}/2$ as $Glu \to v$, we find that

$$GSH'(Glu \to v) = -\frac{G_{tot}}{8v}\left(2 + \frac{G_{tot}}{k}\right) \tag{5.15}$$

where the derivative GSH' is with respect to Glu. For a given value of G_{tot}, the larger the k, the smaller is the slope of the $GSH(Gluc)$ curve at the inflection point. Thus k can be interpreted as a slope with which the inflection is expressed; in other words, the rate of recovery. A smaller k implies that the GSH becomes rapidly near-maximal as Glu crosses below the v threshold.

93

5.5.2 GSH_t-glucose dose-response curves for above 40 and below 40 age-groups

GSH-glucose dose-responses for above and below 40 age-groups are presented separately in the Figures 5.10 and 5.11, respectively. The mean G_{tot} of above 40 age-group is lower compared to mean G_{tot} of below 40 age-group (above 40 mean $G_{tot} = 695$ against below 40 mean $G_{tot} = 924$). However, there is no much difference with respect to mean v and mean k between the two groups of the curves. The lower mean G_{tot} in the above 40 age-group may be ascribed to lower non-diabetic age-adjusted GSH values used for the curve fitting procedure. Although, low number of cases (n=5) in below 40 age-group, may not signify this effect.
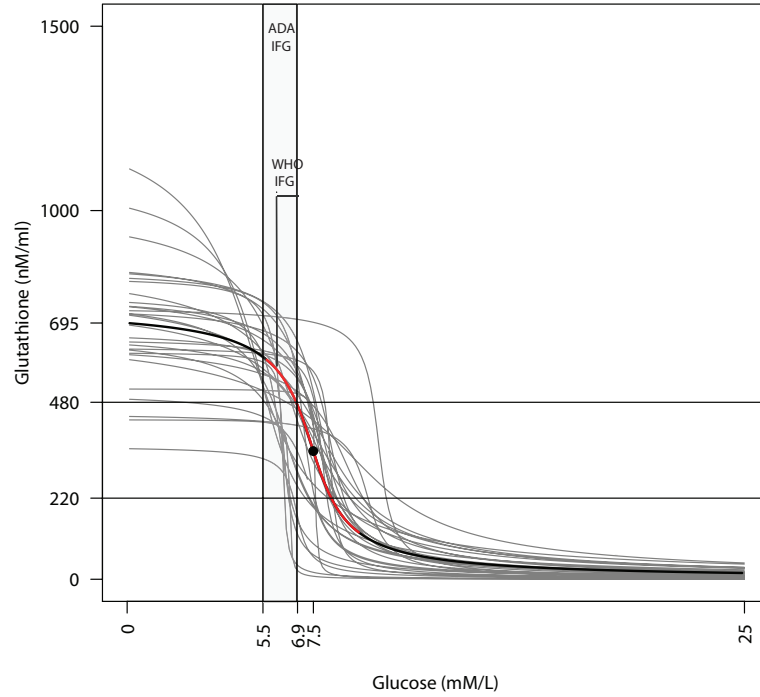
Figure 5.10: GSH-glucose dose-responses for diabetics above-40 age-group (n=29). We could obtain 29 of 38 dose-responses (thin gray lines) in the above-40 age-group using a minimal mathematical model. A PAC is shown by a bold black line. The PAC is parameterised by a threshold glucose value (black dot), v = 7.5 mmol/L ; G_{tot} = 695 and k=43. An inflection regime with an approximate width of one fourth of V (1.87 mmol/L) is marked in red. The GSH band at 220-480 represents the recovery phase for treated diabetics. The ADA impaired fasting glucose (IFG) range (5.5-6.9 mmol/L) and WHO IFG range (6.1-6.9 mmol/L) is superimposed for the reference. Interestingly, IFG occupies the upper portion of the red curve, and 8-weeks patients lie in the lower portion of the red curve. This figure is reproduced from Kulkarni *et al.* [126], published as Figure S24 in the supplementary information.

Figure 5.11: GSH-glucose dose-responses for diabetics below-40 age-group (n=5). Thin gray lines show individual GSH-glucose response curves for diabetic patients in below 40 age-group (n= 5 out of 11) along with the PAC (bold black line). The PAC has a glucose threshold (black dot), v = 7.4 mmol/L; $G_{tot} = 924$ and k=48.7. The red portion of the PACF indicates an inflection regime of width approximately one fourth of V, 1.85 mmol/L. ADA and WHO IFG-ranges are shown for the reference. This figure is reproduced from Kulkarni *et al.* [126], published as Figure S25 in the supplementary information.

5.5.3 Individual diabetic GSH_t-glucose dose-response curves

The GK functional form was used to obtain individual diabetic fits as described in the Section 5.2. We could fit 34 out of 49 diabetic cases, which have meaningful physiological parameter values. Figures 5.12-5.20 show results of 49 individual fits, with data points represented as □: 0-week, ○: 4-weeks and △:8-weeks and ▲: non-diabetic, GSH-glucose pairs. The physiological parameters v, k, and G_{tot} are provided for the reference for each diabetic case.

Figure 5.12: Individual diabetic GSH_t-glucose dose-response curves for the cases 1-7. Minimal model was fitted to diabetic patient's GSH_t-glucose pairs at 0-week ($\square$), 4-weeks ($\circ$) and 8-weeks ($\triangle$). Asymptotic GSH_t-glucose point was age-matched non-diabetic data point ($\blacktriangle$) using regression fit. Parameters v, k and G_{tot} estimated from a fit are displayed for each diabetic case. This panel figure is reproduced from Kulkarni *et al.* [126], published as Figure S15 in the supplementary information.
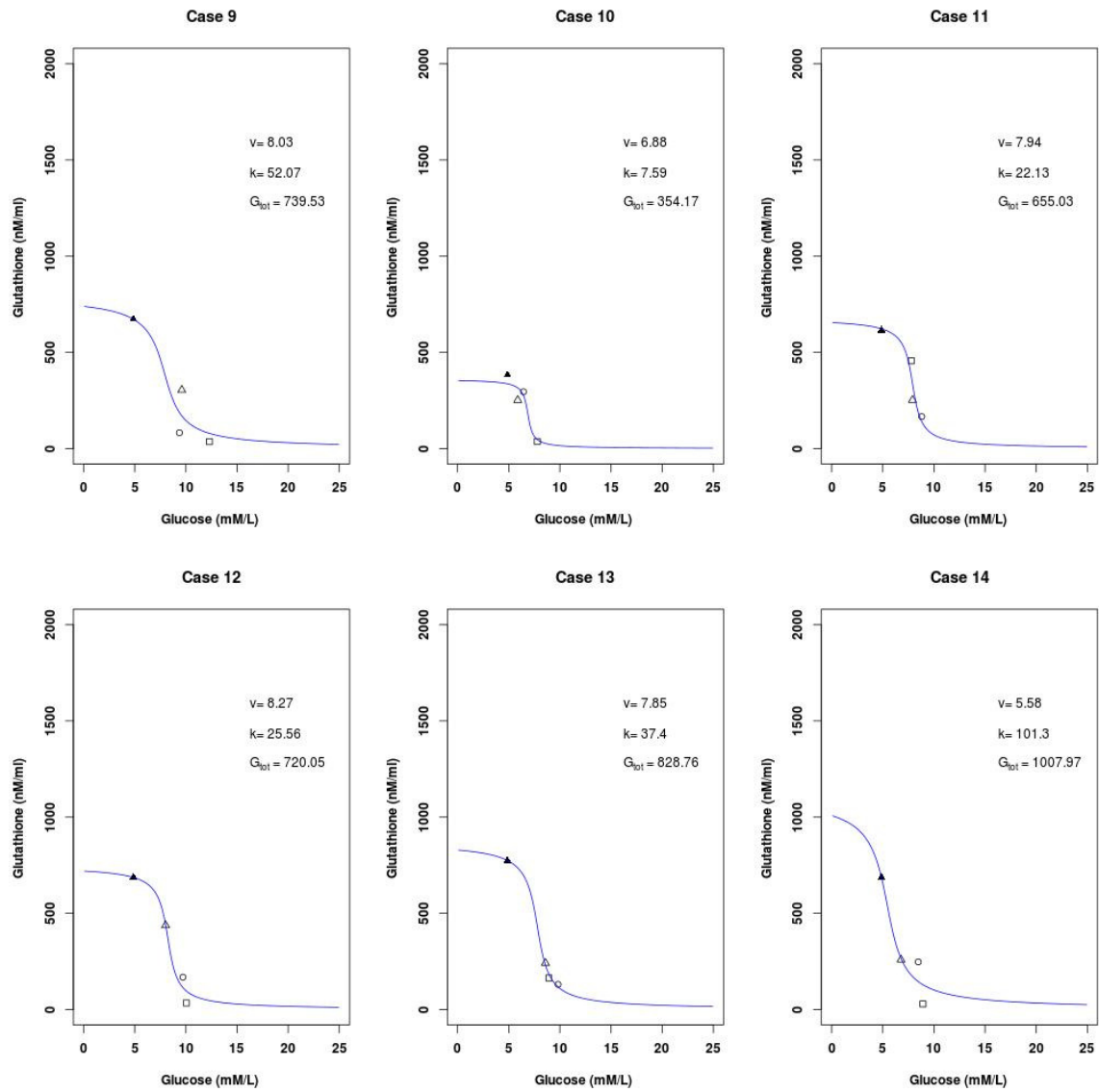
Figure 5.13: Individual diabetic GSH_t-glucose dose-response curves for the cases 9-14. Minimal model was fitted to diabetic patient's GSH_t-glucose pairs at 0-week ($\square$), 4-weeks ($\circ$) and 8-weeks ($\triangle$). Asymptotic GSH_t-glucose point was age-matched non-diabetic data point ($\blacktriangle$) using regression fit. Parameters v, k and G_{tot} estimated from a fit are displayed for each diabetic case. This panel figure is reproduced from Kulkarni *et al.* [126], published as Figure S16 in the supplementary information.
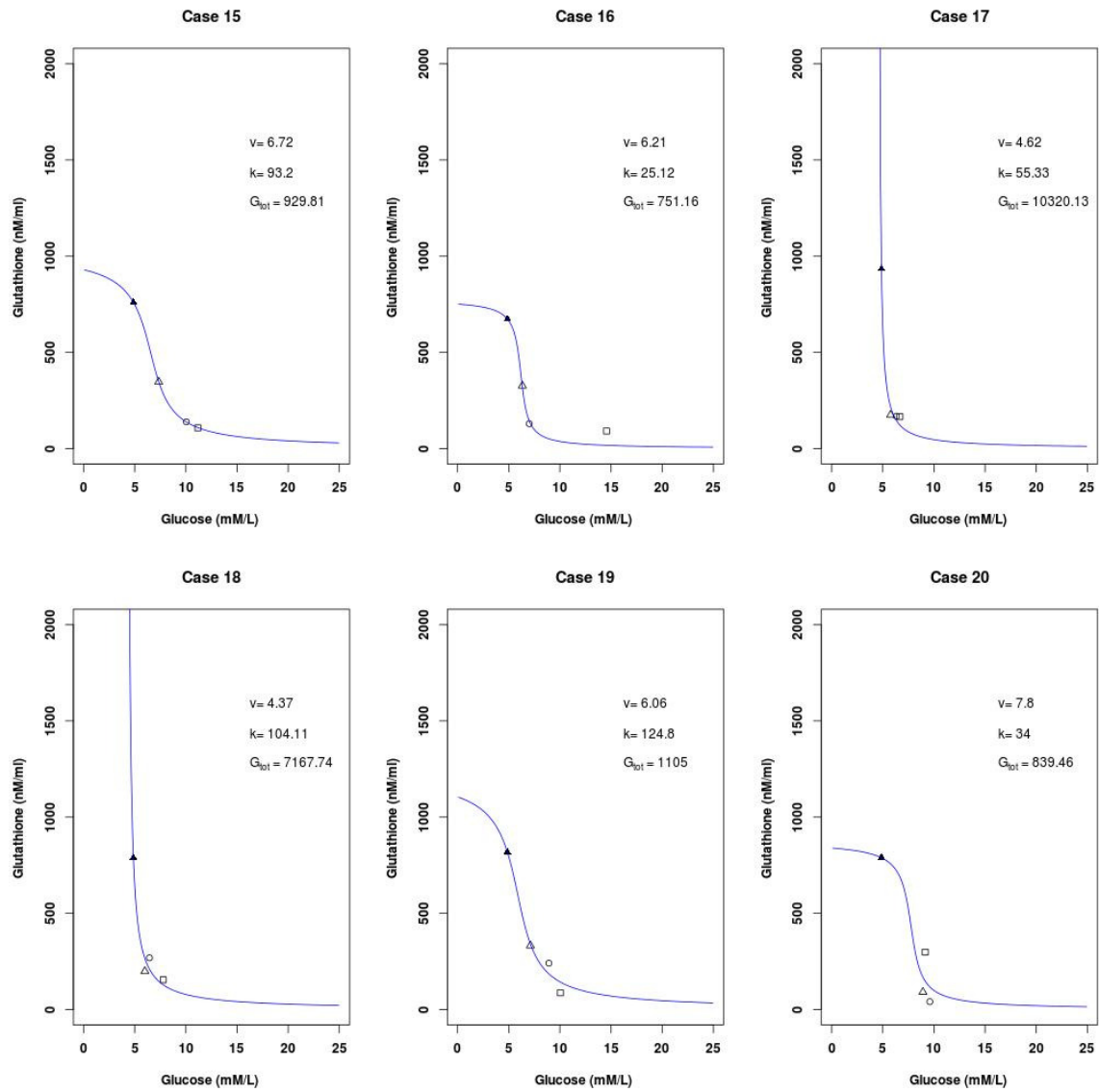
Figure 5.14: Individual diabetic GSH_t-glucose dose-response curves for the cases 15-20. Minimal model was fitted to diabetic patient's GSH_t-glucose pairs at 0-week ($\square$), 4-weeks ($\circ$) and 8-weeks ($\triangle$). Asymptotic GSH_t-glucose point was age-matched non-diabetic data point ($\blacktriangle$) using regression fit. Parameters v, k and G_{tot} estimated from a fit are displayed for each diabetic case. This panel figure is reproduced from Kulkarni *et al.* [126], published as Figure S17 in the supplementary information.
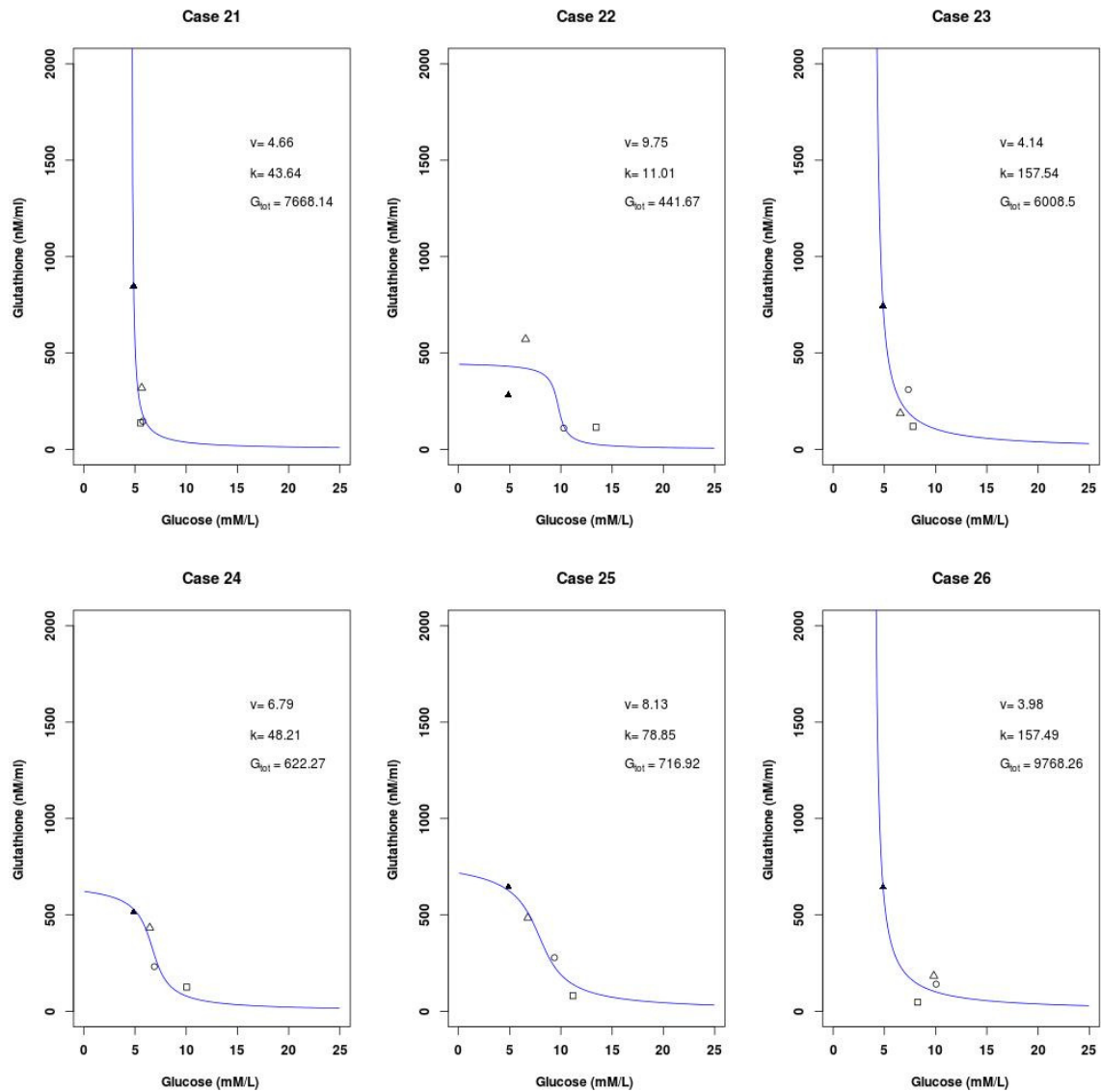
Figure 5.15: Individual diabetic GSH_t-glucose dose-response curves for the cases 21-26. Minimal model was fitted to diabetic patient's GSH_t-glucose pairs at 0-week ($\square$), 4-weeks ($\circ$) and 8-weeks ($\triangle$). Asymptotic GSH_t-glucose point was age-matched non-diabetic data point ($\blacktriangle$) using regression fit. Parameters v, k and G_{tot} estimated from a fit are displayed for each diabetic case. This panel figure is reproduced from Kulkarni *et al.* [126], published as Figure S18 in the supplementary information.
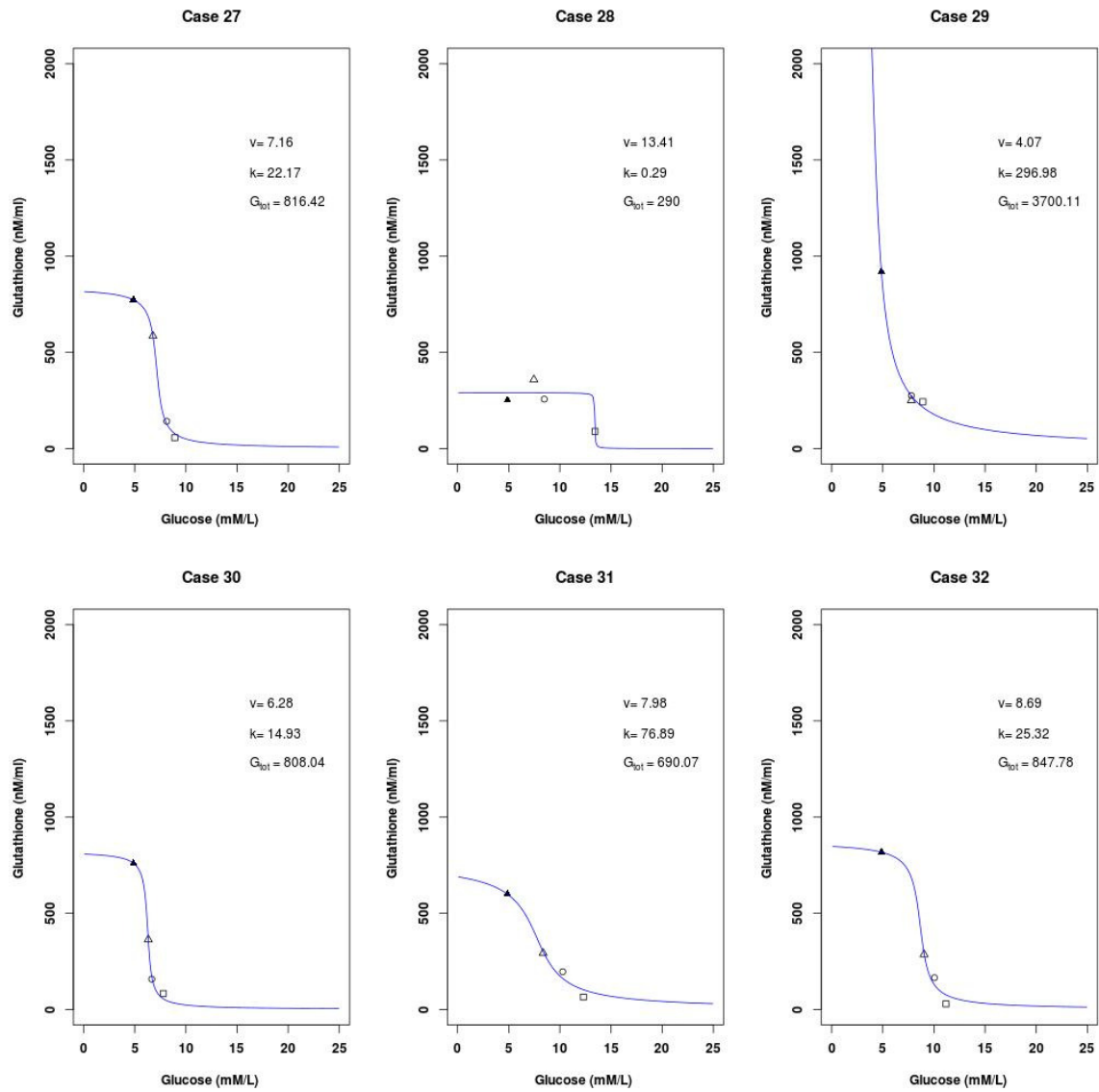
Figure 5.16: Individual diabetic GSH_t-glucose dose-response curves for the cases 27-32. Minimal model was fitted to diabetic patient's GSH_t-glucose pairs at 0-week ($\square$), 4-weeks ($\circ$) and 8-weeks ($\triangle$). Asymptotic GSH_t-glucose point was age-matched non-diabetic data point ($\blacktriangle$) using regression fit. Parameters v, k and G_{tot} estimated from a fit are displayed for each diabetic case. This panel figure is reproduced from Kulkarni *et al.* [126], published as Figure S19 in the supplementary information.

101
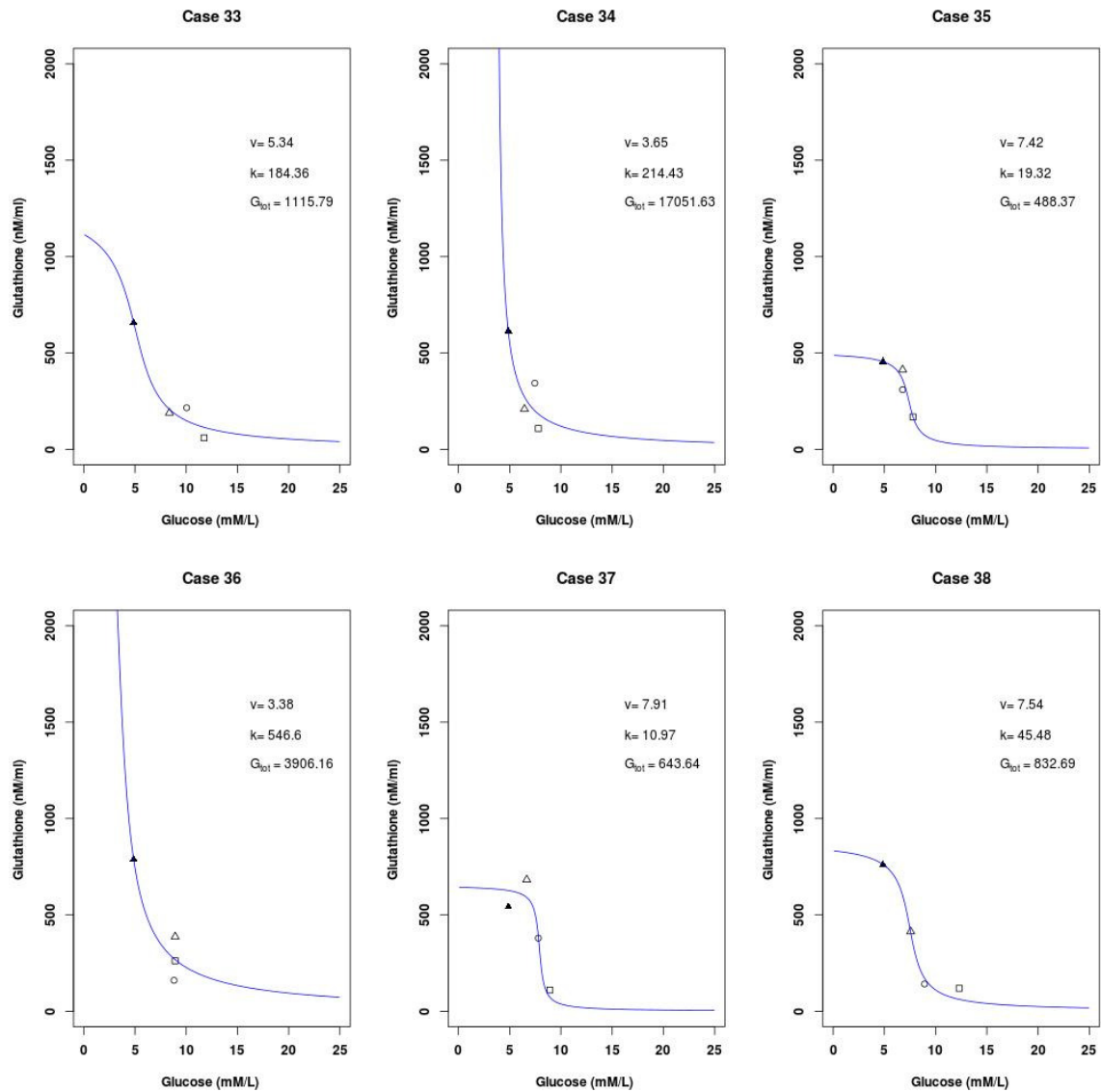
Figure 5.17: Individual diabetic GSH_t-glucose dose-response curves for the cases 33-38. Minimal model was fitted to diabetic patient's GSH_t-glucose pairs at 0-week (□), 4-weeks (○) and 8-weeks (△). Asymptotic GSH_t-glucose point was age-matched non-diabetic data point (▲) using regression fit. Parameters v, k and G_{tot} estimated from a fit are displayed for each diabetic case. This panel figure is reproduced from Kulkarni *et al.* [126], published as Figure S20 in the supplementary information.
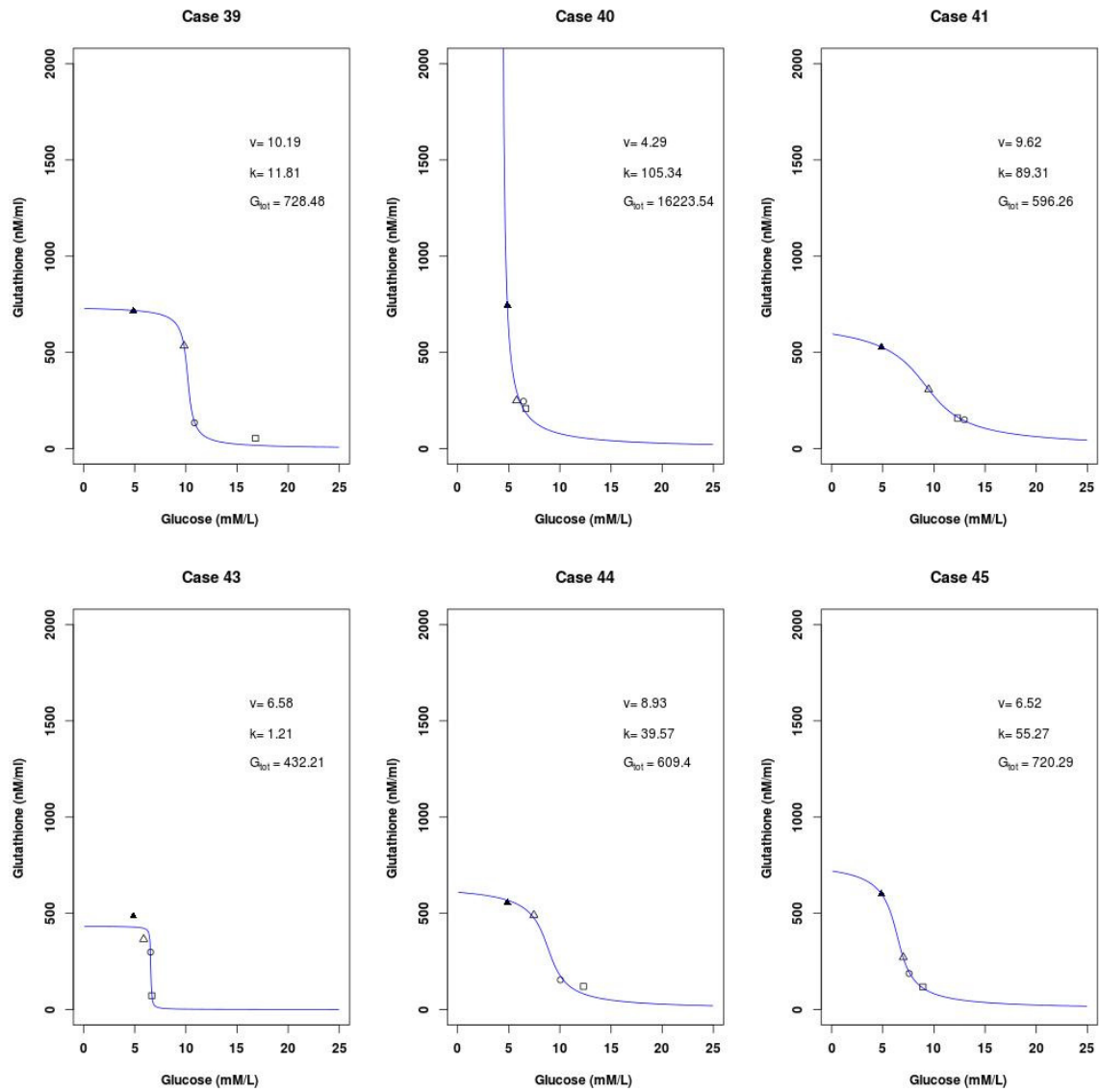
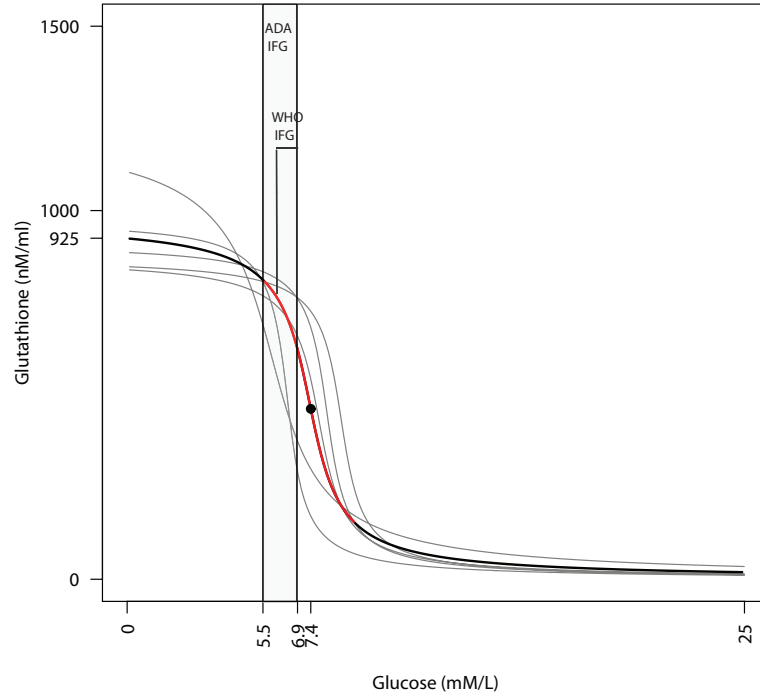**Figure 5.18:** Individual diabetic GSH_t-glucose dose-response curves for the cases 39-45. Minimal model was fitted to diabetic patient's GSH_t-glucose pairs at 0-week ($\square$), 4-weeks ($\circ$) and 8-weeks ($\triangle$). Asymptotic GSH_t-glucose point was age-matched non-diabetic data point ($\blacktriangle$) using regression fit. Parameters v, k and G_{tot} estimated from a fit are displayed for each diabetic case. This panel figure is reproduced from Kulkarni *et al.* [126], published as Figure S21 in the supplementary information.
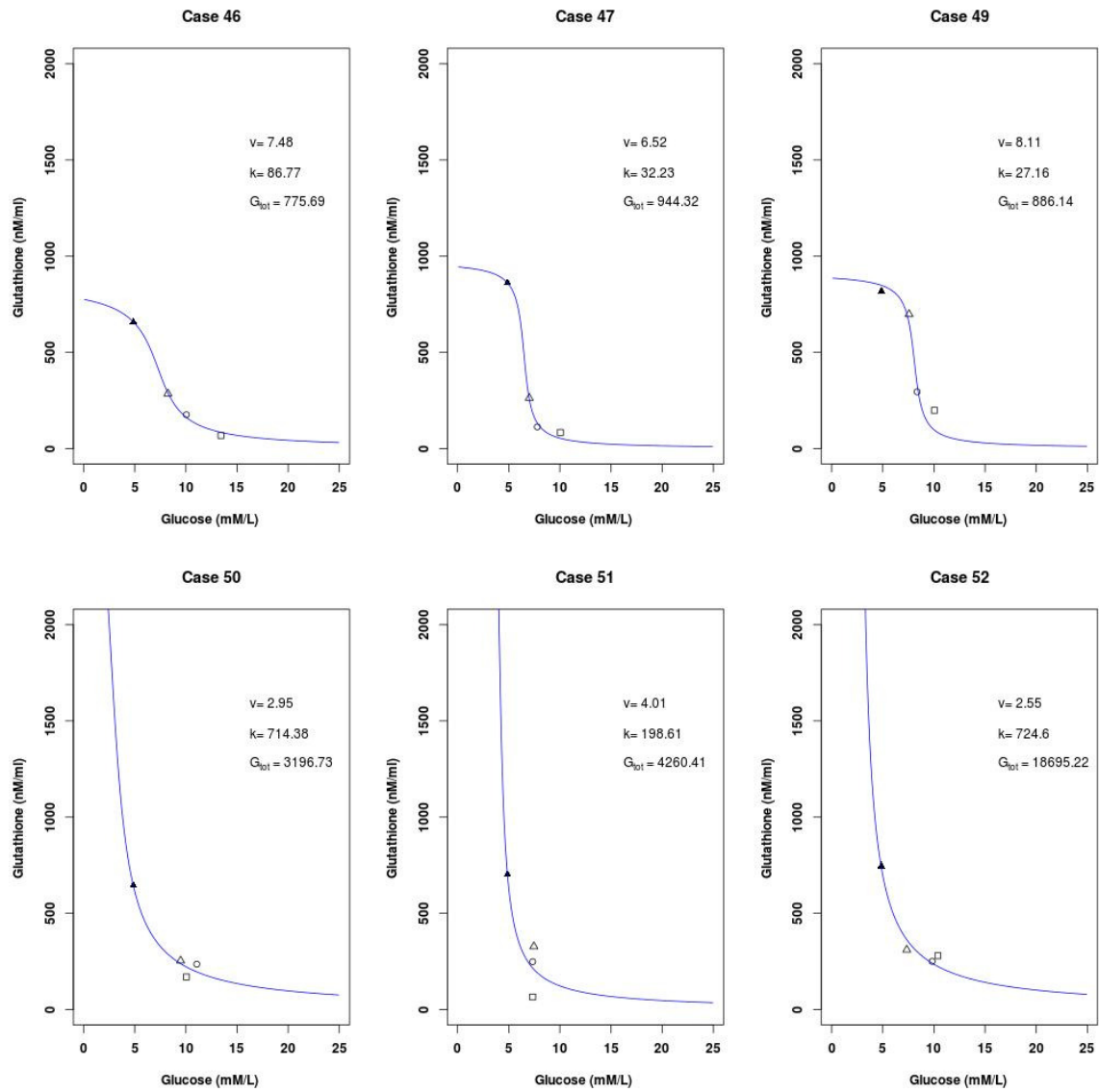
Figure 5.19: Individual diabetic GSH_t-glucose dose-response curves for the cases 46-52. Minimal model was fitted to diabetic patient's GSH_t-glucose pairs at 0-week ($\square$), 4-weeks ($\circ$) and 8-weeks ($\triangle$). Asymptotic GSH_t-glucose point was age-matched non-diabetic data point ($\blacktriangle$) using regression fit. Parameters v, k and G_{tot} estimated from a fit are displayed for each diabetic case. This panel figure is reproduced from Kulkarni *et al.* [126], published as Figure S22 in the supplementary information.
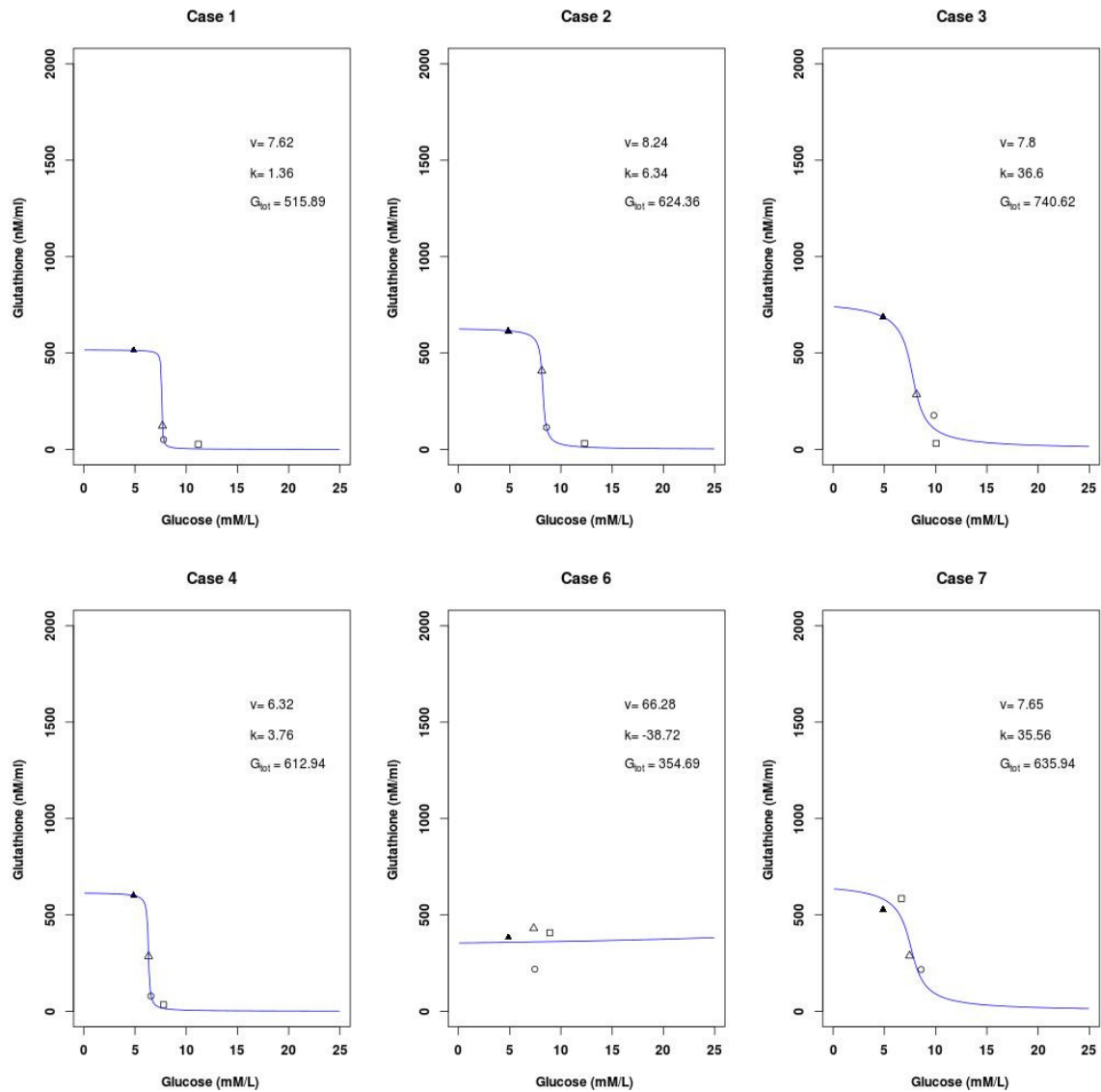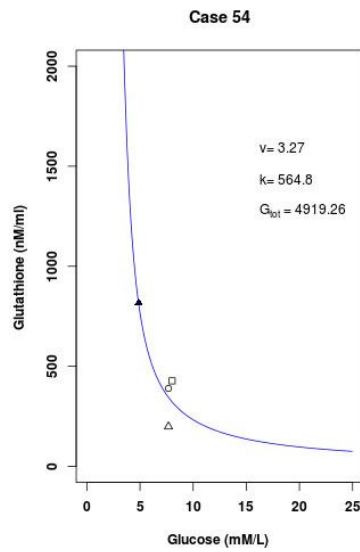
Figure 5.20: Individual diabetic GSH_t-glucose dose-response curves for the case 54. Minimal model was fitted to diabetic patient's GSH_t-glucose pairs at 0-week ($\square$), 4-weeks ($\circ$) and 8-weeks ($\triangle$). Asymptotic GSH_t-glucose point was age-matched non-diabetic data point ($\blacktriangle$) using regression fit. Parameters v, k and G_{tot} estimated from a fit are displayed for each diabetic case. This panel figure is reproduced from Kulkarni *et al.* [126], published as Figure S23 in the supplementary information.

Chapter 6

A phenomenological model of OS-GS trajectories

6.1 Introduction

We have found that the markers of glutathione metabolism responded rapidly to the changes in the GS. Further, we proposed that the OS-GS dose-responses would have "non-linear inverse" relationship in diabetic patients. In Chapter 5, we presented a physiologically-driven minimal mathematical model to capture this **non-linear inverse** relationship between systemic OS (GSH_t) as a function of GS. We used simple GSH-glucose biochemistry to capture changes in the OS response to GS at steady-state (for more information see 4, Section 5.2). Thereafter, we show that the GSH-glucose dose-responses could be individualised. Further, we hypothesised that EC_{50} or threshold glucose value, v can be used to predict personalised glucose targets.

We proposed a minimal model based on a simple glutathione-glucose biochemistry; however, glutathione metabolism is made up of an intricate network of biochemical reactions. Impaired glutathione metabolism and OS are known to be involved in multiple diseases like Alzheimer's, Parkinson's, Down's syndrome, cardiovascular disorders, cancer, autism, and diabetes (Marvin and Farook [150]; Townsend *et al.* [151]; Wu *et al.* [152]). Glutathione

is a tripeptide, synthesised from the amino acids cysteine, glutamate and glycine, of which cysteine is the rate-limiting amino acid. GSH, the reduced form of glutathione scavenges free radicals, primarily produced due to energy metabolism. The net glutathione levels are therefore determined not only by the OS present inside the cell but also due to changes in the amino acid pools. Besides, GSSG, an oxidised form of glutathione is transported out of the cell to maintain reducing GSH levels inside the cell. Systemically, glutathione is produced in the liver and transported to the various tissues through the plasma. Elaborate mathematical models have been developed to understand the role of glutathione metabolism at the cellular and systemic level to understand diseased conditions. For example, Reed *et al.* developed a model of glutathione metabolism in the liver with respect to changes in the amino acid pools in the blood [32]. They used this modelling study to understand glutathione metabolism in the context of Down's syndrome and autism. Another dynamic mathematical model of hepatic glutathione metabolism was proposed by Vali *et al.*, to decipher the role of glutathione metabolism in Parkinson's disease [153]. Raftos *et al.* developed a steady-state kinetic model of erythrocyte glutathione metabolism. It is a complex model with about 26 biochemical reactions [33]. Further, a review of computational studies of glutathione metabolism is given by Presnell *et al.* [154].

We have proposed a minimalistic model to understand changes in the erythrocytic glutathione pool in response to glycemic control in diabetic patients. Considering the complexity of glutathione metabolism, our mechanistic model has limitations. Some of the pitfalls of the GSH-glucose minimal model are as follows:

1. To start with, we assumed that the total glutathione pool (GSH_t) (made up of GSH and GSSG) would be conserved over the two months study period (for more information see 4, Section 5.2). According to this assumption, at the beginning of the study, GSSG levels would be higher compared to the GSH levels; as the GS is reduced over the study period, GSSG gets converted into GSH. However, at any given instant, more than 90% of the erythrocytic GSH_t pool is made up of GSH (Srivastava and Beutler [155]; Nur *et al.* [156]) and therefore, this assumption may not hold true in reality.

107

2. Secondly, glutathione-glucose physiology is made up of a complex biochemical reactions network. Therefore, apart from GSH-GSSG interconversion, there might be some other mechanisms that would give rise to **non-linear inverse** OS-GS relation. For example, changes in transport rates of GSSG and amino acid pools required for synthesis of GSH may contribute to the observed phenomenon (Reed *et al.* [32]; Raftos *et al.* [33]).

3. Most importantly, the GK functional form, with its complexity, is not convenient to readily use in a clinical set-up.

To overcome these shortcomings we employed a simple **phenomenological** model to capture OS-GS relationship in these diabetic patients. A phenomenological model would reduce the uncertainty in the assumptions of the mechanistic model. Additionally, a phenomenological model would have an advantage of being simple and predictive, at the same time.

In this chapter, a phenomenological logistic sigmoid function (LS) is used to derive the OS-GS trajectory for an individual diabetic patient (see Section 6.2.1). We apply another curve-fitting algorithm and fit 48 (out of 49, compared to 34 out of 49 in Chapter 5) diabetic curves using LS and GK functional forms. We also found that LS model is a statistically better alternative to the GK model. Hence, we propose that the LS model is suitable to use in a clinical set-up (a) to monitor antidiabetic treatment using OS of an individual diabetic patient, and (b) to define personalised glucose targets. Nonetheless, the physiological GK model has its advantages, and we close this chapter by presenting a comparative account between the phenomenological and physiological models.

This work is published as a BIOMAT 2015 conference proceedings book chapter (Kulkarni R [157]).

6.2 Methods

6.2.1 A phenomenological model and data fitting

In chapter 5 a mechanistic model was proposed to account for the steady state GSH_t-glucose dose-response trajectories in newly-diagnosed diabetic patients (Kulkarni *et al.* [157]). The

steady-state functional form of the GK model is provided in the Appendix Section 6.5.1. In this chapter, a simple statistical function is used to capture the graded dose-response between GSH_t and glucose. The LS model has a monotonically decreasing functional form, which is given by:

$$GSH_t(glucose) = GSH_{min} + \frac{GSH_{diff}}{1 + e^{k(glucose-v)}} \tag{6.1}$$

The additional details about the mathematical properties of the LS model are provided in the Appendix Section 6.5.2. The LS model has an extra parameter, GSH_{min}, in comparison to the GK model. GSH_{min} stands for the baseline GSH_t value at the 0-week. We note that in the LS model, $GSH_{diff} = GSH_{max} - GSH_{min}$. Both the GK and LS models have three parameters:

1. GSH_{max}[1]: the maximal GSH_t corresponding to normoglycemia

2. k: the recovery rate parameter of the curve

3. v: the threshold glucose value, GSH_t is half maximal

The curve fitting procedure was performed as described in Chapter 5, Section 5.3, with few modifications. In Chapter 5 we observed that curve fitting procedure predicted unphysiological glucose threshold values below 5 mM, in few diabetic cases. To avoid this, the lower value of v, the threshold glucose value, was set to 5mM. Thus, even in cases where curve fitting did not produce meaningful curves, it would predict standard glucose target.

6.2.2 Statistical analysis

Student's t-test was used to compare the best fit parameter distributions obtained by the GK and LS models at 95% CI. Model selection criteria Akaike's Information Criterion (AIC) and sum of squared errors (SSE) were used to compare the model performances. The *aic()* function in statistical package R was used to calculate AIC scores.

---

[1]In Chapter 5, the maximal GSH pool parameter was referred to as G_{tot}. For the sake of comparison between the two models, the same parameter is referred to as GSH_{max} in this chapter.

6.3 Results

6.3.1 Phenomenological model is parametrically comparable to the physiological model

We compared the fits obtained from GK and LS models to the diabetic patient data. The LS model details are provided in the Section 6.2.1, and steady-state form of GK function is provided in the Section 6.5.1. We could fit 48 out of 49 diabetic GSH-glucose dose-responses, for each model. Both the models have three comparable parameters GSH_{max}, v, and k; as described in the Section 6.2.1. Figure 6.2 compares the parameter distributions obtained by two models over the 48 fitted GSH-glucose trajectories. Of the three parameters, v and GSH_{max} have physiological relevance. However, the origin of the slope parameter k in the GK model is convoluted and may not be readily comparable with the slope parameter of the LS model. We found that distributions of v and GSH_{max} do not differ significantly (Figure 6.1). The $mean \pm sd$ values of v for GK and LS models being 6.9 ± 1.7 and 6.6 ± 1.4, respectively. Also, $mean \pm sd$ values for GSH_{max} parameter were not found to be statistically different (905 ± 346 and 846 ± 276 for GK and LS models, respectively). But, distributions of the slope parameter k differ significantly between the two models, with $mean \pm sd$ values of 82.2 ± 98 and 4.4 ± 5.2 corresponding to GK and LS models.

The GSH-glucose dose-responses obtained by fitting GK and LS models are shown in the Figures 6.2(a) and 6.2(b), respectively (Figure 6.2). The grey lines in the background are individual diabetic dose-response curves. The "population-averaged curve" (PAC) for both the models are depicted by a dotted bold curve with population-averaged values of GSH_{max}, k, and v over the 48 individual curves. We note that the PAC for the LS model (parameterized by GSH_{max}=846, GSH_{diff}=712, v=6.6, and k=4.4) has a steeper slope but otherwise comparable to the GK model (parametrized by GSH_{max}=905, v=6.9, and k=82.2). Glutathione responds in a biphasic manner in the inflection region (the solid bold middle portion of the PAC, approximately $\frac{v}{4}$ around the threshold glucose or the inflection point, v depicted by the solid black dot on the PAC). The hyperglycemic region corresponds to
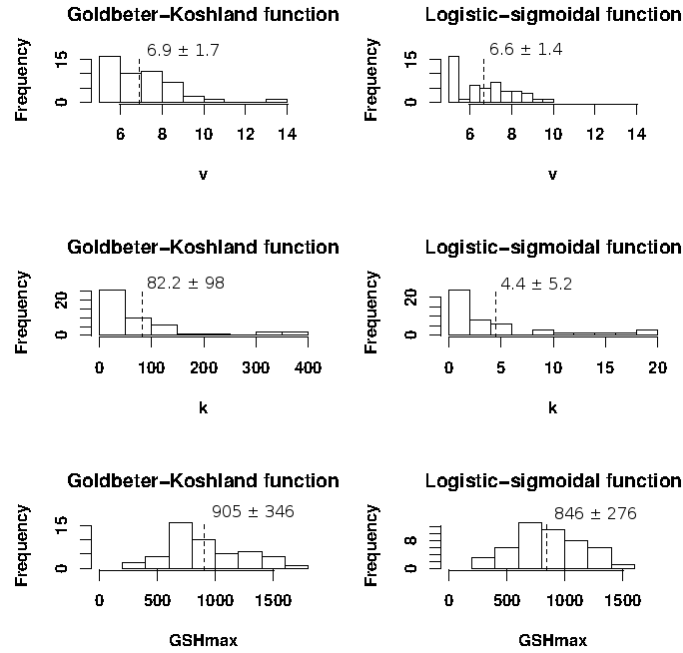
Figure 6.1: Comparison of fitted parameter distributions namely, GSH_{max}, v and k for GK and LS models (n=48). $Mean \pm sd$ values for parameter distributions are represented by vertical black dotted lines. The distributions of the parameters v and GSH_{max} obtained by the LS and GK models are comparable (p-values: 0.44 and 0.36 at 95% confidence interval, respectively), although, the distributions of the slope parameter k differ by an order of magnitude of ten. This figure is reproduced from Kulkarni R [157], published as Figure 2 in the main text.

lower GSH_t asymptote and switches to maximal GSH_t asymptote with non-diabetic glucose range, around the inflection point. The LS-PAC also shows a feature earlier observed in the GK model. The upper portion of the inflection region overlaps with the "impaired fasting glucose" (IFG) ranges defined by ADA (5.5-6.9mM glucose) and WHO (6.1-6.9 mM glucose). Also, after-therapy diabetic GSH_t levels occupied the lower portion of both the PACs. *Essentially, we conclude that LS model fits preserve the features of GK model fits,* and therefore LS model can be used for capturing GSH-glucose dose-responses.
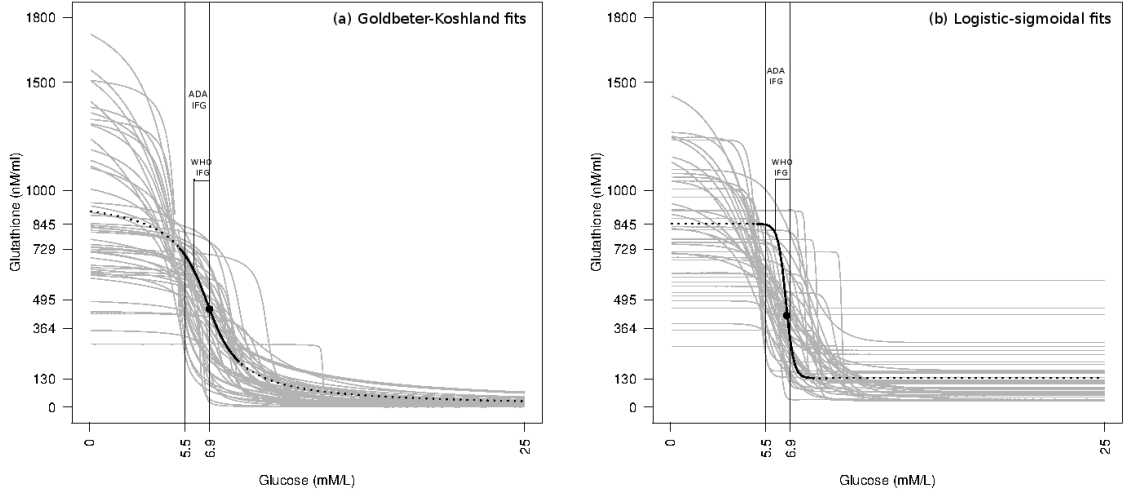
Figure 6.2: Figure panels 1a and 1b show individual diabetic GSH_t-glucose dose-response trajectories (n = 48 of 49) obtained by fitting GK and LS models, respectively. Grey lines in the background depict individual diabetic fits which show considerable variation with respect to glucose control. The PAC is represented by a dotted bold black curve. The black dot on the PAC represents an inflection point (v), the threshold glucose at which GSH_{max} is half-maximal. The solid black curve is the sensitive portion of the PAC defined as "inflection region" (roughly $\frac{v}{4}$ on both sides of the inflection point). The PAC for the LS model is parameterized by v=6.6, k=4.4, GSH_{diff}=712 and GSH_{max}=846) and that of GK model is parameterized by v=6.9, k=82.2 and GSH_{max}=905. PAC of the LS model is steeper than the GK model. ADA (5.5-6.9 mM/L) and WHO (6.1-6.9 mM/L) IFG-ranges are provided for the reference. IFG-ranges occupy the upper portion of the solid black curve. This region is the most sensitive portion of the curve, and individuals having glucose values in this band are prone to develop diabetes at a faster rate. Also, 80% of the 8-weeks GSH_t values lie in the lower portion of the solid black curve which represents the recovery phase from the glycemic treatment. This figure is reproduced from Kulkarni R [157], published as Figure 1 in the main text.

6.3.2 LS model performs statistically better over the GK model

We used two measures of model selection to compare the performances of the model fits: a sum of squared errors (SSE) and Akaike's Information Criterion (AIC). The details of SSE and AIC calculations are provided in the Section 6.2.2. Briefly, lower the SSE and AIC, better the quality of fits. Figure 6.3 shows distributions of SSE scores obtained for each diabetic fit, with GK and LS models. The LS model fits had statistically significant lower SSE scores with the $mean \pm sd$ value of 6.7 ± 3.8 compared to the $mean \pm sd$ value for GK model of

8.4 ± 1.9 (*p-value* for the comparison between the means being <0.003). Additionally, AIC scores were also found to be significantly lower for the LS model ($mean \pm sd$ value of 27 ± 15) as against the GK model ($mean \pm sd$ value of 34 ± 7) with the *p-value <0.003*, for comparison of the means. Hence, both the measures suggest that LS model fits are better over the GK fits.
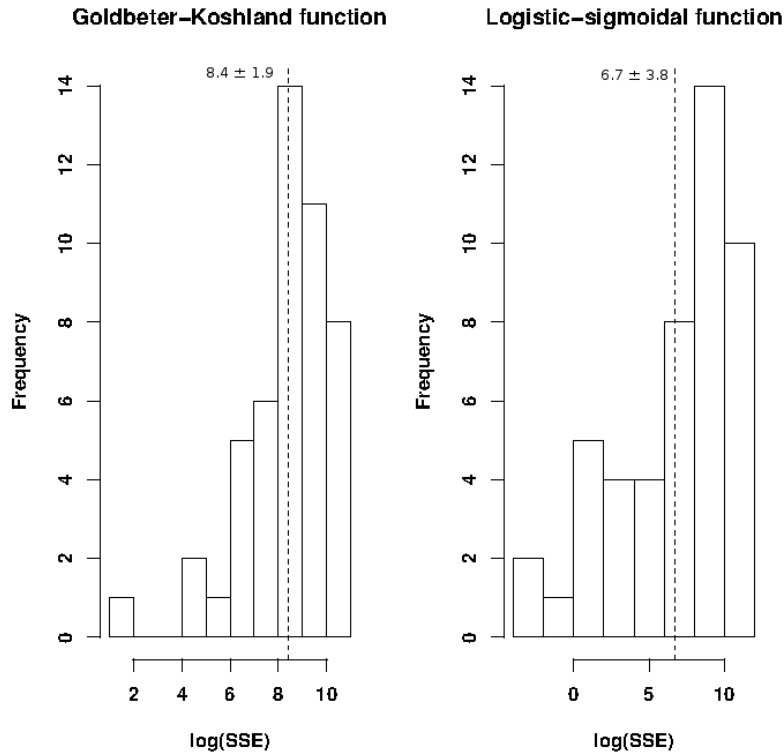
Figure 6.3: Comparison of SSE scores obtained by the GK and LS fits (n=48). Population-averages SSEs ($mean \pm sd$) are represented by the vertical black dotted lines on the histograms. The average SSE score differ significantly between the two models; SSE score found to be lower for LS model (p-value <0.05). This figure is reproduced from Kulkarni R [157], published as Figure 3 in the main text.

6.4 Discussion

We adapted statistical LS model to obtain GSH_t -glucose dose-responses. Our most important aim was to relax the assumptions of the mechanistic model while retaining predictive power. We compared the LS and GK model fits and showed that LS model performs sta-

tistically better over the GK model (see Section 6.3.2). The distributions of the parameters v and GSH_{max} were found to be comparable (Figure 6.1). However, the distributions of the slope parameter k differ significantly, by order of magnitude of 10. We speculate that this difference is due to the complicated functional form of the GK model. We note that such complexity is not present in the LS model, and interpretation of the slope parameter is not complicated. Furthermore, mathematical properties of the LS model suggest that the predicted threshold glucose target (v) is slightly greater than $\frac{GSH_{max}}{2}$ (refer to Appendix Section 6.5.2). However, the slight increase in the v would be on average within the standard deviation of the v for the PAC for the LS model (Figure 6.2), and this may not affect the predictive power.

We performed GSH_t -glucose curve-fitting simulation with 15-30% daily variation around GSH-glucose time point (refer to Chapter 4, Section 5.3.2). We note an interesting feature in the simulated curves: the patient cases whose v is roughly in the range of 5-5.6 mM, show fragility in the curve fitting. These cases show bimodal distributions of the parameters. In short, two different curves are possible for a given set of simulated GSH-glucose time-points. However, no such phenomenon was observed for cases having v >5.6 mM. We speculate that steeper dose-responses are sensitive towards the small fluctuations in the GSH values. Further, the sensitive range for v, would not affect the predictive power of the model, since in these cases optimal glucose control would be the standard prescribed glucose limit. Nonetheless, higher number of time points would reduce the fragility in these cases.

We used statistical analysis to show that the simple LS model is suitable to use in the clinical set-up as compared to the GK model. However, physiologically inspired GK model has its advantages (refer to Table 6.1). For instance, both the GK and LS models can predict optimal glucose targets v, but LS model is not suitable for predicting recovery from the diabetes treatment. On the contrary, slope parameter (k) in the GK model has a complex physiological origin and hence useful in defining recovery from the diabetes treatment. Besides, GSH-glucose physiology is complicated, and, therefore, intricate details of the physiology can be incorporated in the GK model provided more number of data points

GK Model	LS Model
GK functional form though explains OS-GS trajectories is too complex to put into the clinical practice	LS functional form is simpler and can be readily used in the clinical practice
The origin of slope parameter k in the GK model has complex physiological origin. Therefore, GK model can be used predict better recovery rates.	The slope parameter may not be assigned any physiological origin. Therefore, LS model can predict glucose targets comparable to the physiological model, but not recovery from the diabetes treatment.
GK model can be extended to add complex mechanisms, provided more data points are available	Statistical functional form, not assumption based.

Table 6.1: A comparative account of GK (physiological) against LS (phenomenological) models.

are available. In other words, there is scope to extend the existing minimal model and build elaborate mathematical models to predict GSH-glucose dose-responses.

6.5 Appendix

6.5.1 Goldbeter-Koshland functional form

The GK functional form is reproduced for the reference (see Equ.6.2). The detailed derivation can be found in the Chapter 3, Appendix Section 5.1.

$$GSH_t(glucose) = \frac{-(v \cdot GSH_{max} - v \cdot k - Glu \cdot k - GSH_{max} \cdot Glu) - \sqrt{\begin{array}{c} v^2 \cdot GSH_{max}^2 + \\ v^2 \cdot k^2 + k^2 \cdot glucose^2 \\ +glucose^2 \cdot GSH_{max}^2 + \\ 2 \cdot glucose^2 \cdot k \cdot GSH_{max} \\ -2 \cdot GSH_{max}^2 \cdot glucose \cdot v + \\ 2 \cdot k^2 \cdot v \cdot glucose \\ +2 \cdot v^2 \cdot k \cdot GSH_{max} - \\ 4 \cdot glucose \cdot GSH_{max} \cdot v \cdot k \end{array}}}{2 \cdot (glucose - v)} \tag{6.2}$$

6.5.2 Physiological explanation of the phenomenological model

The LS model is characterised by three parameters, v, k and GSH_{max}. GSH_{diff} is the difference between $GSH_{max} - GSH_{min}$. The physiological interpretation can be obtained as follows:

1. By putting Glu = 0, in the Equ. 6.1,

   the denominator in the term $\frac{GSH_{diff}}{1+e^{k(glucose-v)}}$ tends towards 1. This leads to $GSH_t(glucose) = GSH_{min} + GSH_{diff} = GSH_{max}$. Therefore, at the low glucose GSH_{max} is reached.

2. By putting Glu = v, in the Equ. 6.1, we obtain,

   $GSH_t(glucose) = GSH_{min} + \frac{GSH_{diff}}{2} = \frac{GSH_{max}+GSH_{min}}{2}$

   Therefore, v is the threshold of glucose where GSH_t is slightly greater than $\frac{GSH_{max}}{2}$. This mathematical explanation is reproduced from Kulkarni [157], published as Appendix Section 5.3.

3. Differentiating Equ. 6.1 and taking the limits $GSH \to G_{tot}/2$ as $Glu \to v$, we find that

$$GSH'(Glu \to v) = -\frac{GSH_{diff} \times k}{4} \tag{6.3}$$

where the derivative GSH' is with respect to Glu. For a given value of G_{tot}, the larger the k, the larger is the slope of the $GSH(Gluc)$ curve at the inflection point. In oppose to the interpretation of k for the GK model, larger k in the LS model implies that the GSH becomes rapidly near-maximal as Glu crosses below the v threshold (see Chapter 5 Appendix Section 5.5.1). The slope parameter k in the GK model has an upper limit (as $k \to$ infinity) but the slope parameter k in the LS model is not capped.

Chapter 7

Blood glutathione is a covariate of glucose during recovery from diabetes

7.1 Introduction

Persistent hyperglycemia leads to the development of microvascular and macrovascular impairment over the time. Therefore, management of hyperglycemia - the primary cause of diabetic complications - poses a significant challenge to diabetes control. This concern is not unreasonable since clinical studies show there is a considerable interpatient variation in response to antidiabetic treatment and as diabetes progresses, it becomes difficult to achieve the standard glucose control goal of $HbA_{1c} < 7\%$ (Gavin and Bahnnon [158]). Therefore, designing antidiabetic drug treatments to rationalise interpatient variation is an important motivation behind developing "patient-centered" antidiabetic therapies (Inzucchi *et al.* [23]). On these lines, predictive algorithms have been developed to define combinations of antidiabetic drugs to account for underlying pathophysiological changes to achieve standard glycemic goals (Tsang [159]).

In our population study, we examined changes in the HbA_{1c} levels of diabetic patients
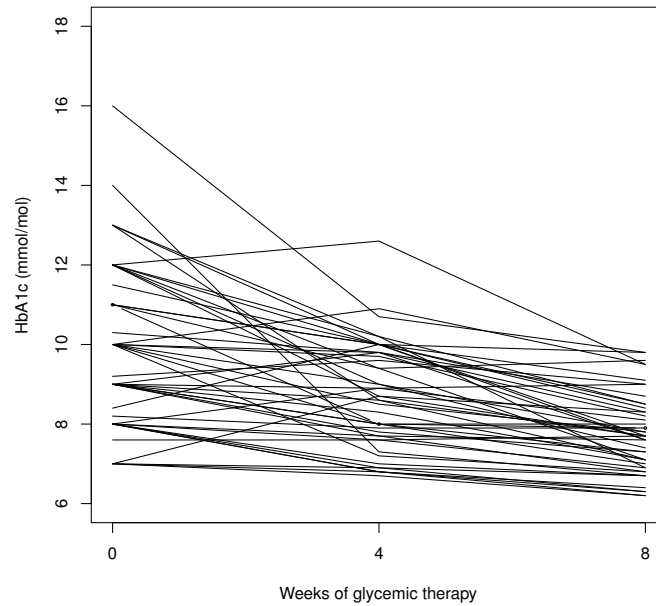
Figure 7.1: HbA_{1c} levels fall consistently in the diabetic patients over the study period (n=43). However, the fall in the GS show considerable variability in the diabetic patients. Figure reproduced from Kulkarni *et al.* [160], published as Figure 2 in the main text.

over the study period (see Figure 7.1). We observed that there is a remarkable interpatient variation in the decline of GS among the diabetic patients. Additionally, in Chapter 5 we also modelled variable recovery rates of diabetic patients kept on the antidiabetic treatment (see Chapter 5, Section 5.3.1). These observations lead to an interesting question: **what determines the variability in the recovery trajectories of diabetic patients?**

Pharmacogenomic and pharmacokinetic studies have been conducted to assess variations to the antidiabetic drugs like biguanides and sulfonylureas. These studies have identified genetic polymorphisms in drug targets in diabetic patients (Daniels *et al.* [161]). However, identification of genetic variants has not turned out to be conclusive in defining personalised therapies (Engelbrechtsen *et al.* [162]). Clearly, there are other pathophysiological components like lipid, liver and skeletal muscle metabolism which potentially contribute towards differential responses to antidiabetic treatments (Becker *et al.* [163]).

OS is known to be causal in the development of PDCs. OS also plays an instrumental

role in the development of hyperglycemia. Studies in cell lines and animal models established that OS is an influential factor in the development of insulin resistance (Houstis *et al.* [164]; Hoehn *et al.* [165]) and β-cell dysfunction (Drews *et al.* [166]; Evans *et al.* [167]). Clinical trials have shown a strong association of OS with insulin resistant states in pre-diabetic conditions (Naota *et al.* [168]). For example, the Framingham study (Meigs *et al.* [169]) shows that insulin resistance in the non-diabetic state is strongly associated with enhanced OS. Therefore, OS might be a potential pathophysiological feature influencing the recovery from the diabetes treatment. Our analysis of OS markers showed that glutathione is an excellent biomarker suitable to represent OS state in the progression of diabetes. Additionally, Thomas *et al.* showed that glutathione levels show considerable variation at the population level, and this variation may be due to genetic components [170]. **Thus, we hypothesise that GSH_t as a measure of OS might influence recovery from the diabetes treatment.**

In this chapter, we seek to answer whether OS status measured as GSH_t is a *co-determinant* of recovery from the diabetes treatment along with GS? We expect that GS of an individual at the beginning of the therapy would influence how much benefit a patient would get out of the antidiabetic treatment. Since OS seems to be affected by changes in the GS, it is plausible that OS could also **co-determine** recovery from treatment. We show that recovery from the diabetes is positively correlated with the baseline GSH_t levels but negatively influenced by initial HbA_{1c} levels.

This result has been previously published as Kulkarni *et al.* [160].

7.2 Statistical methods

7.2.1 Multiple linear regression of recovery rate against 0-week HbA_{1c} and 0-week GSH_t in diabetic patients

Recovery rate (RR) was defined as a difference between 8-weeks HbA_{1c} and 0-week HbA_{1c}. All the three variables, RR, 0-week HbA_{1c}, and 0-week GSH_t were normalised to obtain standard normal distributions. A multiple linear regression was performed with RR as

a dependent variable and 0-week HbA_{1c} and 0-week GSH_t as independent variables. A multiple linear regression was performed using the lm() function in statistical package R (version 2.14.1).

7.3 GSH_t is a covariate of recovery from the diabetes treatment

To establish whether antioxidant defence status or GSH_t influences recovery from the antidiabetic treatment, we defined a term called as recovery rate (RR) - difference between 8-weeks HbA_{1c} and 0-week HbA_{1c}. RR implied how fast or slow a diabetic patient would respond to the antidiabetic treatment. Since we have not monitored diabetic patients long enough to develop PDCs, we assume that RR would be indirectly and inversely related to the rate of development of PDCs.

We performed a multiple linear regression (MLR) of RR against 0-week HbA_{1c}, 0-week GSH_t, and age of a diabetic patient, n=48 (details of the MLR are provided in Section 7.2.1). Table 7.1 shows results of the MLR. Our analysis demonstrated that recovery from the diabetes treatment is significantly correlated to initial GS (0-week HbA_{1c}) and OS (as defined by 0-week GSH_t), but not age. We expected that a-priory glucose levels before starting of the antidiabetic treatment would influence recovery trajectory of a diabetic patient; however, interestingly we also found that pre-treatment GSH_t levels also affect the outcome of the diabetes therapy. In that, RR is significantly but negatively correlated with 0-week HbA_{1c} (coefficient: 1.23; p-value: <0.001)) but positively influenced by 0-week GSH_t pools (coefficient: 0.33; p-value: <0.006).

The results of MLR imply that antioxidant defence status of a diabetic patient is featured prominently in response to the treatment. In other words, higher the antioxidant defence status of a diabetic patient better is the recovery from the diabetes therapy. This would have important implication in determining the diabetes therapy.

120

Independent variable	Coefficient	p-value
Intercept	-1.69	0.01 *
0-week A1C	-1.23	<0.001 *
0-week GSH	0.33	0.006 *
Age	-0.006	0.65

Table 7.1: Multiple linear regression of recovery rate against 0-week HbA_{1c} and 0-week GSH_t. RR is negatively influenced by 0-week GS but positively influenced by 0-week OS (as measured by GSH_t). Table adapted from Kulkarni *et al.* [160].

7.4 Discussion

In this chapter, we sought to understand whether OS (measured as GSH_t) co-determines recovery from the diabetes treatment along with the GS. We regressed recovery rate against 0-week GSH_t and 0-week HbA_{1c} from the diabetes therapy. We found that OS, measured in terms of pre-treatment GSH_t levels, emerged as a *covariate* of recovery along with GS. In other words, OS together with GS contributes towards the outcome diabetes treatment.

We thus observe that OS is an **independent** predictor of RR along with GS. This observation suggests that the contribution of OS to the development of PDCs has a component independent of GS. Undoubtedly, a major portion of OS would be contributed by glucose metabolism. However, OS might also be affected due to factors other than glucose. For example, lipid metabolism and inflammation are known to induce excessive ROS and this may contribute towards hampered OS **independently, and in addition** to, glucose metabolism. These observations, although based on small sample size and short study period, suggest that further substantial effort is required to investigate the complex origins of OS in the progression of diabetes.

We have clearly not waited long enough to see whether diabetic patients develop diabetic complications over the span of years. However, RR of the diabetes treatment can be looked at as a proxy for how OS would influence the rate of diabetic complications in the long run. Hyperglycemia undoubtedly needs to be controlled in the diabetes treatment since it is one of the primary causes of OS. However, our results show that the recovery from the diabetes

$$FFA, Infl. \dashrightarrow OS$$
$$OS \to RR \to PDCs$$
$$GS \to RR$$
$$GS \to OS$$
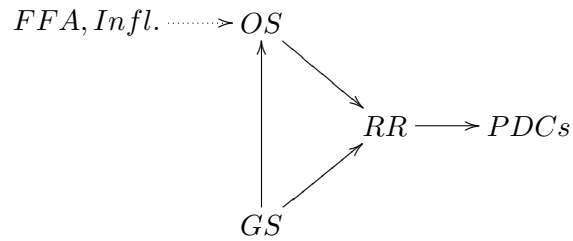
Figure 7.2: OS co-determines recovery from the diabetes treatment along with GS. This observation suggests that there might be other factors which influence OS status apart from GS. These other factors may include free fatty acid metabolism (FFA) and inflammatory responses (Infl). Therefore, involvement of OS in development of PDCs could have multiple nonlinear origins than represented in the minimal model (see **Chapter 5**).

treatment depends not only on the initial glycemic load but also on the initial OS status of a diabetic patient. We speculate that OS holds an additional information which should be incorporated when defining glucose targets.

Chapter 8

Conclusions and future directions

The role of ROS as secondary messenger molecules has been well documented in the human physiology. Impaired ROS responses are an important and emerging area in the study of human disease physiology. The imbalance of redox state - either due to overactivity of pro-oxidant mechanisms or insufficient antioxidant defence systems, or both - has been shown to be involved in the production of OS in the neurodegenerative disorders, cancer and diabetes. In this thesis we have studied the role of OS in the context of hyperglycemia-mediated development of PDCs. Recent findings in cell-lines, animal models and clinical trials establish the central causal role of overproduction of mitochondrial ROS in the development of PDCs. We have focused on investigating OS reduction during the diabetes therapy because augmentation of an antioxidant defence mechanism is likely to be a prominent protective mechanism underlying glycemic control.

In **Chapter 3** we study serial changes in the ten OS markers in response to the glucose control treatment. In particularly, we look for the two features in the OS markers: (a) how quickly does an OS marker respond to changes in the glucose over a short period of 8-weeks, and (b) whether it demarcates a diabetic state from the non-diabetic state? These features could suggest that a particular OS marker is plausibly involved in the pathophysiology of diabetes and can potentially track diabetes progression. Most importantly, such an OS marker would likely manipulable using antidiabetic drug treatment. We show that glutathione pools

recover rapidly in response to antidiabetic drug treatment over the short study period of 8-weeks. In **Chapter 4** we observe an interesting feature of glutathione metabolism in response to changes in the GS. We show that glutathione alone can be used to classify individuals into distinct diabetic states, consistent with the glucose based classification. In other words, glutathione can be a useful measure for tracking diabetes progression.

Although on average, GSH_t pools show rapid recovery over the 8-weeks we observe that the extent and rate of recovery of GSH_t pools show variation among diabetic patients. We propose a biophysically motivated minimal mathematical model to capture these individual differences in responses to antidiabetic treatment, **Chapter 5**. The model indicates that changes in the OS are non-linearly related to reduction in the GS. We were able to compute OS-GS trajectories in 34 of 49 patients. For each case, the recovery trajectory is characterised by a size of the maximal glutathione pools (GSH_t), threshold glucose value when GSH is half-maximal (v), and recovery rate or slope parameter of the curve (k). We hypothesise that controlling glucose until it is well below the threshold glucose value is an optimal glucose target. We explain how these results can be used in a clinical setup (see **Chapter 5, Section 5.3.3**).

The fitted v and k values for the GSH-glucose curves indicate the inherent maximal antioxidant capacity and how rapidly it can be attained. There is an important mechanistic insight coming out of the modelling study, which is justified by few human studies. Our analysis showed that v, the threshold glucose value would be a glucose target for a given diabetic patient. The threshold glucose value v is the ratio of maximal enzymatic reaction rates ($v_1/v_2 * \beta$), where v_1 is the maximum enzymatic reaction rate for GR and v_2 is the maximum enzymatic reaction rate for GPx. v_1 has units of concentration/time and v_2 has unit of (1/time). This means the rate at which GSH is replenished is limited to available GSSG pool but v_2 acts in proportion to glucose load and OS is essentially linearly increased in proportion to glycemic load. This mechanistic understanding suggests two possible ways to control diabetes. First, a standard way is to reduce glucose load so that v_2 will be lowered and antioxidant defence capacity would be sufficient to cope up with the OS stress. Another

way is to improve v_2, which means to increase antioxidant capacity of the cell. Increase in v_1 or decrease in v_2 both will lead to higher glucose threshold levels suggesting that antioxidant capacities would be enough to cope up with the OS. Though our strategy doesn't suggest GSH supplementation, there are several studies available on GSH supplementation in diabetic individuals which showed that improvement in GSH levels leads to relief from the diabetic symptoms and better glucose control. A detailed account of these studies has been given in Chapter 4, Section 4.1 (Introduction). In Chapter 7 we also establish that the initial antioxidant capacity influences the rate of recovery from the diabetes treatment. Therefore, increasing v_1 or GSH inside that cell can be beneficial in diabetes control. Although our strategy is not based upon GSH supplementation, it does suggest the possibility that improving GSH internally can help control the diabetes status.

Although the minimal model is used to describe the non-linear OS-GS relationship, it comes with disadvantages. First, the complex functional form of the minimal model may not be readily usable in the clinical setup. Secondly, glutathione-glucose physiology is more complicated than represented in the minimal model. There might be multiple mechanisms which may contribute towards the observed function relationship between the OS and GS. Thus, employ a phenomenological logistic sigmoid function to reconstruct OS-GS trajectories in **Chapter 6**. The phenomenological model retains the predictive power with its readily usable simple functional form.

In both modelling procedures we show that curve fitting is robust to small but substantial perturbations in glutathione values (see **Chapter 5, Section 5.3.2**). A major strength of this modelling study is that a simple measurement of GSH thrice in 8-weeks can give a quantitative measure of how stringent glucose control needs to be.

One reason for keeping the model minimal is to avoid overfitting due to the availability of only three data points. This is also a limitation of the study. More frequent measurements of GSH might be helpful in improving model estimates and building more complex models of GSH-glucose physiology. Thus, we propose that GSH measurements should be carried out for longer time duration in order to make precise inferences about glucose targets.

We have used mathematical modelling approaches to decipher individual differences to the glucose control treatment. We ask: what factors may influence intrinsic responses to diabetes treatment? In **Chapter 7** we attempted to deconstruct variations in the recovery rates of diabetic patients. We show an intriguing result: initial OS independently co-determines recovery from the diabetes treatment together with initial GS. This result indicates that OS-GS relationship is more complex than represented in the model. OS capacity can be influenced by glucose-dependent, as well as glucose-independent metabolic processes. OS is influenced by **glucose-independent** factors like free fatty acid metabolism, inflammatory responses due to infections as well as aging. We show that changes in the GSH in our study are not correlated to BMI or age (see **Chapter 4, Section 4.5.4**). However, in other population studies diabetes-associated comorbodities may need be considered while modelling OS responses. Another important factor which may contribute towards changes in the OS is antidiabetic drug treatment. Antidiabetic drugs like Glimepiride and Repaglinide have shown to reduce OS without affecting lipid parameters in the blood (Chen [171]). Another study indicates that Miglitol, an oral-antidiabetic drug improves endothelial cell function by suppressing ROS production (Aoki *et al.* [172]).

Glucose-dependent changes in the OS are more intricate than appear in the minimal model (see Figure 8.1). The development of diabetes (in patients with pre-diabetic state) is characterised by two main features: insulin resistance and impaired β-cell dysfunction. The interplay between these two features leads to the development of hyperglycemia. Lipid metabolism, inflammation and gut microbial changes are known to develop insulin resistance and impaired insulin secretion by inducing OS (Houstis *et al.* [164]; Hoehn *et al.* [165]; Johnson and Olfesky [46]). Furthermore, human clinical trials also showed that OS is positively associated with insulin resistance in non-diabetic obese individuals (Meigs *et al.* [169]). Anderson et al. showed that muscle biopsies of obese individuals have a higher rate of mitochondrial superoxide production compared to the lean study subjects and is associated with the higher insulin resistant state (Anderson *et al.* [173]). Additionally, hyperglycemia hampers insulin secretion, aggravates insulin resistance, and contributes to the diabetic pro-

gression via enhanced production of ROS (Ceriello and Motz [174]). This intricate web of reactions depict the non-linear feedback mechanisms which can affect OS state in more than one way. We observe that antidiabetic treatment leads to the reduction in the GS as well as OS. The reduction in the hyperglycemia is likely due to the action of drugs on the insulin sensitivity and insulin secretion responses. These changes can further influence the observed GS state. We realise that it is difficult to decipher individual contributions of these mechanisms to the changes in the OS and GS in a complex physiological network.

$$FFA, Infl., Gut\ microbiome \dashrightarrow OS \longrightarrow PDCs$$
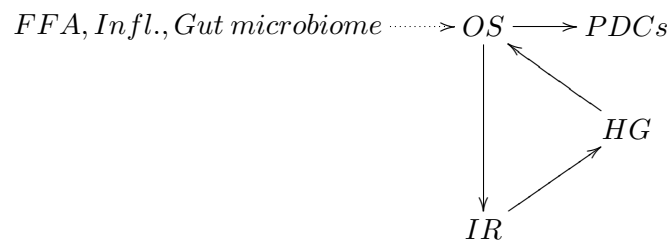
Figure 8.1: The complex origin of OS in the development and progression of diabetes. OS: oxidative stress; IR: insulin resistance; HG: hyperglycemia; PDCs: post-diabetic complications. OS might be influenced due to glucose-independent metabolic insults like free fatty acid metabolism (FFA), inflammation (Infl.) and gut-microbial changes. OS may be influenced due to glucose-dependent changes. For example, changes in the IR can feedback into HG influencing the OS.

Although we have modelled variations in the OS in response to changes in the hyperglycemia, in reality, we have modelled overall changes in the systemic OS in response to the systemic GS changes. Despite these shortcomings, our modelling study suggests the scope to construct complex physiological models incorporating various sources of OS to better distinguish the origin of individual differences.

Finally, we conclude that our modelling effort renders a quantitative tool which can be readily applicable in a clinical setup to define glucose targets over the short monitoring period of two months. We note that, although the predictions of the model are interesting and give valuable insights about defining personalised glucose targets, they are speculative at this stage. Future efforts will determine the efficiency of our approach and further modifications would follow. Nonetheless, understanding the redox regulation in the development

and progression of diabetes would not only help us in designing better diabetic treatments but may also help in building preventive measures. **We hope that our OS profiling to predict personalised glucose targets is a small but significant step towards that endeavour.**

Publications

The work presented in this thesis has appeared in the following publications:

1. **Rashmi Kulkarni**, Jhankar Acharya, Saroj Ghaskadbi and Pranay Goel, "Oxidative Stress as a Covariate of Recovery in Diabetes Therapy", **Frontiers in Endocrinology, 5(89)**, (2014).

2. **Rashmi Kulkarni**, Jhankar Acharya, Saroj Ghaskadbi and Pranay Goel, "Thresholds of Oxidative Stress in Newly Diagnosed Diabetic Patients on Intensive Glucose-Control Therapy", **PLoS ONE, 9(6): e100897**, (2014).

3. **Rashmi Kulkarni**, "A Simple Logistic Sigmoidal Model Predicts Oxidative Stress Thresholds in Newly Diagnosed Diabetics on Glucose Control Therapy", **BIOMAT 2015, 379-394**,(2016).

Bibliography

[1] Alberti, G. *et al.* Type 2 diabetes in the young: The evolving epidemic. *Diabetes Care* **27**, 1798–1811 (2004).

[2] The diabetes control and complications trial research group, The effect of intensive treatment of diabetes on the development and progression of long-term complications in insulin-dependent diabetes mellitus. *New England Journal of Medicine* **329**, 977–986 (1993).

[3] American diabetes association, 2. classification and diagnosis of diabetes **39**.

[4] The international expert committee. International expert committee report on the role of the a1c assay in the diagnosis of diabetes. *Diabetes Care* **32**, 1327–1334 (2009).

[5] *International Diabetes Federation Diabetes Atlas : sixth edition* (International Diabetes Federation, 2013).

[6] Yoon, K.-H. *et al.* Epidemic obesity and type 2 diabetes in asia. *The Lancet* **368**, 1681 – 1688 (2006).

[7] Kahn, S. E., Hull, R. L. & Utzschneider, K. M. Mechanisms linking obesity to insulin resistance and type 2 diabetes. *Nature* **444**, 840 – 846 (2006).

[8] Tuomilehto, J. *et al.* Prevention of type 2 diabetes mellitus by changes in lifestyle among subjects with impaired glucose tolerance. *New England Journal of Medicine* **344**, 1343–1350 (2001).

[9] Hamilton, M. T., Hamilton, D. G. & Zderic, T. W. Role of low energy expenditure and sitting in obesity, metabolic syndrome, type 2 diabetes, and cardiovascular disease. *Diabetes* **56**, 2655–2667 (2007).

[10] Hu, F. & V.S., M. Sugar-sweetened beverages and risk of obesity and type 2 diabetes: Epidemiologic evidence. *Physiol Behav.* **100**, 47–54 (2010).

[11] Pereira, M. A. *et al.* Fast-food habits, weight gain, and insulin resistance (the cardia study): 15-year prospective analysis. *The Lancet* **365**, 36–42 (2016).

[12] Sigal, R. J., Kenny, G. P., Wasserman, D. H., Castaneda-Sceppa, C. & White, R. D. Physical activity/exercise and type 2 diabetes. *Diabetes Care* **29**, 1433–1438 (2006).

[13] Colberg, S. R. *et al.* Exercise and type 2 diabetes. *Diabetes Care* **33**, e147–e167 (2010).

[14] Harris, M. I., Eastman, R. C., Cowie, C. C., Flegal, K. M. & Eberhardt, M. S. Racial and ethnic differences in glycemic control of adults with type 2 diabetes. *Diabetes Care* **22**, 403–408 (1999).

[15] Abate, N. & Chandalia, M. The impact of ethnicity on type 2 diabetes. *Journal of Diabetes and its Complications* **17**, 39–58 (2003).

[16] DeFronzo, R. A., Ferrannini, E., Keen, H. & Zimmet, P. *International Textbook of Diabetes Mellitus: Third Ed.* (Wiley-Blackwell Publishers, 2004).

[17] da Rocha Fernandes, J. *et al.* *IDF* diabetes atlas estimates of 2014 global health expenditures on diabetes. *Diabetes Research and Clinical Practice* **117**, 48–54 (2016).

[18] Zhang, P. *et al.* Global healthcare expenditure on diabetes for 2010 and 2030. *Diabetes research and clinical practice* **87**, 293–301 (2010).

[19] Zhuo, X., Zhang, P. & Hoerger, T. J. Lifetime direct medical costs of treating type 2 diabetes and diabetic complications. *American Journal of Preventive Medicine* **45**, 253–261 (2013).

[20] Klein, R. Hyperglycemia and microvascular and macrovascular disease in diabetes. *Diabetes care* **18**, 258–268 (1995).

[21] Singh, V. P., Bali, A., Singh, N. & Jaggi, A. S. Advanced glycation end products and diabetic complications. *Korean J Physiol Pharmacol* **18**, 1–14 (2014).

[22] Turnbull, F. M. *et al.* Intensive glucose control and macrovascular outcomes in type 2 diabetes. *Diabetologia* **52**, 2288–2298 (2009).

[23] Inzucchi, S. E. *et al.* Management of hyperglycemia in type 2 diabetes, 2015: A patient-centered approach: Update to a position statement of the american diabetes association and the european association for the study of diabetes. *Diabetes Care* **38**, 140–149 (2014).

[24] Ceriello, A. *et al.* Personalized therapy algorithms for type 2 diabetes: a phenotype-based approach. *Pharmgenomics Pers Med.* **7**, 129–136 (2014).

[25] Virkamäki, A. & Saltevo, J. Finnish current care guideline for diabetes: interactive approach to improve individualised treatment. *Diabetologia* **54**, 1264–1265 (2011).

[26] Brownlee, M. The pathobiology of diabetic complications. *Diabetes* **54**, 1615–1625 (2005).

[27] Giacco, F. & Brownlee, M. Oxidative stress and diabetic complications. *Circulation Research* **107**, 1058–1070 (2010).

[28] Acharya, J. D., Pande, A. J., Joshi, S. M., Yajnik, C. S. & Ghaskadbi, S. S. Treatment of hyperglycaemia in newly diagnosed diabetic patients is associated with a reduction in oxidative stress and improvement in β-cell function. *Diabetes Metabolism Research and Reviews* **30**, 590–598 (2014).

[29] Golbidi, S., Ebadi, S. A. & Laher, I. Antioxidants in the treatment of diabetes. *Curr Diabetes Rev.* **7**, 106–125 (2011).

[30] Johansen, J. S., Harris, A. K., Rychly, D. J. & Ergul, A. Oxidative stress and the use of antioxidants in diabetes: Linking basic science to clinical practice. *Cardiovascular Diabetology* **4**, 5 (2005).

[31] Bajaj, S. & Khan, A. Antioxidants and diabetes. *Indian J Endocrinol Metab.* **16**, S267–271 (2012).

[32] Reed, M. C. *et al.* A mathematical model of glutathione metabolism. *Theoretical Biology and Medical Modelling* **5**, 1–16 (2008).

[33] Raftos, J. E., Whillier, S. & Kuchel, P. W. Glutathione synthesis and turnover in the human erythrocyte: Alignment of a model based on detailed enzyme kinetics with experimental data. *J Biol Chem.* **285**, 23557–23567 (2010).

[34] Jacek, Z., Anil, S., Parini, P. & Poretsky, L. *Main Events in the History of Diabetes Mellitus* (Springer, 2009).

[35] von Mering, J. & Minkowski, O. Diabetes mellitus nach pankreasexstirpation. *O. Archiv f. experiment. Pathol. u. Pharmakol* **26** (1890).

[36] FG, B., CH, B., JB, C., WR, C. & AA, F. Pancreatic extracts in the treatment of diabetes mellitus: preliminary report. **145**, 1281–6.

[37] Himsworth, H. Diabetes mellitus: Its differentiation into insulin-sensitive and insulin-insensitive types. *The Lancet* **227**, 127 – 130 (1936).

[38] Yalow, R. & Berson, S. Immunoassay of endogenous plasma insulin in man. *J Clin Invest* **39**, 1157–75 (1960).

[39] Shen, S. W., Reaven, G. M. & Farquhar, J. W. Comparison of impedance to insulin mediated glucose uptake in normal and diabetic subjects. *J. Clin. Invest.* **49**, 2151–2160 (1970).

[40] DeFronzo, R. A., Tobin, J. D. & Andres, R. Glucose clamp technique: a method for quantifying insulin and resistance. *Am. J. Physiol.* **237**, E214–E223 (1979).

[41] Ginsberg, H., Kimmerling, G., Olefsky, J. M. & Reaven, G. M. Demonstration of insulin resistance in untreated adult onset diabetic subjects with fasting hyperglycemia. *J. Clin. Invest.* **55**, 454–461 (1975).

[42] Reaven, G. M. Insulin resistance in non insulin-dependent diabetes mellitus: does it exist and can it be measured ? *Am J Med.* **74**, 3–17 (1983).

[43] Warram, J. H., Martin, B. C., Krowlewski, A. S., Soeldner, J. S. & Kahn, C. R. Slow glucose removal rate and hyperinsulinemia precede the development of type ii diabetes in the off-spring of the diabetic parents. *Ann Intern Med.* **113**, 909–915 (1990).

[44] Lillioja, S. *et al.* Insulin resistance and insulin secretory dysfunction as precursors of non-insulin-dependent diabetes mellitus: Prospective studies of pima indians. *N Engl J Med.* **27**, 1988–1992 (1993).

[45] DeFronzo, R. A. The triumvirate: β-cell, muscle, liver: A collusion responsible for niddm. *Diabetes* **37**, 667–687 (1988).

[46] Johnson, A. & Olefsky, J. The origins and drivers of insulin resistance. *Cell* **152**, 673–684 (2013).

[47] DeFronzo, R. A. & Tripathy, D. Skeletal muscle insulin resistance is the primary defect in type 2 diabetes. *Diabetes Care* **32**, S157–63 (2009).

[48] Corkey, B. E. Diabetes: Have we got it all wrong? *Diabetes Care* **35**, 2432–2437 (2012).

[49] Corkey, B. E. Banting lecture 2011: Hyperinsulinemia: Cause or consequence? *Diabetes* **61**, 4–13 (2012).

[50] DeFronzo, R. A. From the triumvirate to the ominous octet: A new paradigm for the treatment of type 2 diabetes mellitus. *Diabetes* **58**, 773–795 (2009).

[51] The action to control cardiovascular risk in diabetes study group. Effects of intensive glucose lowering in type 2 diabetes. *New England Journal of Medicine* **358**, 2545–2559 (2008).

[52] The advance collaborative group. Intensive blood glucose control and vascular outcomes in patients with type 2 diabetes. *New England Journal of Medicine* **358**, 2560–2572 (2008).

[53] Uk prospective diabetes study (ukpds) group. Intensive blood-glucose control with sulphonylureas or insulin compared with conventional treatment and risk of complications in patients with type 2 diabetes (ukpds 33). *Lancet* **352**, 837–853 (1998).

[54] Neugebauer, R., Fireman, B., Roy, J. A. & O'Connor, P. J. Impact of specific glucose-control strategies on microvascular and macrovascular outcomes in 58,000 adults with type 2 diabetes. *Diabetes Care* **36**, 3510–3516 (2013).

[55] Dailey, G. Early and intensive therapy for management of hyperglycemia and cardio-vascular risk factors in patients with type 2 diabetes. *Clinical Therapeutics* **33** (2011).

[56] Chokrungvaranon, N., Deer, J. & Reaven, P. Intensive glycemic control and cardio-vascular disease: are there patients who may benefit? *Postgrad Med.* **123**, 114–123 (2011).

[57] Inzucchi, S. E. *et al.* Management of hyperglycemia in type 2 diabetes, 2015: A patient-centered approach: Update to a position statement of the american diabetes association and the european association for the study of diabetes. *Diabetes Care* **38**, 140–149 (2014).

[58] Gallagher, E. J., LeRoith, D., Stasinopoulos, M., Zelenko, Z. & Shiloach, J. Polyol accumulation in muscle and liver in a mouse model of type 2 diabetes. *Journal of Diabetes and Its Complications* **30**, 999–1007 (2016).

[59] Chung, S. S., Ho, E. C., Lam, K. S. & Chung, S. K. Contribution of polyol pathway to diabetes-induced oxidative stress. *Journal of the American Society of Nephrology* **14**, S233–S236 (2003).

[60] Tang, W., Martin, K. & Hwa, J. Aldose reductase, oxidative stress, and diabetic mellitus. *Frontiers in Pharmacology* **3**, 87 (2012).

[61] Li, S. *et al.* Redox state-dependent and sorbitol accumulation-independent diabetic albuminuria in mice with transgene-derived human aldose reductase and sorbitol dehydrogenase deficiency. *Diabetologia* **47**, 541–548 (2004).

[62] Bravi, M. C. *et al.* Polyol pathway activation and glutathione redox status in non-insulin-dependent diabetic patients. *Metabolism - Clinical and Experimental* 1194–1198.

[63] Hotta, N. *et al.* Long-term clinical effects of epalrestat, an aldose reductase inhibitor, on diabetic peripheral neuropathy. *Diabetes Care* **29**, 1538–1544 (2006).

[64] Schleicher, E. D. & Weigert, C. Role of the hexosamine biosynthetic pathway in diabetic nephropathy. *Kidney International* **58, Supplement 77**, S13–S18 (2000).

[65] Du, X.-L. *et al.* Hyperglycemia-induced mitochondrial superoxide overproduction activates the hexosamine pathway and induces plasminogen activator inhibitor-1 expression by increasing sp1 glycosylation. *Proceedings of the National Academy of Sciences* **97**, 12222–12226 (2000).

[66] Sharma, K. & Ziyadeh, F. N. Hyperglycemia and diabetic kidney disease: The case for transforming growth factor–β as a key mediator. *Diabetes* **44**, 1139–1146 (1995).

[67] James, L. R. *et al.* Flux through the hexosamine pathway is a determinant of nuclear factor Îžb– dependent promoter activation. *Diabetes* **51**, 1146–1156 (2002).

[68] Buse, M. G. Hexosamines, insulin resistance and the complications of diabetes: current status. *Am J Physiol Endocrinol Metab* **290**, E1–E8 (2006).

[69] Kaneto, H. *et al.* Activation of the hexosamine pathway leads to deterioration of pancreatic β-cell function through the induction of oxidative stress. *Journal of Biological Chemistry* **276**, 31099–31104 (2001).

[70] Geraldes, P. & King, G. L. Activation of protein kinase *C* isoforms and its impact on diabetic complications. *Circulation Research* **106**, 1319–1331 (2010).

[71] Shiba, T. *et al.* Correlation of diacylglycerol level and protein kinase *C* activity in rat retina to retinal circulation. *American Journal of Physiology - Endocrinology and Metabolism* **265**, E783–E793 (1993).

[72] Xia, P. *et al.* Characterization of the mechanism for the chronic activation of diacylglycerol-protein kinase *C* pathway in diabetes and hypergalactosemia. *Diabetes* **43**, 1122–1129 (1994).

[73] Craven, P. A., Davidson, C. M. & DeRubertis, F. R. Increase in diacylglycerol mass in isolated glomeruli by glucose from de novo synthesis of glycerolipids. *Diabetes* **39**, 667–674 (1990).

[74] Inoguchi, T. *et al.* Preferential elevation of protein kinase c isoform beta ii and diacylglycerol levels in the aorta and heart of diabetic rats: differential reversibility to glycemic control by islet cell transplantation. *Proc Natl Acad Sci U S A.* **89**, 11059–11063 (1992).

[75] Brownlee, M. Advanced protein glycosylation in diabetes and aging. *Annual Review of Medicine* **46**, 223–234 (1995).

[76] Taher, M., Garcia, J. & Natarajan, V. Hydroperoxide-induced diacylglycerol formation and protein kinase *C* activation in vascular endothelial cells. *Archives of Biochemistry and Biophysics* **303**, 260 – 266 (1993).

[77] Evcimen, N. D. & King, G. L. The role of protein kinase c activation and the vascular complications of diabetes. *Pharmacological Research* **55**, 498 – 510 (2007).

[78] Lei, S. *et al.* Hyperglycemia-induced protein kinase C $\beta 2$ activation induces diastolic cardiac dysfunction in diabetic rats by impairing caveolin-3 expression and Akt/eNOS signaling. *Diabetes* **62**, 2318–2328 (2013).

[79] Durpès, M.-C. *et al.* Pkc-β activation inhibits il-18-binding protein causing endothelial dysfunction and diabetic atherosclerosis. *Cardiovascular Research* **106**, 303–313 (2015).

[80] Idris, I. & Donnelly, R. Protein kinase c beta inhibition: A novel therapeutic strategy for diabetic microangiopathy. *Diab Vasc Dis Res.* **3**, 172–178 (2003).

[81] Bansal, D., Badhan, Y., Gudala, K. & Schifano, F. Ruboxistaurin for the treatment of diabetic peripheral neuropathy: A systematic review of randomized clinical trials. *Diabetes Metab J.* **37**, 375–384 (2013).

[82] Goldin, A., Beckman, J. A., Schmidt, A. M. & Creager, M. A. Advanced glycation end products. *Circulation* **114**, 597–605 (2006).

[83] Goh, S.-Y. & Cooper, M. E. The role of advanced glycation end products in progression and complications of diabetes. *The Journal of Clinical Endocrinology & Metabolism* **93**, 1143–1152 (2008).

[84] Stiltt, A. W. Advanced glycation: an important pathological event in diabetic and age related ocular disease. *British Journal of Ophthalmology* **85**, 746–753 (2001).

[85] Milne, R. & Brownstein, S. Advanced glycation end products and diabetic retinopathy. *Amino Acids* **44**, 1397–1407 (2013).

[86] Forbes, J. M., Cooper, M. E., Oldfield, M. D. & Thomas, M. C. Role of advanced glycation end products in diabetic nephropathy. *Journal of the American Society of Nephrology* **14**, S254–S258 (2003).

[87] Minoru, Y. & Soroku, Y. Role of advanced glycation end products in diabetic neuropathy. *Current Pharmaceutical Design* **14**, 953–961 (2008).

[88] Meerwaldt, R. *et al.* The clinical relevance of assessing advanced glycation endproducts accumulation in diabetes. *Cardiovascular Diabetology* **7**, 29 (2008).

[89] Ahmed, N. Advanced glycation end products: role in pathology of diabetic complications. *Diabetes Research and Clinical Practice* **67**, 3–21 (1999).

[90] Neumann, A., Schinzel, R., Palm, D., Riederer, P. & Munch, G. High molecular weight hyaluronic acid inhibits advanced glycation endproduct-induced *NF-ÎžB* activation and cytokine expression. *FEBS Letters* **453**, 283–287 (1999).

[91] Ramasamy, R., Yan, S. F. & Schmidt, A. M. Receptor for age (RAGE): signaling mechanisms in the pathogenesis of diabetes and its complications. *Ann N Y Acad Sci* **1243**, 88–102 (2011).

[92] Nishikawa, T. *et al.* Normalizing mitochondrial superoxide production blocks three pathways of hyperglycaemic damage. *Nature* **404**, 787–790 (2000).

[93] Halliwell, B. Antioxidant characterization. *Biochemical Pharmacology* **49**, 1341–1348 (1995).

[94] Augustin, A. J., Dick, H. B., Koch, F. & Schmidt-Erfurth, U. Correlation of blood-glucose control with oxidative metabolites in plasma and vitreous body of diabetic patients. *Eur J Ophthalmol.* **12**, 94–101 (2002).

[95] Sampson, M. J., Gopaul, N., Davies, I. R., Hughes, D. A. & Carrier, M. J. Plasma f2 isoprostanes. *Diabetes Care* **25**, 537–541 (2002).

[96] Kaviarasan, S., Muniandy, S., Qvist, R. & Ismail, I. S. F(2)-isoprostanes as novel biomarkers for type 2 diabetes: a review. *J Clin Biochem Nutr.* **45**, 1–8 (2009).

[97] Iino, K. *et al.* Serum vitamin c levels in type 2 diabetic nephropathy. *Diabetes Care* **28**, 2808–2809 (2005).

[98] Lonn, E. *et al.* Effects of vitamin e on cardiovascular and microvascular outcomes in high-risk patients with diabetes. *Diabetes Care* **25**, 1919–1927 (2002).

[99] Lagman, M. *et al.* Investigating the causes for decreased levels of glutathione in individuals with type ii diabetes. *PLOS ONE* **10**, 1–19 (2015).

[100] Akkus, I. *et al.* Leukocyte lipid peroxidation, superoxide dismutase, glutathione peroxidase and serum and leukocyte vitamin c levels of patients with type ii diabetes mellitus. *Clinica Chimica Acta* **244**, 221–227 (1996).

[101] Bhatia, S., Shukla, R., Madhu, S. V., Gambhir, J. K. & Prabhu, K. M. Antioxidant status, lipid peroxidation and nitric oxide end products in patients of type 2 diabetes mellitus with nephropathy. *Clinical Biochemistry* **36**, 557 – 562 (2003).

[102] Song, F. *et al.* Oxidative stress, antioxidant status and dna damage in patients with impaired glucose regulation and newly diagnosed type 2 diabetes. *Clinical Sciences* **112**, 599–606 (2007).

[103] Akerboom, T. P. & Sies, H. Assay of glutathione, glutathione disulfide, and glutathione mixed disulfides in biological samples. *Methods Enzymol.* **77**, 373–382 (1981).

[104] Scholz, R. W., Graham, K. S., Gumpricht, E. & Redde, C. C. Mechanism of interaction of vitamin e and glutathione in the protection against membrane lipid peroxidation. *Annals of the New York Academy of Sciences* **570**, 514–517 (1989).

[105] Grant, C. M. Role of the glutathione/glutaredoxin and thioredoxin systems in yeast growth and response to stress conditions. *Molecular Microbiology* **39**, 533–541 (2001).

[106] Prasad, A., Andrews, N. P., Padder, F. A., Husain, M. & Quyyumi, A. A. Glutathione reverses endothelial dysfunction and improves nitric oxide bioavailability. *Journal of the American College of Cardiology* **34**, 507 – 514 (1999).

[107] Atakisi, O. *et al.* Effects of reduced glutathione on nitric oxide level, total antioxidant and oxidant capacity and adenosine deaminase activity. *Eur Rev Med Pharmacol Sci.* **14**, 19–23 (2010).

[108] Kumar, C. *et al.* Glutathione revisited: a vital function in iron metabolism and ancillary role in thiol-redox control. *The EMBO journal* **30**, 2044–2056 (2011).

[109] Lu, S. C. Glutathione synthesis. *Biochimica et Biophysica Acta (BBA) - General Subjects* **1830**, 3143–3153 (2013).

[110] Jones, D. P. *[11] Redox potential of GSH/GSSG couple: Assay and biological significance*, vol. 348 of *Methods in Enzymology* (Academic Press, 2002).

[111] Owen, J. B. & Butterfield, D. A. *Measurement of Oxidized/Reduced Glutathione Ratio* (Humana Press, 2010).

[112] Jones, D. P. *et al.* Redox state of glutathione in human plasma. *Free Radical Biology and Medicine* **28**, 625 – 635 (2000).

[113] Peppa, M., Uribarri, J. & Vlassara, H. Glucose, advanced glycation end products, and diabetes complications: What is new and what works. *Clinical Diabetes* **21**, 186–187 (2003).

[114] Stirban, A., Gawlowski, T. & Roden, M. Vascular effects of advanced glycation end-products: Clinical effects and molecular mechanisms. *Molecular metabolism* **3**, 94–108 (2013).

[115] Thornalley, P. J., McLellan, A. C., Lo, T. W., Benn, J. & Sonksen, P. H. Negative association between erythrocyte reduced glutathione concentration and diabetic complications. *Clin Sci (Lond).* **91**, 575–582 (1996).

[116] Samiec, P. S. *et al.* Glutathione in human plasma: Decline in association with aging, age-related macular degeneration, and diabetes. *Free Radical Biology and Medicine* **24**, 699 – 704 (1998).

[117] Dincer, Y., Tulay, A., Zeynep, A. & Ilkova, H. Effect of oxidative stress on glutathione pathway in red blood cells from patients with insulin-dependent diabetes mellitus. *Metabolism - Clinical and Experimental* **51**, 1360–1362 (2002).

141

[118] Nwose, E. U., Jelinek, H. F., Richards, R. S. & Kerr, P. G. Changes in the erythrocyte glutathione concentration in the course of diabetes mellitus. *Redox Report* **11**, 99–104 (2006).

[119] Yoichi, T. *et al.* High concentration of glucose causes impairment of the function of the glutathione redox cycle in human vascular smooth muscle cells. *{FEBS} Letters* **421**, 19–22 (1998).

[120] Murakami, K. *et al.* Impairment of glutathione metabolism in erythrocytes from patients with diabetes mellitus. *Metabolism* **38**, 753–758 (1989).

[121] Whillier, S., Raftos, J. E. & Kuchel, P. W. Glutathione synthesis by red blood cells in type 2 diabetes mellitus. *Redox Report* **13**, 277–282 (2008).

[122] Paolisso, G. *et al.* Glutathione infusion potentiates glucose-induced insulin secretion in aged patients with impaired glucose tolerance. *Diabetes Care* **15**, 1–7 (1992).

[123] De Mattia, G. *et al.* Influence of reduced glutathione infusion on glucose metabolism in patients with non-insulin-dependent diabetes mellitus. *Metabolism* **47**, 993–997 (1998).

[124] Marfella, R. *et al.* Glutathione reverses systemic hemodynamic changes induced by acute hyperglycemia in healthy subjects. *American Journal of Physiology - Endocrinology and Metabolism* **268**, E1167–E1173 (1995).

[125] Sekhar, R. V. *et al.* Glutathione synthesis is diminished in patients with uncontrolled diabetes and restored by dietary supplementation with cysteine and glycine. *Diabetes Care* **34**, 163–167 (2011).

[126] Kulkarni, R., Acharya, J., Ghaskadbi, S. & Goel, P. Thresholds of oxidative stress in newly diagnosed diabetic patients on intensive glucose-control therapy. *PLoS ONE* **9**, 1–8 (2014).

[127] Kregel, K. C. & Zhang, H. J. An integrated view of oxidative stress in aging: basic mechanisms, functional effects, and pathological considerations. *American Journal of Physiology - Regulatory, Integrative and Comparative Physiology* **292**, R18–R36 (2006).

[128] Finkel, T. & Holbrook, N. J. Oxidants, oxidative stress and the biology of ageing. *Nature* **408**, 239–247 (2000).

[129] Muniyappa, R., Lee, S., Chen, H. & Quon, M. Current approaches for assessing insulin sensitivity and resistance in vivo: advantages, limitations, and appropriate usage. *American Journal of Physiology* **291**, E15–E26 (2008).

[130] Matthews, D. *et al.* Homeostasis model assessment: insulin resistance and β-cell function from fasting plasma glucose and insulin concentrations in man. *Diabetologia* **28**, 412–419 (1985).

[131] Levy, J. C., Matthews, D. R. & Hermans, M. P. Correct homeostasis model assessment (*HOMA*) evaluation uses the computer program. *Diabetes Care* **21**, 2191–2192 (1998).

[132] Bonora, E. *et al.* Homeostasis model assessment closely mirrors the glucose clamp technique in the assessment of insulin sensitivity: studies in subjects with various degrees of glucose tolerance and insulin sensitivity. *Diabetes Care* **23**, 57–63 (2000).

[133] Davidson, M. B., Bate, G. & Kirkpatrick, P. Exenatide. *Nat Rev Drug Discov* **4**, 713–714 (2005).

[134] Di Leo, M. A. S. *et al.* Potential therapeutic effect of antioxidants in experimental diabetic retina: a comparison between chronic taurine and vitamin *E* plus selenium supplementations. *Free Radic Res.* **37**, 323–30 (2003).

[135] Kowluru, R. A., Tang, J. & Kern, T. S. Abnormalities of retinal metabolism in diabetes and experimental galactosemia. *Diabetes* **50**, 1938–1942 (2001).

[136] Kedziora-Kornatowska, K. *et al.* Effect of vitamin E and vitamin C supplementation on antioxidative state and renal glomerular basement membrane thickness in diabetic kidney. *Nephron Exp Nephrol* **95**, e134–e143 (2003).

[137] Oyenihi, A. B., Ayeleso, A. O., Mukwevho, E. & Masola, B. Antioxidant strategies in the management of diabetic neuropathy. *BioMed Research International* **2015** (2015).

[138] Shay, K. P., Moreau, R. F., Smith, E. J., Smith, A. R. & Hagen, T. M. Alpha-lipoic acid as a dietary supplement: Molecular mechanisms and therapeutic potential. *Biochimica et Biophysica Acta (BBA) - General Subjects* **1790**, 1149 – 1160 (2009).

[139] Golbidi, S., Alireza Ebadi, S. & Laher, I. Antioxidants in the treatment of diabetes. *Current Diabetes Reviews* **7**.

[140] Gaede, P., Poulsen, H. E., Parving, H.-H. & Pedersen, O. Double-blind, randomised study of the effect of combined treatment with vitamin C and E on albuminuria in type 2 diabetic patients. *Diabetic Medicine* **18**, 756–760 (2001).

[141] Bursell, S. E. *et al.* High-dose vitamin E supplementation normalizes retinal blood flow and creatinine clearance in patients with type 1 diabetes. *Diabetes Care* **22**, 1245–1251 (1999).

[142] Chowienczyk, P. J. *et al.* Oral treatment with an antioxidant (raxofelast) reduces oxidative stress and improves endothelial function in men with type ii diabetes. *Diabetologia* **43**, 974–977 (2000).

[143] Millen, A. E. *et al.* Relation between intake of vitamins c and e and risk of diabetic retinopathy in the atherosclerosis risk in communities study. *The American Journal of Clinical Nutrition* **79**, 865–873 (2004).

[144] Poh, Z. & Goh, K. A current update on the use of α-lipoic acid in the management of type 2 diabetes mellitus. *Endocrine, Metabolic & Immune Disorders-Drug Targets* **9**, 392–398 (2009).

[145] Hector, G.-A., Celia, I. S. V. & Silverio, I. M. Treatment with α-lipoic acid over 16 weeks in type 2 diabetic patients with symptomatic polyneuropathy who responded to initial 4-week high-dose loading. *Journal of Diabetes Research* **2015**, 1–8 (2015).

[146] Blanco, R. *et al. D*iurnal variation in *GSH* and cysteine redox states in human plasma. *Am. J. Clin. Nutr.* **86** (2007).

[147] Selvin, E. *et al.* glycated hemoglobin, diabetes, and cardiovascular risk in nondiabetic adults. *N Engl J Med* **362**, 800–811 (2010).

[148] Chakravarty, S. & Rizvi, S. Day and night *GSH* and *MDA* levels in healthy adults and effects of different doses of melatonin on these parameters. *International Journal of Cell Biology* **2011** (2011).

[149] Tyson, J., Chen, K. & Novak, B. Sniffers, buzzers, toggles and blinkers: dynamics of regulatory and signaling pathways in the cell. *Curr. Opin. Cell Biol.* **15** (2003).

[150] Reid, M. & Jahoor, F. Glutathione in disease. *Curr Opin Clin Nutr Metab Care* **4**, 65–71 (2001).

[151] Townsend, D., Tew, K. D. & Tapiero, H. The importance of glutathione in human disease. *Biomedicine & Pharmacotherapy* **57**, 145–155 (2003).

[152] Wu, G., Fang, Y.-Z., Yang, S., Lupton, J. R. & Turner, N. D. Glutathione metabolism and its implications for health. *The Journal of Nutrition* **134**, 489–492 (2004).

[153] Vali, S. *et al.* Integrating glutathione metabolism and mitochondrial dysfunction with implications for ParkinsonâĂŹs disease: A dynamic model. *Neuroscience* **149**, 917–930 (2007).

[154] Presnell, C. *et al.* Computational insights into the role of glutathione in oxidative stress. *Current Neurovascular Research* **10**, 185–194 (2013).

[155] Srivastava, S. & Beutler, E. Oxidized glutathione levels in erythrocytes of glucose-6-phosphate-dehydrogenase-deficient subjects. *The Lancet* **292**, 23–24 (1968).

[156] Nur, E. *et al.* Increased efflux of oxidized glutathione (GSSG) causes glutathione depletion and potentially diminishes antioxidant defense in sickle erythrocytes. *Biochimica et Biophysica Acta (BBA) - Molecular Basis of Disease* **1812**, 1412–1417 (2011).

[157] Kulkarni, R. A simple logistic sigmoidal model predicts oxidative stress thresholds in newly diagnosed diabetics on glucose control therapy. *BIOMAT 2015* 379–394 (2016).

[158] Gavin, J. R. & Bohannon, N. J. A review of the response to oral antidiabetes agents in patients with type 2 diabetes. *Postgraduate Medicine* **122**, 43–51 (2010).

[159] Tsang, M.-W. The management of type 2 diabetic patients with hypoglycaemic agents. *ISRN Endocrinol.* **2012** (2012).

[160] Kulkarni, R., Acharya, J., Ghaskadbi, S. & Goel, P. Oxidative stress as a covariate of recovery in diabetes therapy. *Frontiers in Endocrinology* **5**, 89 (2014).

[161] Daniels, M. A. *et al.* Pharmacogenomics in type 2 diabetes: oral antidiabetic drugs. *Pharmacogenomics J* **16**, 399–410 (2016).

[162] Engelbrechtsen, L., Andersson, E., Roepstorff, S., Hansen, T. & Vestergaard, H. Pharmacogenetics and individual responses to treatment of hyperglycemia in type 2 diabetes. *Pharmacogenet Genomics.* **25**, 475–484 (2015).

[163] Becker, M., Pearson, E. & Tkac, I. Pharmacogenetics of oral antidiabetic drugs. *International Journal of Endocrinology* **2013** (2013).

[164] Houstis, N., Rosen, E. & Lander, E. Reactive oxygen species have a causal role in multiple forms of insulin resistance. *Nature* **440** (2006).

[165] Hoehn, K. L. *et al.* Insulin resistance is a cellular antioxidant defense mechanism. *Proceedings of the National Academy of Sciences* .

[166] Drews, G., Krippeit-Drews, P. & Düfer, M. Oxidative stress and beta-cell dysfunction. *Pflügers Archiv - European Journal of Physiology* **460**, 703–718 (2010).

[167] Evans, J. L., Goldfine, I. D., Maddux, B. A. & Grodsky, G. M. Are oxidative stress-activated signaling pathways mediators of insulin resistance and β-cell dysfunction? **52**, 1–8 (2003).

[168] Naoto, M.-N. *et al.* Increased oxidative stress precedes the onset of high-fat diet-induced insulin resistance and obesity. *Metabolism* **57**, 1071 – 1077 (2008).

[169] Meigs, J. B. *et al.* Association of oxidative stress, insulin resistance, and diabetes risk phenotypes: the framingham offspring study. *Diabetes Care* **30**, 2529–2535 (2007).

[170] van't Erve, T. J., Wagner, B. A., Ryckman, K. K., Raife, T. J. & Buettner, G. R. The concentration of glutathione in human erythrocytes is a heritable trait. *Free Radic Biol Med.* **65**, 742–749 (2013).

[171] Chen, K. Athero-protective actions of two oral antidiabetic drugs: Suppression of inflammation and oxidative stress. *J Cardiovasc Dis Res.* **3**, 3–4 (2012).

[172] Aoki, C. *et al.* Miglitol, an anti-diabetic drug, inhibits oxidative stress induced apoptosis and mitochondrial ros over-production in endothelial cells by enhancement of amp-activated protein kinase. *Journal of Pharmacological Sciences* **120**, 121–128 (2012).

[173] Johnson, A. & Olefsky, J. Mitochondrial h2o2 emission and cellular redox state link excess fat intake to insulin resistance in both rodents and humans. *Cell* **119**, 573–581 (2009).

[174] Ceriello, A. & Motz, E. Is oxidative stress the pathogenic mechanism underlying insulin resistance, diabetes, and cardiovascular disease? the common soil hypothesis revisited. *Arterioscler Thromb Vasc Biol.* **24**, 816–823 (2004).